Analysis of *COP1/SPA* signalling events in plant developmental responses

Inaugural-Dissertation

zur

Erlangung des Doktorgrades

der Mathematisch-Naturwissenschaftlichen Fakultät

der Universität zu Köln

vorgelegt von

Natalia Maria Ordoñez Herrera

Aus Bogota, Kolumbien

Köln 28.04 2017

Berichterstatter: Prof. Dr. Ute Höcker

                                              Prof. Dr. Martin Hülskamp

Prüfungsvorsitzender: Prof. Dr. Wolfgang Werr

Tag der mündlichen Prüfung: April 28th, 2017

Abbreviations

35S	*35S* promoter of Cauliflower Mosaic virus
B	blue light
BBX	B-box protein
bp	base pair, DNA sequence position
°C	degree Celsius
µl	micro liter
µg	micro gram
cDNA	complementary DNA
CDS	coding sequence
CCT	CO, CO-Like, TOC1
CFP	Cyan fluorescent protein
Col	Columbia; ecotype of *Arabidopsis thaliana*
COL	CONSTANS-LIKE
Co-IP	Co - immunoprecipitation
cm	centimeter
D	darkness
Da	Dalton
DNA	deoxyribonucleic acid
FLIM	Fluorescence-lifetime imaging microscopy
FRET	Förster resonance energy transfer
Fr	far-red light
h	hour
HA	human influenza hemagglutinin
HEK293	human embryonic kidney 293
HRP	horseradish peroxidase
his	Histidine, aminoacid
k	kilo
L	liter
leu	Leucin, amino acid
LUMIER	luminescence-based mammalian interactome
LD	long day
M	molar; mol/l
mg	milligram
mM	millimolar
min	minute
MS	Murashige and Skoog medium
NLS	nuclear localization signal/sequence
OD	Optical density
PCR	polymerase chain reaction
PVDF	polyvinyledene difluoride
Pfr	red light absorbing phytochrome conformation
Phy	phytochrome
Pr	red light absorbing phytochrome conformation
R	red light

RNA	ribonucleic acid
RT-PCR	reverse-transcription-PCR
RLuc	renilla luciferase
SAM	shoot apical meristem
s	second
SD	short day
SE	standard error, statistics
SDS	sodium dodecyl sulfate
StDev	Standard deviation of the mean, statistics
SUC2	*SUCROSE TRANSPORTER 2*
TF	Transcription factor
trp	tryptophan, amino acid
Wc	continuous white light
WT	wild type
Y2H	Yeast-two-hybrid
YFP	yellow fluorescent protein
ZT	Zeitgeber

Nomenclature

Nomenclature of Arabidopsis genes and proteins

SPA1	Gene, locus, wild-type allele
spa1	Mutant allele
SPA1	Protein

Exception: Nomenclature of photoreceptors

PHYB	Gene, locus, wild-type allele
phyB	Mutant allele
PHYB	Apoprotein
phyB	Holoprotein (with chromophore)

Abstract

Plants are able to perceive the light cues and adjust its development according to the prevalent conditions. An essential core component of the light signaling is the CONSTITUTIVELY PHOTOMORPHOGENIC1/SUPPRESSOR OF PHYA-105 (COP1/SPA) complex, that operates downstream of the photoreceptors to inhibit the light responses. Thus, the COP1/SPA complex is involved in the regulation of a variety of plant developmental processes, such as the timing of flowering and seedling growth. At the molecular level, COP1/SPA acts as an E3 ubiquitin ligase that promotes the selective degradation of its substrates, which mainly consist of transcription factors, i.e. CONSTANS (CO/BBX1). Since the *spanQ* and *cop1* mutants exhibit severe growth and developmental compromises that cannot be explained by the targets described so far, this study aims to identify and characterize a novel COP1/SPA substrate. In addition, COP1 and SPAs have been shown to act in concert to regulate post-embryonic development. However, the degree at which COP1 and SPAs act independently of each other was not addressed so far. Furthermore, it was unknown whether COP1/SPA plays a role in the regulation of embryogenesis. These novel aspects of the COP1/SPAs co-action are addressed in part II of this thesis.

Previously, a screening for interactors of COP1/SPA *in vitro* suggested that several B-Box transcription factors (BBX), that share similarity with CO, interact with COP1 and SPA1. This study confirms that several BBX proteins bind to COP1/SPA *in planta*, and focuses on the phenotypical and molecular characterization of CONSTANS-LIKE 12 (COL12/ BBX10). A domain mapping analysis indicated that the CO, CO-Like, TOC1 (CCT) domain of COL12 is important for binding to COP1 whereas the B-boxes are important for binding to SPA1, indicating that COP1 and SPAs might reinforce substrate binding. In agreement with the protein interactions, the COL12 protein undergoes proteolysis at the 26S proteasome in the darkness in a COP1-dependent manner. Both monochromatic red and blue light enhance COL12 protein stability, which contrasts with the destabilizing effects of red light on CO. Therefore, we conclude that COL12 is a novel COP1/SPA substrate.

The phenotypical analysis reveals that overexpression of COL12 delays the plant flowering time and enhances branching. Importantly, COL12 repression of flowering is photoperiod-dependent indicating that the protein takes part in the photoperiodic pathway that controls flowering. At the center of this pathway, the CO-FT accumulation is restricted to the LD. The visible light has a prominent role as a positive regulator of CO protein levels. Here, biochemical analyses reveal that COL12 physically interacts with the master regulator of flowering CO, possibly antagonizing its function. In addition, *FT* mRNA accumulation is reduced in *COL12 ox* plants compared to WT. Altogether our experiments suggest that COL12 might constitute a fine-tuning mechanism thereby the visible light can enhance CO function by stabilization of the COL12 repressor.

In the second part of this thesis, we isolated the quintuple *cop1-5 spaQn* mutant seedlings, demonstrating that   COP1/SPA do not play a role in embryogenesis. We also isolated the *cop1-4 spaQn* mutant that is completely devoid in the conserved WD-repeats. These quintuple mutant plants resemble the null *cop1-5* mutant. This result indicates that the WD-repeat domains provided by the SPA proteins can partially substitute for the lack of the COP1 WD-repeat domain in the COP1-4 protein. Therefore, the WD-repeats are essential for the signaling activity of COP1/SPA.

Zusammenfassung

Pflanzen sind in der Lage, Lichtsignale wahrzunehmen und ihre Entwicklung den vorherrschenden Bedingungen anzupassen. Eine wesentliche Kernkomponente des Lichtsignaltransduktionswegs ist der CONSTITUTIVELY PHOTOMORPHOGENIC1/SUPPRESSOR OF PHYA-105 (COP1/SPA) Komplex, der im Signaltransduktionsweg nach den Photorezeptoren agiert, um die Lichtreaktionen zu hemmen. So ist der COP1/SPA-Komplex an der Regulierung einer Vielzahl von pflanzlichen Entwicklungsprozessen beteiligt, wie zum Beispiel der Regulierung des Blühzeitpunkts und des Keimlingswachstums. Auf molekularer Ebene wirkt COP1/SPA als E3-Ubiquitin-Ligase, die den selektiven Abbau ihrer Substrate bewirkt, die hauptsächlich aus Transkriptionsfaktoren, z.B. CONSTANS (CO/BBX1) bestehen. Da die spanQ- und cop1-Mutanten starke Wachstums- und Entwicklungsdefizite aufweisen, die durch die bisher bekannten Interaktionspartner nicht erklärt werden konnten, zielte diese Studie darauf ab, ein neuartiges COP1/SPA-Substrat zu identifizieren und zu charakterisieren. Es wurde zudem gezeigt, dass COP1 und SPAs zusammenarbeiten, um die post-embryonale Entwicklung zu regulieren. Der Grad, in dem COP1 und SPAs unabhängig voneinander handeln, wurde jedoch bisher nicht untersucht. Auch ist bisher unbekannt, ob COP1/SPA eine Rolle bei der Regulation der Embryogenese spielt. Diese neuartigen Aspekte der COP1/SPA-Kooperation wurden in Teil II dieser Arbeit behandelt.

Bisher hat eine Suche nach Interaktionspartnern von COP1/SPA in vitro ergeben, dass wahrscheinlich mehrere B-Box-Transkriptionsfaktoren (BBX), die Ähnlichkeit mit CO haben, mit COP1 und SPA1 in Wechselwirkung treten. Die vorliegende Studie bestätigt, dass mehrere BBX-Proteine an COP1/SPA in planta binden und konzentriert sich auf die phänotypische und molekulare Charakterisierung von CONSTANS-LIKE 12 (COL12/BBX10). Eine Analyse der Domänen zeigte, dass die CO-, CO-Like-, und TOC1- (CCT-) Domain von COL12 für die Bindung an COP1 wichtig ist, während B-Box- Transkriptionsfaktoren für die Bindung an SPA1 wichtig sind. Dies lässt darauf schließen, dass COP1 und SPAs die Substratbindung verstärken können. In Übereinstimmung mit den Protein-Wechselwirkungen wird das COL12-Protein COP1-abhängig am 26S-Proteasom in der Dunkelheit abgebaut. Sowohl monochromatisches rotes als auch blaues Licht erhöhen die COL12-Protein-Stabilität, kontrastierend zu der destabilisierenden Wirkung von rotem Licht auf CO. Daher schließen wir, dass COL12 ein neuartiges COP1/SPA-Substrat ist.

Die phänotypische Analyse zeigte, dass die Überexpression von COL12 den Zeitpunkt der Blüte verzögert und die Verzweigungen der Sprossachse der Pflanze erhöht. Die Repression der Blüte durch COl12 ist abhängig von der Photoperiode, was darauf hinweist, dass das Protein Teil des photoperiodischen Signalwegs ist, der die Blütezeit reguliert. Im Zentrum des Signalwegs ist die CO-FT-Akkumulation auf Langtagbedingungen beschränkt. Das sichtbare Licht hat eine herausragende Rolle als positiver Regulator vom CO-Proteingehalt. Biochemische Analysen zeigten hier, dass COL12 physisch mit dem Masterregler des

blühenden CO interagiert und möglicherweise dessen Funktion entgegenwirkt. Darüber hinaus wird die FT-mRNA-Akkumulation in COL12-ox-Pflanzen im Vergleich zum WT reduziert. Insgesamt zeigten unsere Experimente, dass COL12 einen einabstimmungsmechanismus darstellen könnte, durch den das sichtbare Licht die CO-Funktion durch die Stabilisierung des COL12-Repressors verstärken kann.

Im zweiten Teil dieser Arbeit haben wir die Fünffach-cop1-5 spaQn-Mutanten-Sämlinge isoliert und gezeigt, dass COP1/SPA bei der Embryogenese keine Rolle spielt. Wir haben auch die cop1-4 spaQn Mutante isoliert, bei der die konservierte WD-Wiederholungs-Domänen fehlen. Die Fünffach-Mutanten-Pflanzen ähneln der cop1-5-Nullmutante. Dieses Ergebnis deutet darauf hin, dass die von den SPA-Proteinen bereitgestellten WD-Wiederholungs-Domänen teilweise das Fehlen der COP1-WD-Wiederholungs-Domäne im COP1-4-Protein ersetzen können. Daher sind die WD-Wiederholungen für die Signalisierungsaktivität von COP1/SPA unerlässlich.

Table of contents

1 Introduction

1.1 Plants possess a molecular network to perceive the light and adjust development accordingly

Plants are autotrophic organisms that harvest the energy from electromagnetic radiation and use it to power catabolic reactions. In contrast to the heterotrophic counterparts, adaptation to the light conditions is critical for plant survival and reproductive success. Hence, plants have acquired a diversified group of molecules that sense the light signals and control several developmental processes. In higher plants, these include seed germination, seedling de-etiolating, pigments accumulation, plant architecture, and the onset of flowering (Arsovski *et al.*, 2012). The regulation of the phenotypical changes involves transcriptional reprogramming (Jiao *et al.*, 2005) as well as changes in the epigenetic context (He *et al.*, 2011). These are coordinated by the actions of the photoreceptors and downstream molecular players. Plants possess at least five classes of photoreceptors that absorb specific wavelengths of the sunlight spectrum: Phytochromes (Phys) absorb red and far-red light, cryptochromes (CRYs) and phototropins perceive blue light and UV-A, LOV/F-box/Kelch-domain proteins (ZTL, FKF, and LKP2) sense blue-light and UVR8 senses the UV-B region of the spectrum (Kami *et al.*, 2010, Heijde and Ulm, 2012, Losi and Gartner, 2012, Casal, 2013). The information from the light environment is decoded directly into changes in gene expression or indirectly by downstream players such as the CONSTITUTIVE PHOTOMORPHOGENIC1/ SUPPRESSOR OF *phyA-105* (COP1/SPA) complex, COP9 signalosome, COP10-DET1-DAMAGED DNA BINDING PROTEIN 1 (DDB1) (CDD) and the family of bHLH transcription factors PHYTOCHROME INTERACTING FACTORs (PIFs)(Leivar and Quail, 2011, Chen *et al.*, 2014a, Huang *et al.*, 2014, Jung *et al.*, 2016).

1.2 COP1 and SPAs act together as central regulators of light signaling

Central components of the light signaling pathway were identified in a genetic screening for *Arabidopsis thaliana* mutant seedlings exhibiting the phenotypical features of light-grown seedlings in darkness. The group of loci was named as *COP/FUS* (Castle and Meinke, 1994, Lau and Deng, 2012). One of the members of the group, *COP1,* encodes a RING-finger protein present in plant and animal genomes. In mammals, *COP1* in known for its role in the regulation of cell-cycle progression, while in plants *COP1* is a characterized central regulator of development (Yi and Deng, 2005). In plants, biochemical and genetic evidence demonstrated that COP1 forms a tetrameric complex with members of the SPA family and that both molecular entities act in concert to control the light responses (Hoecker, 2005, Zhu *et al.*, 2008). In *Arabidopsis,* the SPA family is composed of four members (SPA1-4) that act partially redundant; the *spa1234* quadruple mutants (*spaQ*) exhibit a severe constitutive photomorphogenic phenotype that resembles that of *cop1* (Laubinger *et al.*, 2004, Fackendahl, 2012). The analysis of *spa* double and triple mutants clarified that each *SPA* family member contributes differentially to specific

phenotypes. Thus, *SPA1* and *SPA2* are important for seedling de-etiolation, *SPA3* and *SPA4* are pivotal for the regulation of vegetative growth, whereas *SPA1* and *SPA4* are the main contributors to the regulation of flowering time (Laubinger *et al.*, 2004, Fittinghoff *et al.*, 2006, Ordonez-Herrera *et al.*, 2015).

At the molecular level, the COP1/SPA complex acts as an E3 ligase that selectively controls the protein stability of its substrates by promoting ubiquitination and subsequent degradation in the 26S proteasome (Lau and Deng, 2012a). *In vitro* ubiquitination assays revealed that COP1 alone is sufficient to promote the ubiquitination of its substrates and that this activity can be fine-tuned by the interactions with the SPAs (Seo *et al.*, 2003). *In vivo*, the four SPAs act cooperatively with COP1 to promote the degradation of HY5 (Zhu *et al.*, 2008). The COP1/SPA complex also integrates as a substrate receptor into a higher order E3 ligase complex together with CULLIN 4 (CUL4)/DAMAGED DNA-BINDING 1 (DDB1)/RING BOX 1 (RBX1), thus *in planta* the E2 activity can be recruited indirectly (Chen *et al.*, 2010, Lau and Deng, 2012).

The visible light inactivates COP1/SPA through the action of the photoreceptors, some of the operating molecular mechanisms have been described, whereas others remain unknown. First, the visible light changes COP1 nucleocytoplasmic partitioning favoring its depletion from the nuclei (Vonarnim and Deng, 1994, Pacin *et al.*, 2014). Second, direct interactions between active photoreceptors (PhyA, PhyB, CRY1) and the SPAs perturb the interactions within the complex promoting its disassembly (Lian *et al.*, 2011, Liu *et al.*, 2011, Zheng *et al.*, 2013, Lu *et al.*, 2015b, Sheerin *et al.*, 2015). Third, light triggers the proteolysis of SPAs, especially the degradation of SPA2 that occurs rapidly and requires COP1 activity (Balcerowicz *et al.*, 2011, Chen *et al.*, 2015). Additional control mechanisms might exist, such as changes in affinity or specificity for the substrates upon interactions with photoreceptors (Menon *et al.*, 2016). As a result of the inactivating action of the Phys and CRYs, the COP1/SPA targets can accumulate in the light. Since most of the targeted proteins are transcription factors, the repression of COP1/SPA causes a massive transcriptional switch driving drastic phenotypic changes (Ma *et al.*, 2002). In contrast to its inhibitory role in the visible light pathways, COP1/SPA acts as a positive regulator in response to photomorphogenic UV-B employing a novel biochemical mechanism (Heijde and Ulm, 2012, Huang *et al.*, 2014). Upon UV-B exposure, UVR8 physically interacts with COP1/SPA displacing the CUL4-DDB1 E3 ligase, thus stabilizing HY5 protein. In this mechanism, COP1/SPA acts as a substrate receptor that recruits UVR8 to the targets instead of being an inducer of proteolysis (Huang *et al.*, 2013b).

1.3   COP1 and SPAs act partially redundantly

The *cop1*-5 allele is a null mutant that carries an early stop codon, also leading to the absence of *COP1* transcripts.   The *cop1-5* homozygous plants undergo embryogenesis but suffer a developmental arrest at the cotyledon stage and the adult plants are not viable (Deng *et al.*, 1992, Castle and Meinke, 1994). Therefore, COP1 is indispensable for seedling growth and development and after the seedling stage the SPAs alone are not sufficient to sustain development. In contrast, the *spa* null quadruple mutant (*spaQn*) develops into a dwarf plant capable of producing seeds and completing its life cycle (Fackendahl, 2012, Ordonez-Herrera *et al.*, 2015). Thus, COP1 is able to act independently of the SPAs, albeit its activity is highly reduced.

Since the SPAs and COP1 exhibit partial functional redundancy, the definite test to determine if the COP1/SPA complex is needed for the early stages of embryo and seedling development is to obtain mutant plants that are devoid in COP1 and the four members of the SPA family. We address this hypothesis by isolating the quintuple *spaQn cop1-5* mutant, and the results are presented in part II of this thesis.

1.4   Domain structure of COP1 and SPA proteins

Plant COP1 and SPA proteins share structural similarities; both possess a WD-repeat domain at the C-terminal part and a coil-coiled domain in the middle portion. Domain mapping analyses evidenced that the WD-repeat of both proteins is essential for protein-protein interactions with the substrates and the DDB1 E3 adaptor (Holm *et al.*, 2001, Saijo *et al.*, 2003, Chen *et al.*, 2010, Maier *et al.*, 2013). In addition, the WD-repeat domain of SPA1 mediates the inhibitory interaction with the photoreceptor CRY1 (Lian *et al.*, 2011, Liu *et al.*, 2011). The coil-coiled domain mediates homodimerization and heterodimerization within the COP1/SPA complex members (Hoecker and Quail, 2001, Saijo *et al.*, 2008b). At the N-terminal region of the proteins the structures diverge: The SPAs carry a kinase-like domain, whereas COP1 possesses a RING domain that confers E3 ligase enzymatic activity *in vitro* (Deng *et al.*, 1992, Hoecker *et al.*, 1999). Previous mutational analysis revealed that the N-terminal region of SPA1 is essential for the protein function in the darkness, in part due to its contribution to heterodimerization with COP1 (Holtkotte *et al.*, 2016). This protein region is also required for the interaction with CRY2 (Zuo *et al.*, 2011). The contribution of the kinase-like domain to the interaction with PHYA is controversial, as yeast-two-hybrid (Y2H) experiments report that this domain is indispensable (Sheerin *et al.*, 2015) for the interaction and another report that the domain is dispensable (Lu *et al.*, 2015a). Strikingly the deletion of the kinase-like domain does not reduce the seedling sensitivity to monochromatic light treatments, presumably because the WD-repeat of the SPAs or COP1 also contributes to the photoreceptors binding (Holtkotte *et al.*, 2016). The protein stability of SPAs is affected by the sequence at the N-terminal region (Fittinghoff *et al.*, 2006, Chen *et al.*, 2016). The structural similarity at the C-terminal part of COP1 and SPAs might contribute to the partial redundancy of their actions.

Furthermore, mutational analysis of some COP1 substrates indicates that the amino acids located at a conserved hydrophobic motif (VPE/D) are needed for the recognition and degradation by COP1 (Holm *et al.*, 2001). The crystal structure of the COP1 WD-repeat domain further confirmed that the VP residues participate in electrostatic interactions essential for substrate binding (Uljon *et al.*, 2016).

The *cop1-4* allele carries an early stop codon generating a truncated protein that lacks the WD-repeat domain (McNellis *et al.*, 1994). Compared to the null *cop1-5* lethal allele, the *cop1-4* mutant exhibits a weaker mutant phenotype, i.e. mutant *cop1-4* plants survive beyond the seedling stage. This indicates that the truncated protein in *cop1-4* confers residual activity. One possible scenario to explain the residual activity in *cop1-4* is that the WD-repeat of the SPA proteins compensate for the activity of this domain. We tested this hypothesis by isolating the quintuple mutant *spaQn cop1-4* and analyzing its phenotype, the results are presented in part II of this thesis.

1.5 The COP1/SPA complex targets transcription factors for degradation

The protein stability of several transcription factors is directly modulated by the COP1/SPA complex, including several members of the B-Box family (BBX) (Lau and Deng, 2012, Gangappa and Botto, 2014). In that way, COP1/SPA directly regulates numerous aspects of plant development. The complex is essential for the regulation of flowering time, targeting CONSTANS (CO/BBX1) (Laubinger *et al.*, 2006, Jang *et al.*, 2008, Liu *et al.*, 2008) and CONSTANS-LIKE3 (COL3/BBX4) (Datta *et al.*, 2006). In addition, the action of COP1/SPA represses seedling de-etiolation, a process that includes hypocotyl shortening, apical hook opening, and cotyledon opening. Positive regulators of this process that are targets of COP1/SPA include ELONGATED HYPOCOTYL 5 (HY5) (Saijo *et al.*, 2008a), BBX21 (STH2) (Xu *et al.*, 2016a), BBX22 (STH3/LZF1) (Datta *et al.*, 2008, Chang *et al.*, 2011) and LONG AFTER FAR-RED LIGHT 1 (LAF1) (Seo *et al.*, 2003). Moreover, *cop1* and *spaQ* mutants do not elongate the leaf hypocotyls in response to simulated shade (Low R:Fr), this function is dependent on the suppression of transcription factors, such as LONG HYPOCOTYL IN FAR-RED LIGHT (HFR1) that activates auxin biosynthetic genes (Yang *et al.*, 2005a, Yang *et al.*, 2005b) . COP1/SPA negatively controls the biosynthesis of anthocyanins by regulating HY5 and the MYB transcription factors PRODUCTION OF ANTHOCYANIN PIGMENT1 (PAP1) and PAP2 (Maier *et al.*, 2013). However, the known COP1/SPA substrates do not account for all the aspects of the COP1/SPA phenotype (Fig 1). For example, downstream molecular effectors that control leaf expansion and plant size are unknown. Therefore, we hypothesize that the COP1/SPA complex targets other substrates than the ones that have been described and aim to identify them.

1.6 The transition from the vegetative to the reproductive stage is a tightly controlled process

Living organisms control the timing of the reproductive transitions to maximize the chances of life-cycle completion and survival of the offspring. In the angiosperms, the dominant group of land plants, the developmental transition from the vegetative to the reproductive stage is defined by the production of flowers. This process takes place at the shoot meristems, the place where new organs are formed, although the regulation is achieved by the convergence of signals originated in different organs of the plant.

Plants adjust the time of the reproductive transitions according to their internal state and to the external conditions (Andres and Coupland, 2012). The main internal factors that determine the onset of flowering are the age of the plant and hormonal status (e.g. Gibberellin (GA) and ABA) while environmental factors include temperature, light quality, and photoperiod. Genes that convey these signals are classified into major flowering time pathways (Fornara *et al.*, 2010): Endogenous, age, GA, vernalization, ambient temperature, and photoperiod. Many of the signals converge in the activation of the main floral integrator genes *FLOWERING LOCUS T* (*FT)* and SUPPRESSOR OF OVEREXPRESSION OF CONSTANS 1 (*SOC1),* encoding a phosphatidylethanolamine-binding protein (PEBP) and a MADS box transcription factor, respectively (Andres and Coupland, 2012). *FT* and its closest relative, *TWIN SISTER OF FT* (*TSF),*

proteins constitute a long-distance florigen signal that initiates in the vasculature of leaves and moves to the shoot apical meristem (SAM) to change the transcriptional program triggering the onset of flowering (Kardailsky *et al.*, 1999, Kobayashi *et al.*, 1999, Corbesier and Coupland, 2006, Jaeger and Wigge, 2007). At the SAM, FT forms a complex with FD (Abe *et al.*, 2005), inducing the expression of SOC1 and the floral
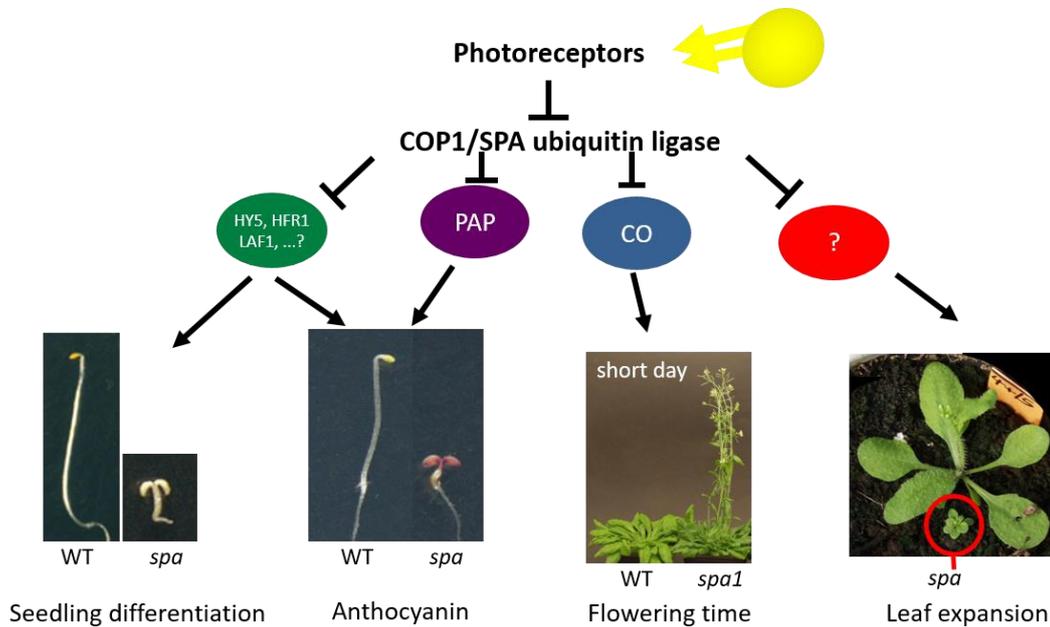
(Laubinger et al. *Plant Cell* 2004; Fittinghoff et al., *Plant J*. 2006; Laubinger et al. *Development* 2006)

Figure 1. The COP1/SPA complex targets unknown targets

COP1/SPA directly modulates the protein stability of several transcription factors. These proteins play a role in the regulation of developmental and physiological processes. For example, HY5, HFR1, and LAF1 control seedling differentiation. PAP proteins are positive regulators of Anthocyanin synthesis. Early flowering time in *spa1 and cop1-4* mutants is correlated with high CO accumulation. However, several aspects of *spaQn* and *cop1* mutants are not explained by the direct action on known targets. This led us to hypothesize that there may be unknown transcription factors targeted by COP1/SPA (Laubinger *et al.*, 2004, Fackendahl, 2012, Maier *et al.*, 2013)

identity genes *LEAFY (LFY), FRUITFULL (FULL)* and *APETALA1 (AP1)* leading to the developmental switch in which the SAM produces cauline leaves and flower buds (Searle and Coupland, 2004, Wigge *et al.*, 2005, Yoo *et al.*, 2005). The competence of the meristem to respond to the inductive stimuli is modulated by repressors, such as *SHORT VEGETATIVE PHASE (SVP)* (Hartmann *et al.*, 2000, Andres *et al.*, 2014) and activators like the S*QUAMOSA PROMOTER BINDING PROTEIN-LIKE genes (SPLs)* (Wang *et al.*, 2009). SVP acts alone or together with other floral repressors, such as FLOWERING LOCUS C (FLC), to repress the transcription of *SOC1* and *FT* (Mateos *et al.*, 2015). *FLC* integrates signals from the autonomous and vernalization pathways, the repressor imposes the requirement of exposure to cold temperatures for *FT* to rise. Important for the understanding of this work, *FT* expression responds to the length of the day/night cycles or photoperiod by a mechanism described below.

1.7 Mechanism of photoperiodic control of flowering in *Arabidopsis thaliana*

Many plants adjust the onset of flowering according to the photoperiod. This property has adaptive value in temperate regions where changes in day-length are associated with seasonal changes (Andres and Coupland, 2012). *Arabidopsis thaliana* is classified as a facultative long-day plant because it flowers when days are long and nights are short, typical of the spring, but eventually flowers under non-inductive short days. Genes that confer sensitivity to photoperiod can be identified because mutant plants flower at a similar time when grown in long days (LD) (16h light/ 8h dark cycles) and short days (SD) (8h light/ 16h dark cycles) (Koornneef *et al.*, 1991). At the center of these group of genes is *CONSTANS* (*CO*); *co* mutant plants flower later than WT in LD, nearly at the same time in LD and SD, whereas *CO* overexpressor plants flower early in both photoperiods (Koornneef *et al.*, 1991, Simon *et al.*, 1996). Hence, *CO* acts as a positive regulator of flowering operating under inductive photoperiods. The molecular cloning of the *CO* gene revealed that it encodes a transcription factor sharing high similarity with B-Box transcription factors present in yeast and mammals (Putterill *et al.*, 1995). In plants, CO promotes flowering mainly by activating the transcription of *FT* and *TSF* in the vasculature of leaves (Samach *et al.*, 2000, Yamaguchi *et al.*, 2005).

The CO protein associates with *cis*-elements in the *FT* promoter, binding directly to CORE elements (Tiwari *et al.*, 2010) and indirectly to the CCAAT elements through the *NUCLEAR FACTOR Y* (*NF-Y*) complex (Ben-Naim *et al.*, 2006, Wenkel *et al.*, 2006). Other transcription factors that target the *FT* promoter can counterbalance or enhance CO action, by changing promoter accessibility. For example, TEMPRANILLO (TEM) proteins bind directly to *FT* promoter repressing flowering. *TEM* genes might work as an antiflorigen signal that balances the florigen signal, as double *CO ox TEM ox* plants exhibit an intermediate flowering time behaving like WT plants. The transcription of *TEM* is regulated by the plant age, thus repression is relieved when plants immerse into the juvenile phase (Castillejo and Pelaz, 2008). *FT* promoter is also bound by the AP2-like proteins TARGET OF EAT (TOE), that can also bind directly to CO antagonizing its action (Zhang *et al.*, 2015). The accessibility to the *FT* promoter is influenced by *trans* elements and epigenetic factors that shape the plant´s ability to flower (Cao *et al.*, 2014, Turck and Coupland, 2014).

Sensing of the photoperiod is accomplished by a fine mechanism in which the coincidence of internal and external signals is required to generate the responses (Buenning, 1936). For Arabidopsis flowering time, the *CO-FT* module constitutes the core of the mechanism. Thus, at specific day-length conditions signals from the circadian clock and the light pathways coincide to trigger the accumulation of CO protein leading to *FT* transcription (Fig 2). In the first part of the mechanism, *CO* mRNA levels are tightly regulated by the circadian clock, restricting its accumulation to the end of the day and night periods (Suarez-Lopez and Coupland, 1998). The photoperiod sensing mechanism fails in mutant plants that have general circadian clock period shifts, such as the *toc1* mutant that exhibits early flowering in SD; also in clock mutants that regulate *CO* mRNA as a direct output, like *gigantea* (*gi)* and *late elongated hypocotyl* (*lhy*) (Yanovsky and Kay, 2002). Transcription of *CO* is enhanced at the afternoon hours of LD, due to the actions of GI and the blue light receptor FKF1 that together relieve the repression imposed by CYCLING DOF FACTORs (*CDFs*). The repressive action of the CDFs is essential to prevent *CO* transcription in the morning hours. The second part of the mechanism involves the action of the

visible light to modulate CO accumulation at the post-translational level. Briefly, the visible light prevents the degradation of CO protein by repression of the COP1/SPA complex. Therefore, CO protein is degraded during the night period. As a result of the regulation on both levels, in SD CO protein is synthesized at a time when there is no light, then proteolysis occurs and the plants are not induced to flower. In LD, the peak of CO transcription at the end of the day coincides with the presence of light, thus CO protein accumulates and triggers FT transcription (Turck *et al.*, 2008). In summary, CO protein levels are the main output of the photoperiod sensing pathway. The molecular players ensure that CO protein accumulation is restricted to the LD when plants are induced to flower.

CO mRNA
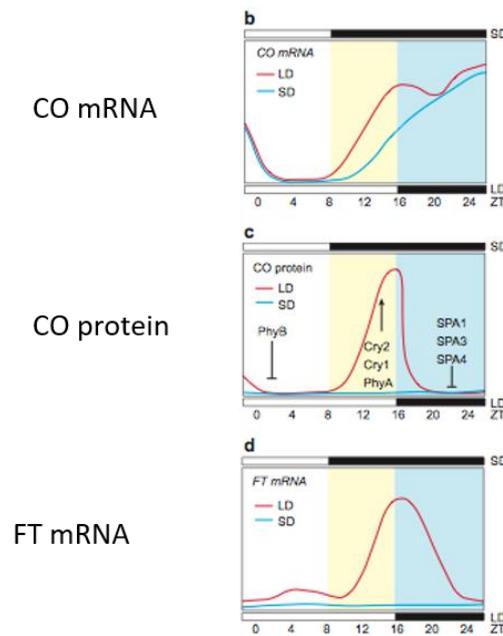
CO protein

FT mRNA

Taken from: Turck & Coupland, 2008

Figure 2. In *Arabidopsis,* the photoperiodic regulation of flowering involves tight regulation of CO-FT accumulation. Accumulation of CO mRNA, CO protein, and FT mRNA fluctuate along the day in a photoperiod-dependent manner. The action of the visible light on the photoreceptors shapes the CO protein accumulation pattern. As a result, FT is transcribed in LD and not in SD (Turck *et al.*, 2008).

1.8   The visible light controls CO protein stability

Visible light exerts a predominant role in the regulation of flowering time, mainly by controlling CO protein stability. However, there is wavelength specificity regarding CO protein accumulation. Indeed, plants growing in continuous blue and far-red light flower earlier than plants growing in white light whereas in red light flowering is delayed (Goto *et al.*, 1991, Guo *et al.*, 1998). In addition, photoreceptor mutants *cry2*, *phyA* and *fkf1* exhibit late-flowering phenotypes, in contrast to *phyB* mutant that has an early flowering phenotype (Goto *et al.*, 1991, Reed *et al.*, 1993, Guo *et al.*, 1998, Imaizumi *et al.*, 2003, Mockler *et al.*, 2003, Valverde *et al.*, 2004). PhyA, CRY1, and CRY2 promote CO protein stabilization, acting redundantly to inactivate the COP1/SPA complex (Valverde *et al.*, 2004, Jang *et al.*, 2008). The blue light receptor FKF1 interacts and

stabilizes CO protein, specifically at the late afternoon of LDs contributing to shape CO protein levels (Song *et al.*, 2014). Modulation of this interaction is achieved by TOE proteins that physically interact with CO and with FKF1, preventing CO stabilization (Zhang *et al.*, 2015). The red light activates PhyB, inducing its conversion into the Pfr form. PhyB Pfr exerts a dual action on CO protein, stabilizing or destabilizing depending on the time of the day and the availability of E3 ligases (Hajdu *et al.*, 2015). In the morning hours, PhyB partners with the E3 ligase OSMOTICALLY RESPONSIVE GENES1 (HOS1) to promote CO degradation (Lazaro *et al.*, 2012, Lazaro *et al.*, 2015). Yeast-two-hybrid and pull-down experiments show that PhyB, CO and HOS1 interact directly with each other and presumably they form a tripartite complex to achieve degradation in presence of red-light (Lazaro *et al.*, 2015). The physical association of CO and PhyB can be also bridged by PHYTOCHROME-DEPENDENT LATE-FLOWERING (PHL) counteracting the red light-dependent CO degradation (Endo *et al.*, 2013). In the beginning of the night, residual levels of PhyB Pfr lead to CO stabilization, presumably by repressing the COP1/SPA complex, this activity explains the early flowering phenotype of the PhyB overexpressor plants (Hajdu *et al.*, 2015). The net effect of the action of PhyB is to promote CO protein degradation, as *phyB* mutants exhibit higher CO protein levels than WT, consistently with its early flowering phenotype (Valverde *et al.*, 2004). The regulation of CO protein by the different light qualities, not only impacts the photoperiodic flowering but also have functional implications in the flowering outcome under different natural illumination conditions such as shade (Kim *et al.*, 2008, Wollenberg *et al.*, 2008).

1.9 Genes that control CO function

To achieve precise *FT* expression patterns under differential conditions, plants also employ molecular components that modulate CO function, these genes are described below. BBX19 encodes another member of the B-Box family of transcription factors, BBX19 and CO form non-active heterodimers preventing binding to the FT-promoter. The N-terminal part of BBX19, specifically the conserved B-Box1 domain is required for the interaction with CO (Wang *et al.*, 2014). Microproteins miP1a and miP1b also exploit the presence of BBXs to interact weakly with CO and bridge the formation of a tripartite complex together with the co-repressors TOPLESS/TOPLESS-RELATED (TPL/TPR) proteins potentially changing the activity of the transcription factor complex (Graeff *et al.*, 2016). The formation of the DNA binding CO - NF-Y complex is disrupted by the DELLA proteins, that directly bind to CO. This mechanism represents a point of crosstalk between the photoperiodic and GA pathways, thereby the hormone reinforces the induction of flowering (Xu *et al.*, 2016b). Molecular mechanisms at different levels govern the regulation of FT, providing enough robustness and plasticity to ensure a consistent outcome in a variety of physiological situations. Many of the genes that participate in the intricated flowering control network have been identified, but the mathematical models predict the existence of additional components (Salazar *et al.*, 2009). This is the case of the new repressor gene that we characterize in this thesis.

1.10 CO and the COLs share homology at conserved domains

The structural analysis of CO revealed that the gene encodes three conserved motifs: At the N-terminus, two zinc-binding B-boxes in tandem and at the C-terminus a CO, CO-Like, TOC1 (CCT) domain. Sequence similarity search shows that this combination of domains is also present in

other 16 *Arabidopsis* genes classified as the CONSTANS-LIKE (COLs) family of TF, which are part of a larger group of 32 genes that contain only the B-box domain named BBX family of TFs (Robson *et al.*, 2001, Gangappa and Botto, 2014). All COLs have a CCT and a B-box1 that are highly conserved and a variable portion in the middle, while at the B-box2 there are different degrees of conservation. Thus, the COLs can be sub-classified according to the conservation of the B-box2 domain: Group I comprises the genes with high conservation (CO, COL1, COL2, COL3, COL4, and COL5), group II includes genes do not possess a B-box2 (COL6, COL7; COL8 and COL16) and group III encompasses genes with intermediate sequence divergence (COL9, COL10, COL11, COL12, COL13, COL14, and COL15)(Griffiths *et al.*, 2003) . This study aims to gain knowledge on *Arabidopsis* COLs that belongs to group III because the functions of many of its members are unknown (Fig 3).

The conserved domains of CO and other COLs have been shown to be functionally relevant and domain mapping analyses have elucidated some of its specific molecular functions (Robson *et al.*, 2001, Gangappa and Botto, 2014). The CCT domain of CO is required for nuclear protein import, as it harbors a nuclear localization signal (NLS) (Robson *et al.*, 2001). Moreover, the CCT domain is needed for the association with DNA: It is important for the binding to the NF-Y, thereby to the CCAAT *cis* elements and for the direct interaction with CORE elements (Ben-Naim *et al.*, 2006, Tiwari *et al.*, 2010). Transactivation assays also show that COL9 and COL15 bind to the same CORE elements *in vitro,* with different affinities than CO, presumably by the CCT domain (Tiwari *et al.*, 2010). The CCT domain of COL7 also mediates binding to the promoter of an auxin-responsive marker (Zhang *et al.*, 2014). Protein-protein interactions with E3 ligases require the CCT domain of CO, specifically this domain is essential for the interactions of CO with COP1 and SPA proteins (Laubinger *et al.*, 2006, Jang *et al.*, 2009). The B-boxes are important for the establishment of protein-protein interactions with other partners and might contribute to transcriptional activation activities (Gangappa and Botto, 2014). Many BBX proteins possess the ability to form homodimers and heterodimers with members of the same family, due to an intrinsic property of the B-box domain (Peng *et al.*, 2000). For example, CO isoforms (named α and β), both containing the N-terminal part, interact with each other leading to the formation of inactive heterodimers (Gil *et al.*, 2017). In a similar way, *CO* interacts with BBX19 through the B-box1 domain (Wang *et al.*, 2014). In synthesis, the COLs proteins exhibit a modular structure that can result in combinatorial properties and multiple functional implications.
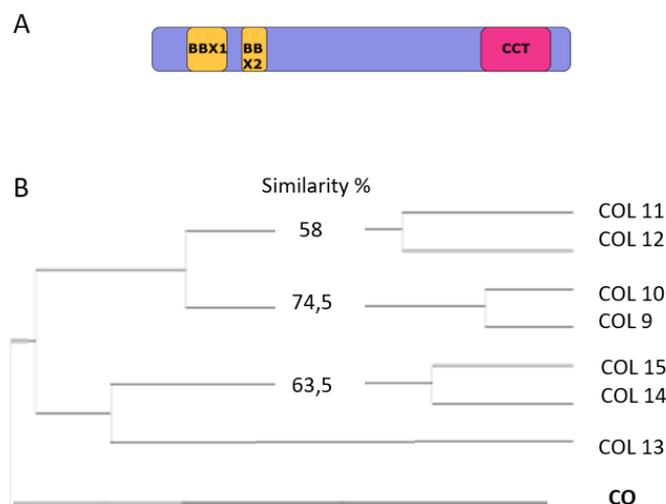
Figure 3. COLs family of transcription factors

(A). Depiction of the protein domain structure of COLs showing the distribution of conserved domains: BBX1, BBX2 and CCT (Griffiths *et al.*, 2003).

(B). Phylogenetic tree of *Arabidopsis thaliana* COLs group III, the tree groups proteins according to its sequence similarity. The percentage of amino acid similarity among closest relatives is shown. Phylogenetic tree calculated with the MegAlign application from LaserGene software.

1.11 Evolutionary history of the COLs

The evolutionary history of COL genes tracks back to the early photosynthetic organisms. There is a single copy gene in the green algae *Chlamydomonas* that contains the three conserved domains clustering with Arabidopsis group I. The ancestral algae gene, CrCO, drives changes in phase transitions in response to photoperiod and light (Serrano *et al.*, 2009). Through evolution the gene family has expanded, resulting in 10 COL members in the moss *Physcomitrella patents* and 17 in *Arabidopsis* (Zobell *et al.*, 2005, Romero-Campero *et al.*, 2013). The appearance of new genes and sequence divergence might have resulted in neo-functionalization. The evolutionary analysis of COLs from the group I in the *Brassicaceae* family revealed that the sequence divergence in the *CO* promoter as well as in the protein coding sequences was fundamental for generating the powerful photoperiodic switch represented by CO in the *Brassicaceae*. New features of CO protein, compared to closest relatives COL1 and COL2, achieve a strong FT induction. In addition, the circadian expression pattern is a novelty conferred by the *CO* promoter (Simon *et al.*, 2015). Numerous angiosperms species, encode CO homologs that control photoperiodic responses, presumably this is due to convergent evolution (Simon *et al.*, 2015).

1.12 The functions of some members of the *Arabidopsis* BBX family of transcription factors are known

In *Arabidopsis,* the functions of some members of the BBX family have been elucidated. These are mainly related to photomorphogenesis, flowering time, abiotic stress tolerance and shade avoidance responses (Gangappa and Botto, 2014). Genes that participate in the control of flowering time include *CO, COL3, COL5, COL9,* and *BBX19*. Similar to the positive regulator *CO*, when overexpressed in *Arabidopsis COL5*, *COL1* and *COL2* promote flowering. However, single loss-of-function lines do not exhibit a mutant flowering phenotype, presumably due to functional redundancy (Hassidim *et al.*, 2009) (Simon *et al.*, 2015). Oppositely to *CO, COL9 and BBX19* act as negative regulators of flowering in a photoperiod-dependent manner, COL9 acts by repressing the *CO* mRNA expression in LD at ZT12 (Cheng and Wang, 2005) and BBX19 represses CO by the formation of non-active heterodimers (Wang *et al.*, 2014). *COL3* represses flowering in a photoperiod-independent manner, this gene is also involved in the promotion of shoot and root branching and inhibition of hypocotyl elongation (Datta *et al.*, 2006). Other BBX proteins participate in the process of photomorphogenesis; genes that act as positive regulators of and repress *COP1* function include *COL3*, *BBX20*, *BBX21* and *BBX22* (Gangappa and Botto, 2014). BBX21 directly binds to *HY5* promoter inducing its expression, the protein stability of both proteins is targeted by COP1, thus the E3 ligase action is reinforced in a positive manner (Xu *et al.*, 2016a). Another group of genes are negative regulators and act as enhancers of *COP1* function in

the control of photomorphogenesis, these include *BBX19*, *BBX24* (*STO*) and *BBX25* (*STH*). *BBX19* plays a pleiotropic role as a negative regulator of photomorphogenesis, acting via a novel mechanism. BBX19 facilitates the COP1-dependent degradation of ELF3 by bridging the proteins, thereby it suppresses the transcription of *PIF4* and *PIF5* that are needed for the inhibition of hypocotyl growth (Wang *et al.*, 2015). BBX24 and BBX25 are COP1/SPA substrates that at the same time interact with HY5 impairing its transcriptional activity. Thus constituting a fine-tuning mechanism of the photomorphogenesis response (Gangappa *et al.*, 2013). BBX24 also promotes the shade-avoidance syndrome (SAS) independently of HY5, rather by repressing the DELLA proteins (Crocco *et al.*, 2015). Another BBX protein involved in the SAS is COL7, acting in an R:Fr-dependent manner to control hypocotyl length and rosette branching (Wang *et al.*, 2013). COL7 promotes branching in high R:Fr but not in low R:Fr due to the protein stabilization by PHYB in high R:Fr which is reduced in the low R:Fr (Zhang *et al.*, 2014). In synthesis, several members of the BBX family play critical roles in the regulation of plant developmental processes, often these genes are part of the light signaling cascade positioned downstream of COP1/SPA.

1.13 Pleiotropic roles of *FT* and *CO*

Besides playing an essential role in the regulation of flowering time, *CO* and *FT* exhibit pleiotropic roles in the control of other developmental processes. In fact, both genes are expressed through vegetative development as well as in reproductive development in structures such as cauline leaves, flowers, and siliques (Schmid *et al.*, 2005, Adrian *et al.*, 2010). Additional phenotypical effects can be linked to the differences in the onset of flowering transition but can also result from the direct effect of the genes on other processes (Huang *et al.*, 2013a). Importantly, plant architecture is changed not only in response to the transformation of the SAM by a signal that moves basipetally but also by *FT* acting independently of flowering time (Hempel and Feldman, 1994, Hiraoka *et al.*, 2013). In this aspect, *FT* is implicated in the formation and speed of growth of axillary branches (Hiraoka *et al.*, 2013). In addition, *FT* expression in the siliques is important for the establishment of seed dormancy and for the maintenance of flowering commitment, thus preventing flowering reversion (Chen *et al.*, 2014b, Liu *et al.*, 2014). In the leaves, overexpression of *FT* leads to reduced leaf size and curly shape in a photoperiod-independent manner (Teper-Bamnolker and Samach, 2005). Rosette leaf size and inflorescence length are reduced by overexpression of *CO* (Simon *et al.*, 1996). In tomato, a perennial plant, the *FT*-related orthologue *SINGLE-FLOWER TRUSS (SFT)* together with the *TFL1* orthologue *SELF-PRUNING (SP) are* part of a systemic signal that elicits major changes in the sympodial growth, activation of the meristems, leaf complexity and growth of stems (Shalit *et al.*, 2009). In other plant species, orthologues of *Arabidopsis CO* and *FT* are involved in the control of developmental switches in response to photoperiodic cues, such as tuberization in potato and cessation of bud growth in trees (Böhlenius *et al.*, 2006, Rodríguez-Falcón *et al.*, 2006). Thus, FT constitutes a versatile transcription factor that triggers developmental transitions in a context-dependent manner, presumably by interactions with different partners (Teper-Bamnolker and Samach, 2005).

In this thesis, we investigate the functional roles and molecular mechanism of COL12, a previously uncharacterized BBX protein. We show that COL12 might have multiple roles in the plant, as overexpression of the gene leads to aberrant architecture and flowering time. Furthermore, we unveiled details of the molecular mechanism thereby COL12 interferes with flowering in a photoperiod-dependent manner. The experiments presented here proved evidence that COL12

physically interacts with CO and that it downregulates FT mRNA expression. Finally, we provide compiling evidence that COL12 is a COP1/SPA substrate and its stability is regulated by the visible light. Therefore, COL12 might constitute part of a fine-tuning mechanism by which the initiation of flowering is adjusted in response to the light.

2 Aims of the dissertation

2.1 Part I - Identification and functional characterization of a novel COP1/SPA substrate

Plants adjust development to prevalent light conditions. A powerful control mechanism encompasses the rapid regulation of gene transcription by selective degradation of transcription factors. The specificity is conferred by the E3 ligases such as the COP1/SPA complex that is active in darkness. Since the action of this complex impacts numerous aspects of plant development. We hypothesize that COP1/SPA controls the stability of unknown targets that account for the regulation of specific aspects of the phenotype. The purpose of this project is, therefore, to identify and characterize a novel COP1/SPA substrate. First by confirming the protein-protein interactions and then by testing whether the protein stability of the putative substrate is modulated by COP1/SPA. Next, the project aims to annotate the function of the gene. Finally, to place the gene into the known molecular network and elucidate its molecular mechanisms.

2.2 Part II - Co-action of COP1 and SPA in the regulation of early developmental stages

Given that: First, COP1 and SPA proteins act partially redundantly to regulate plant development. Partial redundancy of the molecular entities is evidenced by the fact that in the *spanQ* mutant, COP1 is able to function independently of the SPAs, albeit a severe reduction in activity. Second, in the *cop1-5* null mutant, the activity of the SPA proteins is retained and the plants arrest development at seedling stage. Third, the *COP1* orthologue in mammals controls cell cycle progression. Therefore, we aim to test if SPAs have functional activity in the absence of COP1 at the early stages of seedling development. Thus, to clarify whether the COP1/SPA complex plays a role in embryogenesis. To this end, our objective is to isolate the quintuple mutant *spaQ cop1-5* that completely lacks all components of the system.

In *cop1-4* plants, truncated COP1 lacking the WD-repeat domain exhibits residual functional activity. The structure of COP1 and SPAs is highly conserved and both entities encode a WD-repeat domain. Therefore, we hypothesize that the WD-repeat domain of SPAs can functionally compensate for the lack of COP1 WD-repeat. To test this hypothesis, we aim to isolate the *spaQ cop1-4* mutant in which the WD-repeat domains are absent from the complex.

3 Results

3.1 PART I - COL12 is a COP1/SPA substrate that represses flowering in *Arabidopsis* thaliana

3.1.1 Analyses of the protein-protein interactions between COP1/SPA members and COLs (Group III)

The COP1/SPA complex instructs the protein degradation of its targets, thereby regulating many aspects of plant development. To identify novel COP1/SPA interactors, an *in vitro* pulldown screening was performed between COP1, SPA1 and members of the COLs family of transcription factors (Adrian, 2005). These experiments indicated that several COLs (1-12,15) bind to COP1 and SPA1 *in vitro*. We decided to focus our studies on COLs from group III (Griffiths *et al.*, 2003) because the function of many of its members remains unknown. For the initial interaction analyses, all the gene members of this group were investigated.

To further investigate if COLs physically interact with members of the COP1/SPA complex, we performed yeast two-hybrid experiments using SPA1, COP1, and SPA4 as baits and COLs (12, 13, 14 and 15) as preys. In the yeast system, SPA4 interacted strongly with COL13, COL14, and COL15 (Fig 4A) and might have interacted with COL12 (Fig S1B) (This experiment exhibited contradicting results among replicates). SPA1 interacted weakly with COL15 but not with COL12, COL13, and COL14 (Fig 4B and S1A). Using yeast two-hybrid experiments, no interactions between COP1 and COLs were detected (data not shown). Similarly, it was reported in the literature that the interaction between CO and COP1 was not detected by the yeast-two hybrid system but it is detectable with *in vitro* pulldown experiments (Jang *et al.*, 2008). Therefore, we tested the putative interactions using alternative methods.

3.1.2 COL12 physically interacts with SPA1 and COP1 as shown by co-localization and FRET analyses

Then, we inspected the COP1/SPA - COLs (9-15) interactions *in planta* by co-localization analysis. To this end, the proteins of interest were tagged at the N-terminus with CFP, YFP or mCherry fluorophores. The chimeric proteins were transiently expressed in leek epidermal cells using gold particle bombardment. The epifluorescence microscope analysis revealed that all COLs proteins

that belong to group III localize diffusely within the nuclei (Fig 4C and 5B) and (Henschel, 2014). Since both COP1 and the SPAs are known to localize into discrete nuclear bodies (NB), we asked whether they can recruit the COLs to the same location. Hence, chimeric fluorescent COL proteins were transiently co-expressed with either fluorescent COP1 or SPA1 in leek epidermal cells. Strikingly, both YFP-COP1 and YFP-SPA1 recruited mCherry-COL12 into NB (Fig 5B and 5D). A similar result is obtained in co-localization experiments using COL12 fused to CFP and YFP tagged COP1 and SPA1 (6E). Conversely, COLs (9, 10, 11 and 15) fused to CFP are not mobilized into NB by YFP-COP1 nor with YFP-SPA1 (data in Henschel, M. 2014). This difference might be due to hindering effects of the fluorescent tag, it might be useful to employ other fluorophores or positions of the tag.
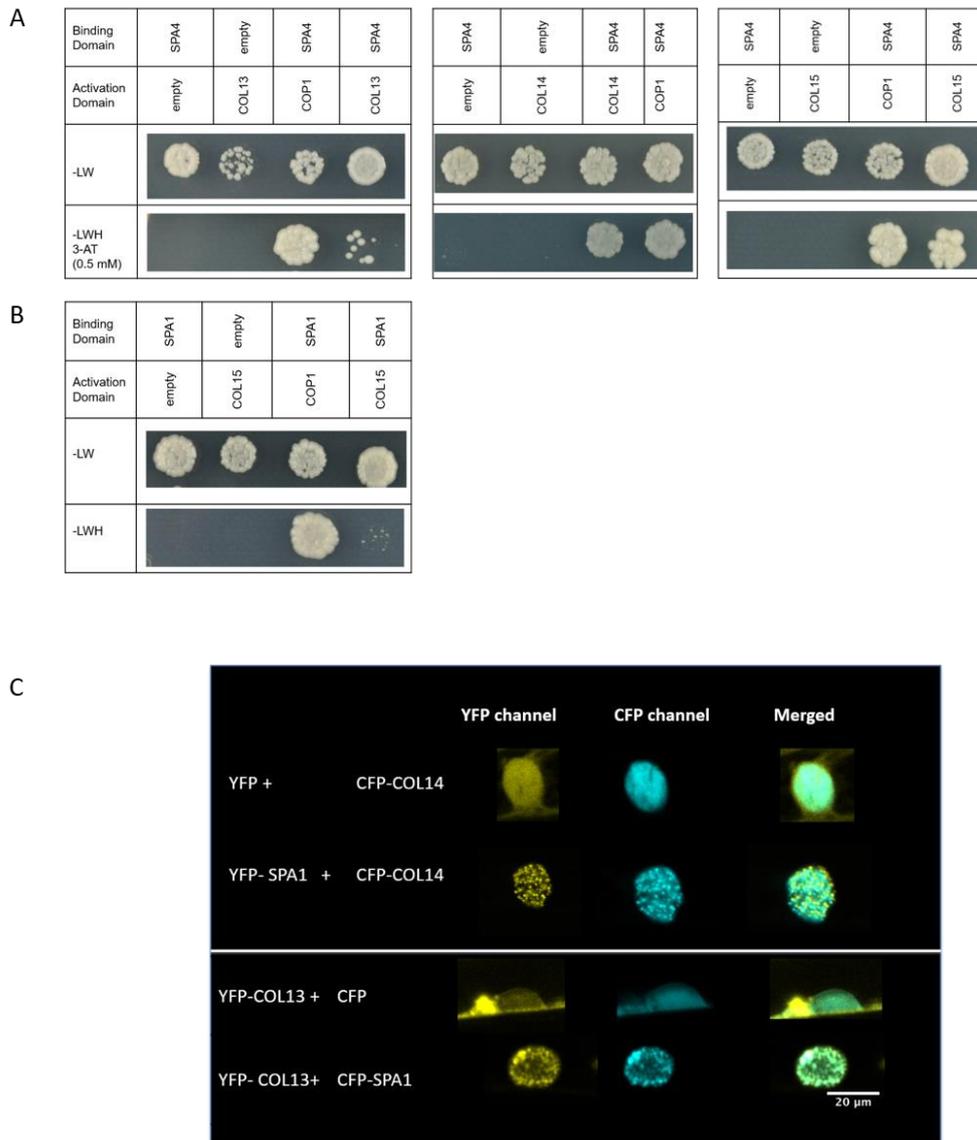
Figure 4. Members of the COP1/SPA complex interact with COLs from group III

Yeast two-hybrid experiments show that SPA4 interacts with COL13, COL14 and COL15 and SPA1 interacts weakly with COL15.

(A) For Y2H, SPA4 was used as bait and COL proteins as prey. Yeast was co-transformed with prey vectors (pACT) and bait vectors (pAS) as indicated. From each co-transformation, 5 colonies were pooled and grown overnight, the OD600 was normalized to 0,1. Cultures were spotted onto non-selective medium

lacking Leu and Trp (–LW) and selective medium without Leu, Trp and His (-LWH) supplemented with 3-AT (0.5mM) if indicated. Growth was analyzed after 3 – 5 days of incubation at 30 °C.

(B) Y2H using SPA1 as bait and COL15 as bait, performed as in A.

(C) Co-localization analysis shows that COL13 and 14 are recruited into nuclear speckles by SPA1. COL14 was fused to CFP and co-bombarded with YFP-SPA1 or YFP as control. COL13 coding sequence combined with YFP tag and co-bombarded with CFP-SPA1 or CFP as a control.
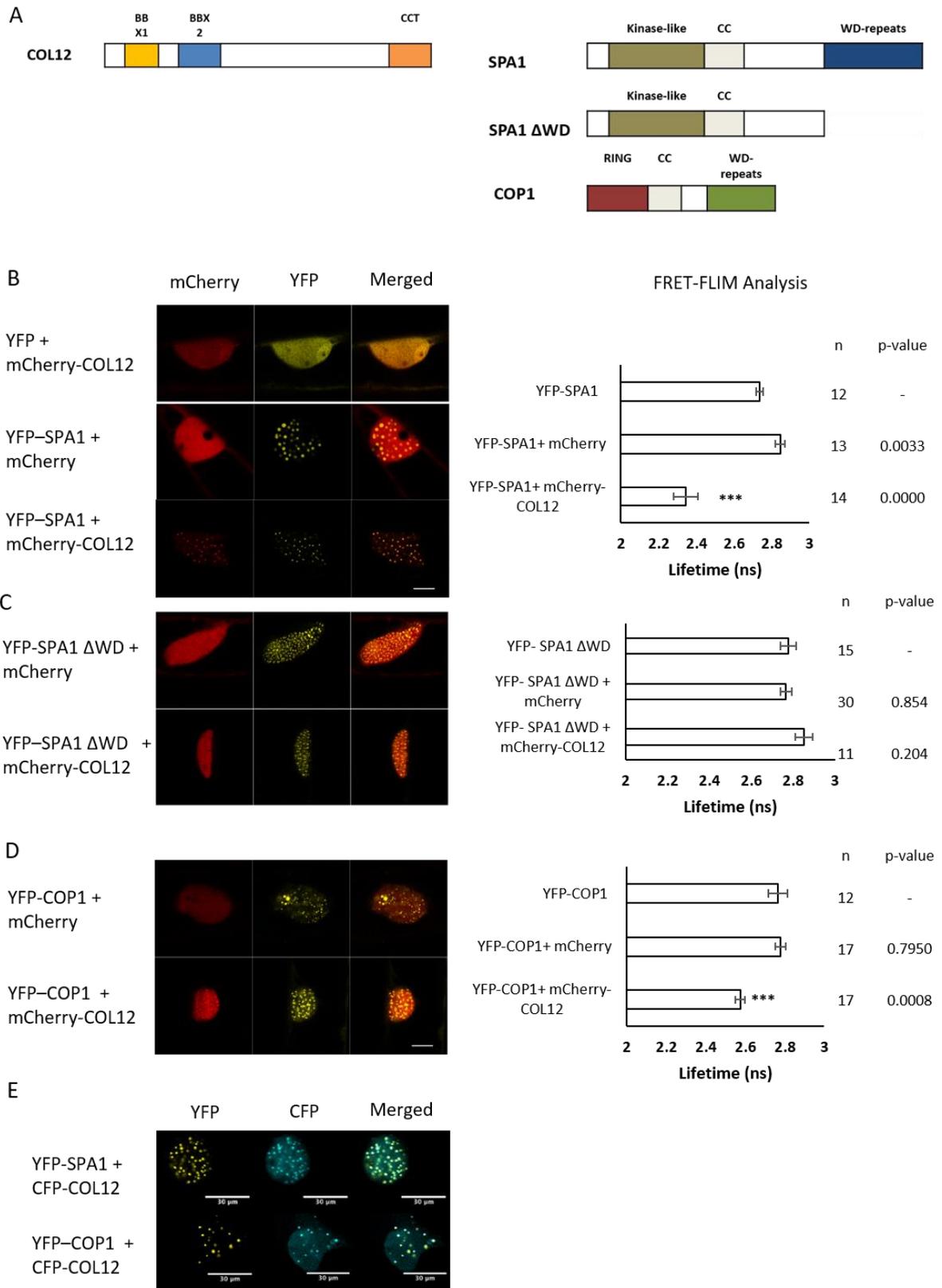
Figure 5. COL12 localizes into the nuclei and is recruited to nuclear bodies by SPA1 and COP1

(A). Domain structures of full-length COL12, COP1, SPA1 and truncated SPA1 proteins.

(B) to **(E)** Fluorescent tags, mCherry, YFP and CFP, were fused to the coding sequences. Chimeric proteins were co-expressed in leek cells using particle bombardment. Plant cells were imaged using confocal microscopy at the indicated channels and merged using FIJI.

(B) to **(D)** Left, representative confocal images. Scale bar = 10 µm. Right, mean lifetime of the YFP donor measured by FRET-FLIM inside nuclear bodies. Bars show the average lifetime of the donor ± SE. n= number of measured cells. Significant differences between donor alone and donor + acceptor were estimated using t-test analysis and the p-value is reported. Co-localization and FRET-FLIM analysis of **(B)** COL12 with SPA1, **(C)** COL12 and truncated ΔWD SPA1, (D) COL12 and COP1. (Menje, M 2016. Bachelor Thesis).

(E) Co-localization of COL12 with SPA1 and COP1, fused to CFP and YFP tags respectively. Scale bar = 30 µm. (Henschel, M. 2014, Bachelor Thesis)

Finally, experiments were performed using CFP- COL13 and CFP-COL14 with the corresponding YFP-COP1 or YFP-SPA1. Both YFP-COL13 and YFP-COL14 exhibited partial co-localization with CFP-SPA1 (Fig 4C) but nor with CFP-COP1 (data not shown). In conclusion, COL12 distributes thoroughly into the nuclei and is recruited into nuclear speckles by COP1 and SPA1 indicating that the proteins physically interact *in planta*.

Given that COL12 interacts strongly with COP1/SPA members, we decided to investigate this gene in depth. To further monitor whether COL12 can be found in close intramolecular proximity with COP1 or SPA1 proteins *in vivo*, we performed fluorescence resonance energy transfer-fluorescence lifetime imaging microscopy (FRET-FLIM) analysis. The YFP-mCherry FRET pair was selected because the YFP donor has high quantum yield and exhibits a mono-exponential decay (Bajar *et al.*, 2016). Thus, FRET was inferred from differences in the lifetime of the YFP donor in absence or presence of the mCherry acceptor. Interestingly, the lifetime of YFP-SPA1 is significantly reduced by the presence of mCherry-COL12 but not with mCherry alone (Fig 5B) indicating the occurrence of FRET. A statistically significant FRET also occur between YFP-COP1 and mCherry-COL12, (Fig 5D). We corroborated that the reduction in the lifetime for the YFP-SPA1 and mCherry-COL12 is specific for this protein pair by using the truncated SPA1 lacking the WD-repeats domain (SPA1 ΔWD) as a control (Fig 5A). In this case, SPA1 ΔWD retains the localization at nuclear bodies but it fails to recruit mCherry-COL12 to these subcellular regions. The spatial distribution correlates with the lack of changes in the lifetime of the YFP- SPA1 ΔWD donor due to mCherry-COL12 (Fig 5C). In conclusion, the FRET-FLIM experiments provide conclusive evidence that COL12 and COP1/SPA1 physically interact and that the WD-repeats domain of SPA1 is necessary for protein binding.

3.1.3   Domain mapping analysis of COL12 interactions with COP1 and SPA1

To map the interacting domains of COL12 with COP1 and SPA1 we performed co-localization and FRET-FLIM analysis using a series of COL12 deletion proteins (Fig 6A). The following COL12 deletion constructs were created using gene specific primers (Table 9): Lacking the N-terminal BBX1 domain (COL12 Δbbx1), without the BBX2 domain (COL12 Δbbx2) and missing the C-terminal CCT domain (COL12 Δcct). All the constructs harbor an additional nuclear localization signal (NLS) to ensure nuclear

Figure 6. Domain mapping analysis of COL12 interactions with COP1 and SPA1

(A) Representation of COL12 structural domains. COL12 full-length, COL12 Δbbx1, COL12 Δbbx2 and COL12 Δcct.

(B) to **(D)** Co-localization and FRET-FLIM analysis were performed as in Fig 1. **(B)** Sub-cellular localization of truncated COL12 fused to mCherry and YFP alone as control. **(C)** and **(D)** Left, FRET-FLIM analysis shows the average lifetime of the YFP donor ± SE. n= number of measured cells. p-value reports statistical differences between donor alone and donor + acceptor, estimated using t-test analysis. Right, representative confocal images with scale bar = 10 μm. Co-localization and FRET-FLIM analysis of truncated COL12 with **(C)** SPA1 and **(D)** COP1. (Menje, M 2016. Bachelor Thesis)

import. Truncated COL12 were fused to N-terminal mCherry tag and expressed in presence of YFP only to assess its sub-cellular localization. COL12 Δcct retains nuclear localization throughout the nuclei whereas COL12 Δbbx1 and COL12 Δbbx2 localize into protein aggregates inside the nuclei (Fig 6B). Subsequently, full-length and truncated COL12 chimeric proteins were co-expressed with either YFP-SPA1 or YFP-COP1 to assess co-localization and FRET-FLIM. Importantly, mCherry-COL12 Δcct lost the ability to mobilize to NB by the presence of YFP-COP1 (Fig 6C). Conversely, mCherry- COL12 Δbbx1 and mCherry-COL12 Δbbx2 co-localize with YFP-COP1 into nuclear aggregates leading to a significant reduction in the YFP donor lifetime (Fig 6C). Hence, the COP1-interacting motif of COL12 resides in the CCT domain and the B-boxes might prevent the exposure of the interaction determinants. In parallel, YFP-SPA1 is still able to recruit the three deletion proteins into co-localizing NB (Fig 6D). In the FRET FLIM analysis with SPA1, mCherry-COL12 Δbbx2 and mCherry-COL12 Δcct lead to a significant reduction in the lifetime of YFP-SPA1 when compared to the control. The truncated ΔBBX1 COL12 display a lower lifetime than YFP-SPA1 alone, albeit it is not significantly different. Thus, the BBX1 might contain determinants that are necessary for the interaction with SPA1. The decreased FRET efficiency in mCherry-COL12 Δbbx2 and mCherry-COL12 Δcct might be due to the presence of interaction determinants that contribute cooperatively to the interaction.

3.1.4 COL12 protein stability is regulated by light

To monitor changes in COL12 protein stability we generated *35S::HA-COL12* transgenic lines and used T3 generation seedlings to monitor protein levels by immunoblot using an anti-HA antibody. The COL12 protein is not solubilized by commonly used protein preparation buffers such as Yoda buffer. Therefore, we employed a previously described protein preparation protocol that enriches the nuclear fraction using a mild buffer supplied with protease inhibitors (Farrona *et al.*, 2011). The COL12 protein contains 364 amino acids and has a predicted molecular size of 40.5 kDa; it is recognized by the HA antibody as a single band (Fig 7) or as a double band (Fig 14) that migrates at approximately 50 kDa in SDS-PAGE gels. In most of the western blot experiments, the 50 kDa protein band is absent from the WT sample, used as a control. However, when some blots were highly exposed, we detected one unspecific signal that migrates at a similar position as the HA-COL12 signal. The appearance of a specific double band may correspond to phosphorylated and unphosphorylated forms of COL12 that can be detected in higher percentage SDS-PAGE gels (15%). It has been reported that CO protein is subjected to phosphorylation and that the phosphorylated form is the preferred substrate for degradation by E3 ligases (Sarid-Krebs *et al.*, 2015).

The action of the COP1/SPA complex leads to protein destabilization of its substrates, particularly in darkness since light strongly inactivates its function (Lau and Deng, 2012). To test if light controls the accumulation of COL12 protein, switch experiments were performed growing seedlings under continuous white light (Wc) and either keeping them exposed to light (L) or transferring them into complete darkness (D) for 24 hours. Dramatic changes in the COL12 protein levels occur in response to the light treatments; COL12 can accumulate in the light and is labile in the darkness (Fig 7A and Fig S3). We performed a time-course experiment to monitor how fast the changes in protein levels can be observed. The time-course reveals that within 16 hours after switching lights off, more than 90% of COL12 protein disappears (Fig 7B).

Selective degradation of ubiquitinated proteins is achieved by the action of the 26S proteasome. To test whether the 26S proteasome is implicated in COL12 degradation, we used a pharmacological approach treating seedlings with or without the proteasome inhibitor MG132 at a concentration of 50 µM. The chemical was supplied to the liquid medium where it can be absorbed by the roots and transported throughout the plant body by bulk flow (Kim *et al.*, 2013). After 4 hours of incubation, plants were exposed to differential light conditions (L or D) and COL12 protein levels monitored by immunoblot. In the dark condition, the degradation of COL12 is overcome by treatment with MG132 and to a little extent the proteasome inhibitor also stabilizes the protein in the light condition (Fig 8). These data demonstrate that COL12 undergoes selective degradation by the 26S proteasome predominantly when seedlings are in the dark and minor degradation might occur in the light.

A

35S::HA-COL12 # 16 - 8				WT	
L		D		L	D
Rep 1	Rep 2	Rep 1	Rep 2		

HA-COL12

Histone 3

B

WT	35S::HA-COL12 #16					
	0	2	4	7	16	**Hours after transfer to darkness**

HA-COL12

Histone 3
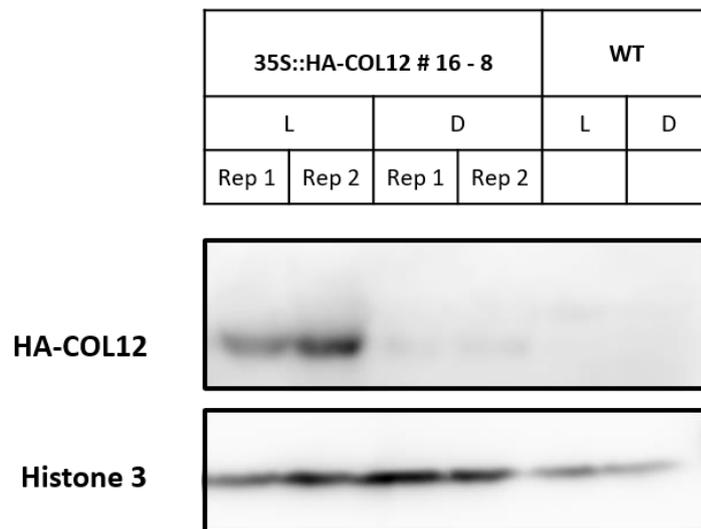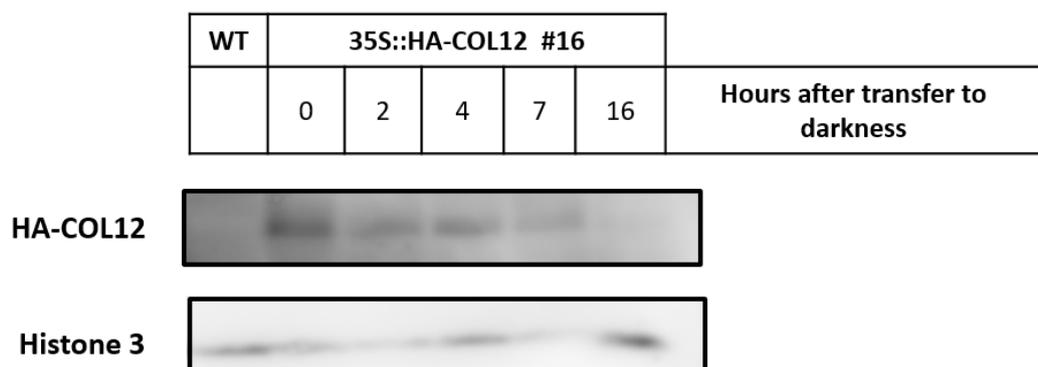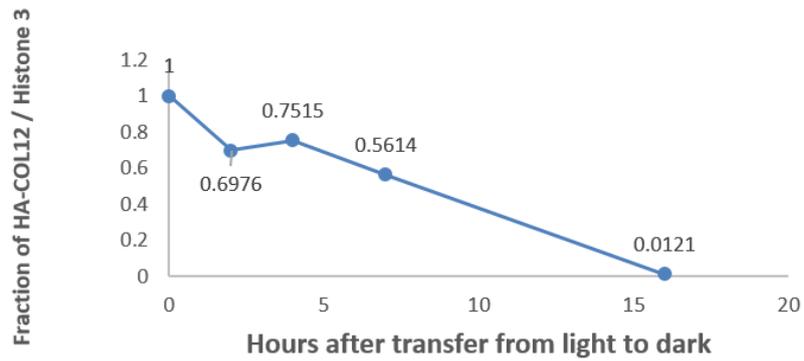
Figure 7. COL12 protein stability is regulated by the light

(A) and **(B)** Immunoblot analyses display the accumulation of COL12 in seedlings in response to light treatments. T3 *35S::HA-COL12* seedlings were grown on MS for 10 days under continuous white light (80 µmol m^{-2} s^{-1}) and either kept in light (L) or switched to complete darkness (D). Nuclear proteins were prepared as described in Materials and Methods and resolved in a 12.5% Acrylamide gel. **(A)** Seedlings were exposed to L or D for 24 hours. Blot shows the result for two biological replicates (Rep), the experiment was repeated at least three times. **(B)** Time-course analysis of the degradation of COL12 upon transfer from light to darkness for different numbers of hours. Relative protein amount was quantified as HA/UBQ10, performed with FIJI.

35S::HA-COL12				
L	L	D	D	**Light treatment**
-	+	-	+	**MG132**
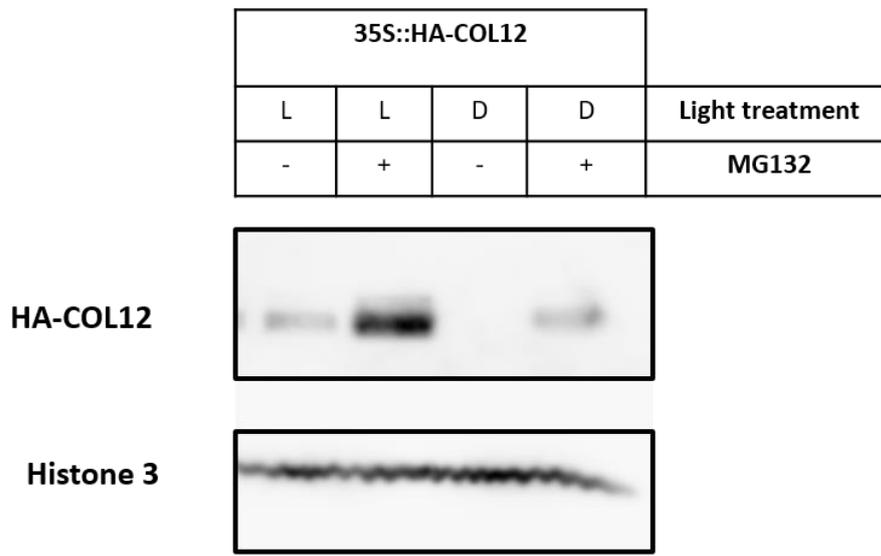
Figure 8. COL12 is degraded by the 26S-proteasome.

Assessment of COL12 accumulation under different light conditions when the 26S proteasome activity was blocked by treatment with MG132 (50µM) or remained active. Seedlings were grown on solid MS for 16 days under continuous white light. Then, they were transferred to either water with MG132 (50uM) (+) or water with DMSO (-). Seedlings were incubated with the chemical for 4 hours under growing conditions. Subsequently, the seedlings were transferred to dark (D) or kept under the light (L) for 14 hours. Protein was extracted as described in Materials and Methods. The experiment was repeated three times with similar results.

3.1.5   The COL12 degradation is dependent on COP1/SPA

The COP1/SPA complex is the main E3 ligase that regulates protein stability in response to darkness (Lau and Deng, 2012). To investigate whether COP1/SPA is the E3 ligase responsible for the destabilization of COL12, *35S::HA-COL12* plants (line #8) were crossed with the *cop1-4* mutant and HA-COL12 protein accumulation was determined. Upon transfer to darkness, COL12 is effectively degraded in the WT background whereas destabilization does not occur in the *cop1-4* background (Fig 9). This experiment clearly demonstrates that the degradation of HA-COL12 is COP1-dependent and thus likely mediated by the COP1/SPA E3 ligase.

35S::HA-COL12 #8				
cop1-4		WT		Background
L	D	L	D	Light treatment
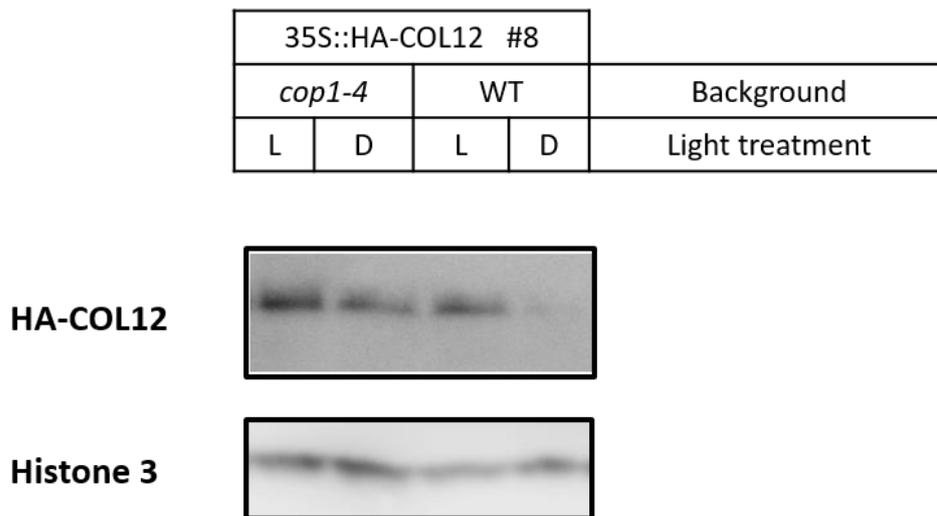
Figure 9. COP1 controls the protein stability of COL12

Immunoblot displays COL12 accumulation in *cop1-4* and WT plants carrying the *35S::HA-COL12* transgene. 10 days-old seedlings were grown on MS media and placed under continuous white light, then were either kept under the light (L) or switched to darkness (D) for 14 hours. Proteins were prepared and separated in acrylamide gels (15%) and detected with HA and Histone3 antibodies. A representative experiment is shown from 3 repetitions, each including different biological replicates.

3.1.6   Functional analysis of COL12 in Arabidopsis

The functional role of many COLs is completely unknown; hence this study aims to uncover new aspects of COL12 function. The genetic analysis started by overexpressing the coding sequences of *COL9*, *COL10*, *COL11*, *COL12* and *COL15* under the constitutive *CaMV 35S* promoter, fused to an HA tag (pEarlyGate 201). The T1 offspring was subjected to selection by Basta, then 10 - 15 resistant plants were recovered, grown to maturation, and selfed. The number of transgene insertions was estimated by analyzing the ratio of T2 Basta resistant/ Basta susceptible (Basta^r/Basta^s) seedlings, the lines that exhibited a 3:1 ratio were selected for further analysis. T2 Basta^r plants were selfed and the T3 homozygous progeny selected based on Basta^r/Basta^s. Strikingly, several T1 *35S::HA-COL12* (COL12 ox) Basta^r plants already exhibited a delayed

flowering time compared to WT under greenhouse conditions. T1 plants carrying *35S::HA-COL9* also showed a late flowering phenotype in the greenhouse. T1 Basta[r] plants overexpressing COL10, COL11 and COL15 did not show any obvious phenotypical changes in greenhouse conditions (data not shown). The protein overexpression was confirmed in T2 generation. We could detect HA-COL9, HA-COL12, and HA-COL15 proteins from pooled T2 seedlings (Fig S2), but not HA-COL10 and HA-COL11.

In parallel, mutant lines harboring mutation inside the COL genes were obtained from *Arabidopsis* public seed repositories (The *Arabidopsis* Information Resource (TAIR) and Nottingham Arabidopsis Seed Center (NASC)). The positions of T-DNA insertions were confirmed by PCR followed by product sequencing using primers listed in Table S1. The list of lines experimentally confirmed to contain T-DNA insertions is presented in Table S1. The Sail line N862394 (Sail_318_F05) contains a T-DNA insertion at position 1089 bp after initiation codon (First ATG) of *COL12* genomic sequence, this is located inside the third exon. We named this insertion line *col12-1* and analyzed it in detail (Fig 10A). To corroborate the insertion site, primers flanking the insertion site (COL12.4 qPCR) were employed to amplify cDNA from WT and *col12* plants. The PCR produces an amplicon from the WT cDNA whereas it fails to amplify from *col12* cDNA (Fig 10B). To test whether *col12* is a null allele or it exhibits reduced transcript levels, a qRT-PCR was performed employing primers that target the first exon (COL12.6 qPCR). The quantification shows that the *col12* line produces similar transcript levels than WT and corroborates that independent COL12 ox lines express high mRNA *COL12* levels (Fig 10C). Thus, *col12* encodes a truncated transcript lacking the fourth exon.

Several aspects of the plant phenotype are aberrant in COL12 ox lines. Importantly, in plants growing in long-day conditions *COL12* overexpression leads to a delayed flowering time, reflected in both higher days from seed sowing to bolting and a higher number of leaves at bolting (Fig 10D, 11E and Table S3). The *col12* plants flower at the same time as WT plants (Fig 10E). When flowering- time was measured under short-day conditions, COL12 ox lines and *col12* are not different from WT plants. Since the effects of *COL12* overexpression on flowering time are dependent on the photoperiod, it is likely that *COL12* interferes specifically with the photoperiodic pathway.

Independent COL12 ox lines also exhibit a reduced inflorescence length and a higher number of rosette branches (Fig 11), these effects are independent of the photoperiod. Therefore, *COL12* might act as a positive regulator of branching. To test whether *COL12* interferes broadly with light perception, the sensitivity of the hypocotyl growth to monochromatic wavelengths of light was monitored at different fluence rates. The hypocotyl growth of COL12 ox seedlings was similar as that of the WT in all light conditions (Fig S4). In summary, *COL12* interferes with the flowering time and plant architecture and this is not due to a general defect in light perception.
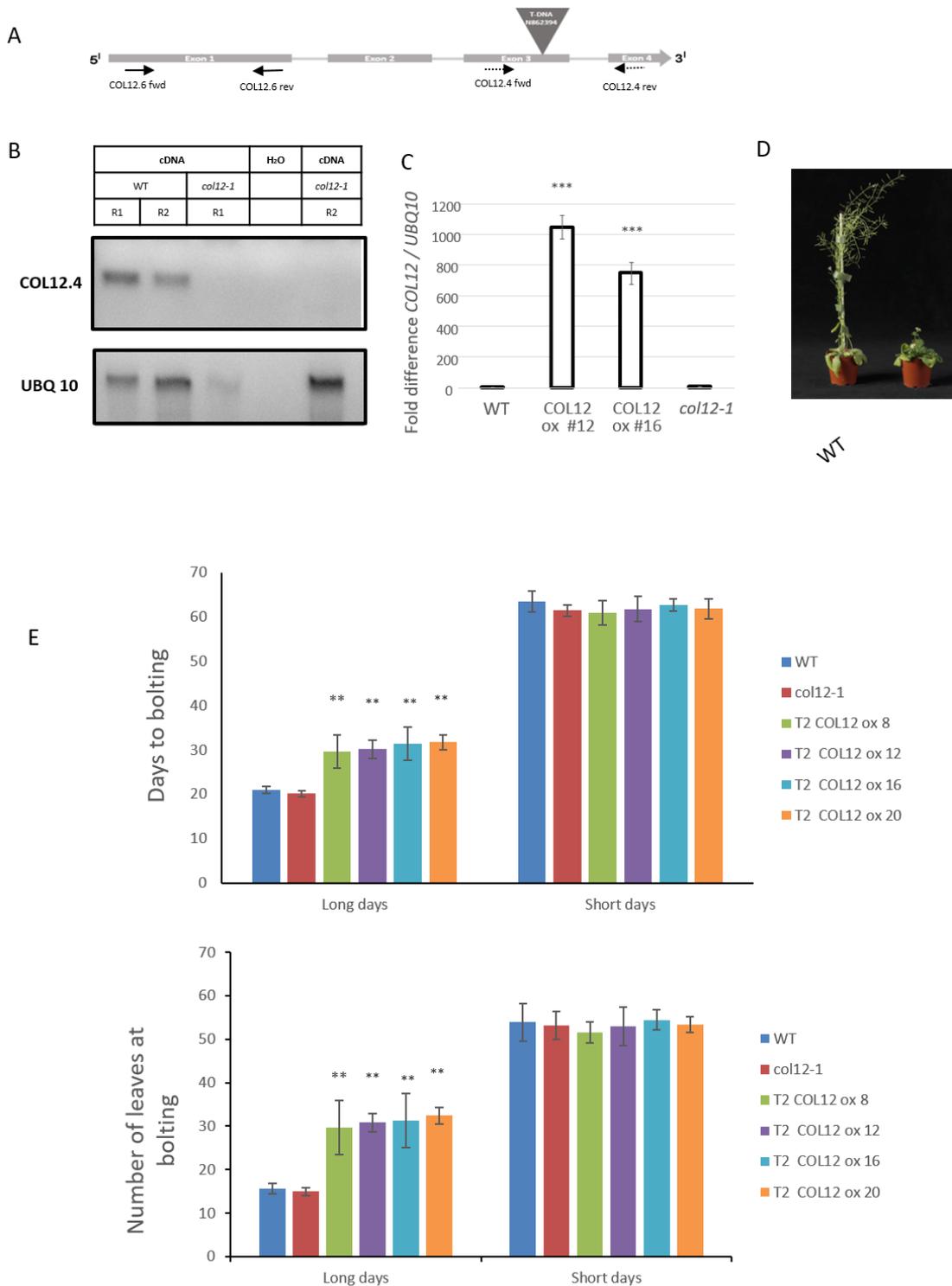
Figure 10. Overexpression of COL12 delays flowering in LD but not in SD

(A) Graphic representation of *COL12* gene indicating the position of the T-DNA insertion in line N862394 (from now on called *col12-1*), continuous arrows denote the position of COL12.6 qPCR primers used to compare the transcript expression of WT and COL12 plants by qRT- PCR. Discontinuous arrows show the position of COL12.4 qPCR primers used to characterize the *col12-1* line.

(B) Molecular characterization of the *col12-1* T-DNA allele using COL12.4 primers that span the *COL12* gene at the position of T-DNA insertion. PCR amplifies cDNA templates from plants of the indicated genotypes and *UBQ10* used as loading control. Two biological replicates were used (R1 and R2) (Trimborn, L. 2015. Bachelor Thesis).

(C) Comparison of relative *COL12* transcript levels in WT, T-DNA line *col12-1* and independent transgenic lines harboring 35S::HA-COL12. Seedlings were grown on soil for under LD conditions for 10 days. Relative transcript levels were measured by qRT-PCR using of COL12.6 qPCR primers and UBQ10 as reference gene (Trimborn, L. 2015. Bachelor Thesis).

(D) WT and COL12-overexpressing plants grown in LD for 45 days.

(E) Flowering time of the indicated genotypes grown in long day or short day. Line numbers indicate independent T2 transgenic lines. Error bars indicate the SE of the mean. Differences between WT and other genotypes were estimated using ANOVA followed by Tukey's Post hoc Tukey test: ****p≤0.0001, ***p≤0.001.
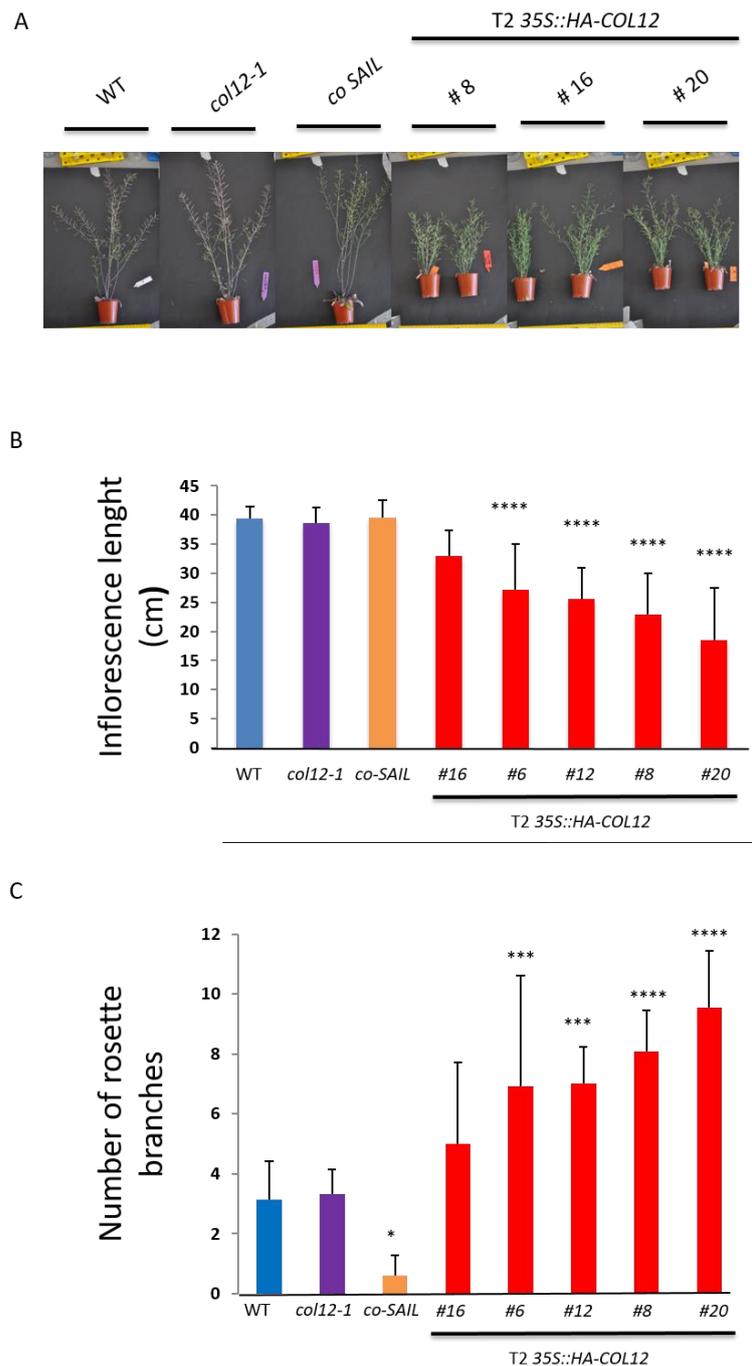
Figure 11. COL12 overexpression led to increased rosette branching and decreased inflorescence length

Plants were grown in LD for 10-weeks, when all the genotypes have stopped growing, the inflorescence length and number of rosette branches measured.

(A) Pictures of 10-week-old plants from different genotypes.

(B) Quantification of inflorescence length (cm). Bars display mean ± Stdev, n= 8 -15. (**** p-value <0.0001, *** p<0.001, *p<0.1 indicating significant differences between WT and denoted genotypes calculated with ANOVA Tukey's Post hoc).

(C) Quantification of rosette branches. Bars display mean ± Stdev, n= 8 -15. (**** p-value <0.0001, *** p<0.001, *p<0.1 indicating significant differences between WT and denoted genotypes calculated with ANOVA Tukey's Post hoc).

3.1.7   COL12 physically interacts with CO

Our experiments revealed that COL12 overexpression causes a significant delay in flowering time in a photoperiod-dependent manner, thus it is expected that *COL12* interferes with the photoperiodic pathway, in which CO acts as a central switch. It has recently been reported that BBX microproteins and BBX19 interact with CO through the B-box conserved domains (Wang *et al.*, 2014, Graeff *et al.*, 2016). Therefore, we hypothesized that COL12 might interact with CO thereby delaying flowering. To test this hypothesis, co-localization and FRET-FLIM analysis were performed using CO-YFP and mCherry-COL12 expressed in *Nicotiana benthamiana*. CO localizes into NB, in contrast to COL12 that distributes throughout the nuclei. When both proteins are co-expressed, COL12 is recruited to the NB (Fig 12A). Concomitantly, the lifetime of CO-YFP drops significantly in presence of mCherry-COL12 indicating the occurrence of FRET (Fig 12A). Confirmation of CO and COL12 interaction *in planta* was conducted by a co-immunoprecipitation experiment in *Nicotiana Benthamiana,* HA-COL12 (pEarlygate 201_*35S::HA-COL12*) was used as bait and CO-YFP as prey (*35S::CO-YFP*) (Fernandez et al., 2016). Immunoprecipitation was performed using anti-HA antibody followed by western blot and immunoblot with GFP and HA antibodies. The CO-YFP is detected in the co-immunoprecipitation fraction when HA-COL12 is present but not in its absence, indicating specific binding of CO to COL12 (Fig 12B). To further validate the interaction, a luminescence-based mammalian interactome (LUMIER) co-immunoprecipitation assay in mammalian cells was conducted. To this end, COL12 was fused to the luciferase coding sequence derived from *Renilla reniformis* (RLuc) and CO to Protein A (ProtA). HEK293TN cells were co-transfected with ProtA and RLuc constructs and total proteins were extracted after incubation for 48 hours. Anti-ProtA magnetic beads were used for immunoprecipitation followed by quantification of luciferase activity. The ratio of RLuc in the immunoprecipitation fraction (IP) to the RLuc in the input fraction was calculated and normalized to the negative control (Rluc + Prot A). The LUMIER experiments show that when using ProtA-CO as bait, the IP fraction is significantly enriched with the prey RLuc-COL12 compared to RLuc alone and the magnitude of the interaction is similar to the positive control RLuc-COP1 (Fig 12C). Altogether the data demonstrate that COL12 physically interacts with CO, both in plants and in the mammalian heterologous system.

To examine the role of the COL12 conserved domains in the interaction with CO, we employed co-localization and FRET-FLIM analysis. Full-length and truncated COL12 versions (COL12 Δbbx1, COL12 Δbbx2, COL12 Δcct and COL12 Δbbx1 bbx2) were transiently co-expressed with CO-YFP in *Nicotiana Benthamiana.* The ability of CO-YFP to recruit COL12 into NB and FRET to occur was

unaffected by the absence of a CCT domain (Fig 13). In contrast, disrupting B-Box1, B-Box2 or the combination reduces the number of cells in which COL12 is recruited into NB and reduces FRET, although CO-YFP still retains the ability to recruit COL12 into NB as observed in some cells (Fig 13). Hence, the CCT of COL12 is not necessary for the interaction with CO whereas the BBX1, BBX2 and the central region might play a redundant role to achieve binding.

A

B

C
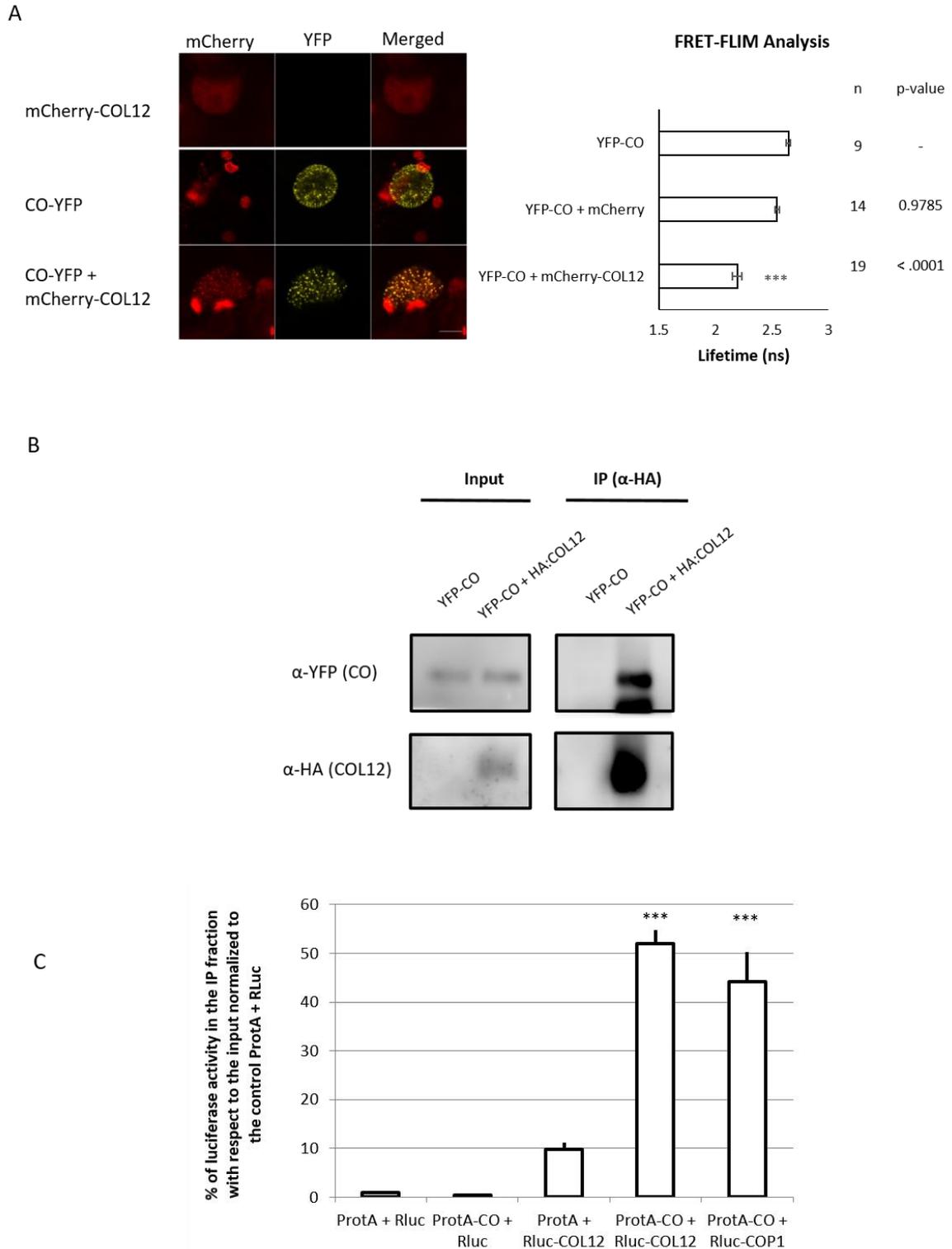
Figure 12. COL12 physically interacts with CO

(A) Co-localization and FLIM-FRET analysis for the interaction between CO and COL12. Fluorescent tags, mCherry and YFP were fused to COL12 and CO respectively. Fused proteins were co-expressed transiently in Tobacco plants (*Nicotiana benthamiana)* using *Agrobacterium* mediated transformation. Infiltrated leaves were imaged with confocal microscopy and lifetime of the CO-YFP donor was measured as described in Materials and methods section. Bars show the mean lifetime of the donor in nanoseconds (ns) ± SE. n= number of measured cells. Significant differences between donor alone and donor + acceptor were estimated using ANOVA followed by Tukey's post hoc analysis and p-value is reported . Scale bar = 5 µm.

(B) CO-YFP is co-pulled down by HA-COL12. *In vivo* co-Immunoprecipitation was performed using anti-HA coupled to magnetic beads on extracts containing only CO-YFP (prey) or CO-YFP + HA-COL12 (prey + bait). Proteins were co-expressed transiently in Tobacco plants (*Nicotiana benthamiana)* using Agrobacterium mediated transformation. The experiment was repeated several times.

(C) Pulldown experiment in mammal cells by LUMIER. COL12 was fused to the *R. reniformis* luciferase (RLuc) and CO to ProtA. Vectors were co-transfected into mammal cell (HEK293TN). Luciferase activity was measured before pulldown in the input fractions and after affinity purification with Dynabeads (magnetic anti-protA). Three experimental replicates were performed. (***p-value <0.001) for the comparison to the control sample ProtA-CO + Rluc, calculated with ANOVA with Tukey's post-hoc.
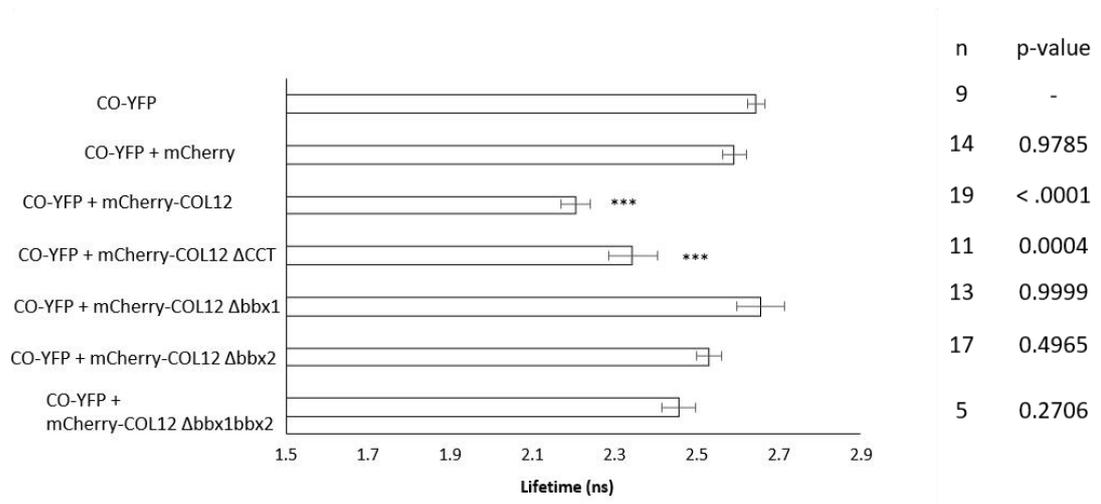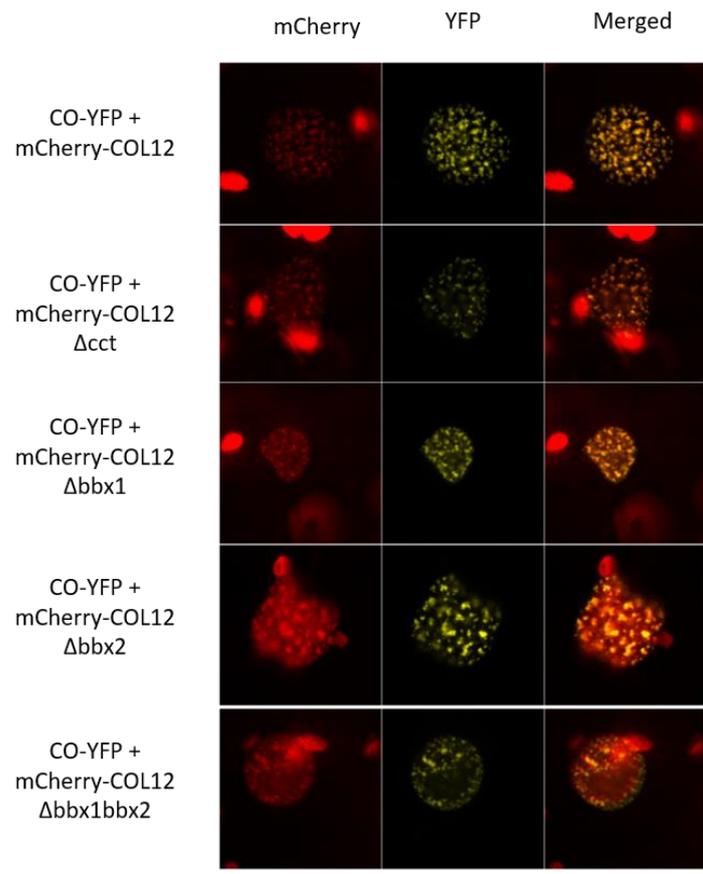
Figure 13. COL12 domain analysis for the interaction with CO

Analysis of the interaction between CO and truncated COL12 proteins by co-localization and FLIM-FRET performed as described in Fig 6.

3.1.8 COL12 does not affect CO protein accumulation at ZT16

Since COL12 associates with both COP1/SPA and CO, one possible mechanism whereby COL12 might interfere with the induction of flowering is to affect the E3 ligase function changing CO

protein stability. To evaluate if COL12 overexpression affects CO protein levels, two independent COL12 ox lines (*35S::HA-COL12*) were crossed with *SUC2::HA-CO co-SAIL* line (Jang *et al.*, 2009) and the levels of both proteins were monitored by immunoblot using anti-HA antibody. Single and double overexpression mutants were grown in LD and harvested at the end of the day (ZT16), the time when the functional activity of CO is maximal. The protein abundance experiment considers biological variability by measuring at least two biological samples in an experimental replicate. HA:CO protein levels in *SUC2::HA-CO* plants are similar to those in *SUC2::HA-CO* x *35S::HA-COL12* plants (Fig 14). Thus, COL12 does not act by interfering with CO accumulation at ZT16.
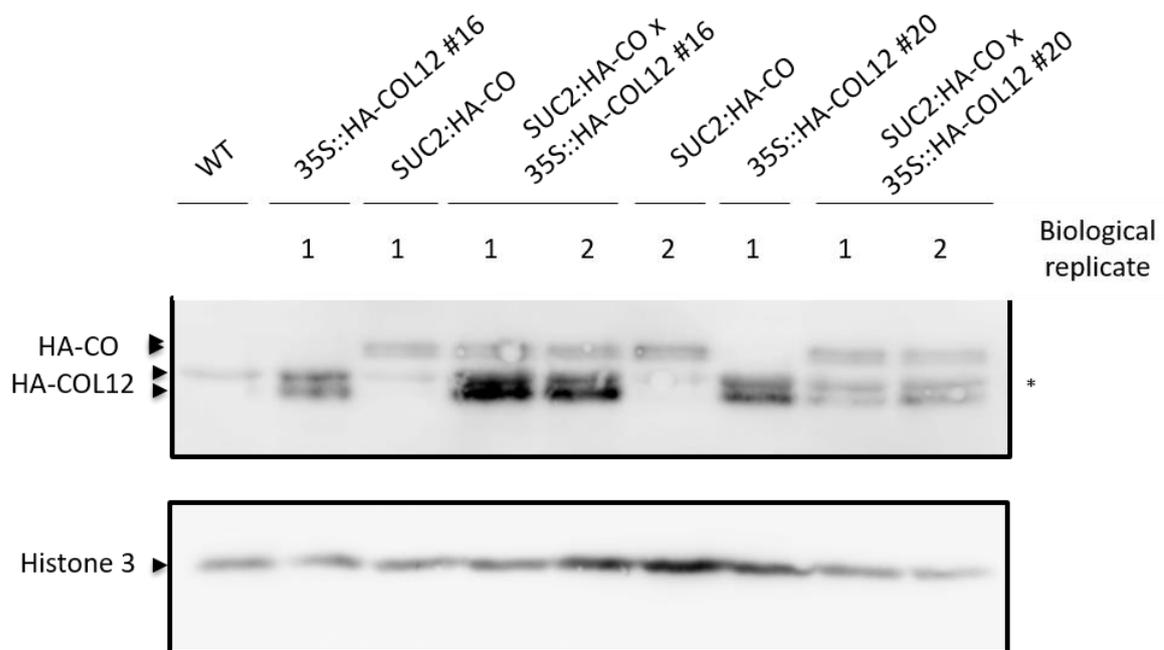
Figure 14. COL12 does not affect CO protein levels

Protein accumulation of HA-CO and HA-COL12 assessed by immunoblot. 10-days-old seedlings growing were grown soil in LD conditions (200 µmol m^{-2} s^{-1}) and tissue was harvested at ZT16. Protein samples prepared as in Material and methods section resolved on 15% acrylamide gels. The following genotypes are compared: WT Col-0, *35S::HA-COL12* (16 and 20), *SUC2::HA-CO* and the double overexpression lines *SUC2::HA-CO* x *35S::HA-COL12* (16 and 20). Blot includes two biological replicates. The experiment was repeated three times with similar results.

3.1.9   COL12 is stabilized by red and blue monochromatic light qualities

The light is the main factor that determines CO accumulation, moreover, specific wavelengths of light exert different effects (Valverde *et al.*, 2004). To elucidate how the different light qualities affect COL12 stability, switch experiments were conducted with treatments applied at low (10 µmol m^{-2} s^{-1}) and very low (1 µmol m^{-2} s^{-1}) fluence rates. Seedlings were grown under continuous

Wc and either kept in Wc or transferred to B, R or D. The protein accumulation was monitored by immunoblot with anti-HA and anti-Histone3 as a loading control. First, it can be observed that in Wc the level of protein accumulation varies with fluence rates; little COL12 protein accumulates in very low Wc and the levels rise in low Wc (Fig 15). Second, in all tested light qualities (B, R, and Wc), COL12 accumulates to higher levels than in darkness (Fig 15). Protein accumulation is higher in B than in Wc whereas there are no dramatic differences between R and Wc treatments. These experiments suggest that COL12 protein is stabilized by B, R, and Wc, contrasting with the stabilizing effects of R in the regulation of CO protein (Valverde *et al.*, 2004).
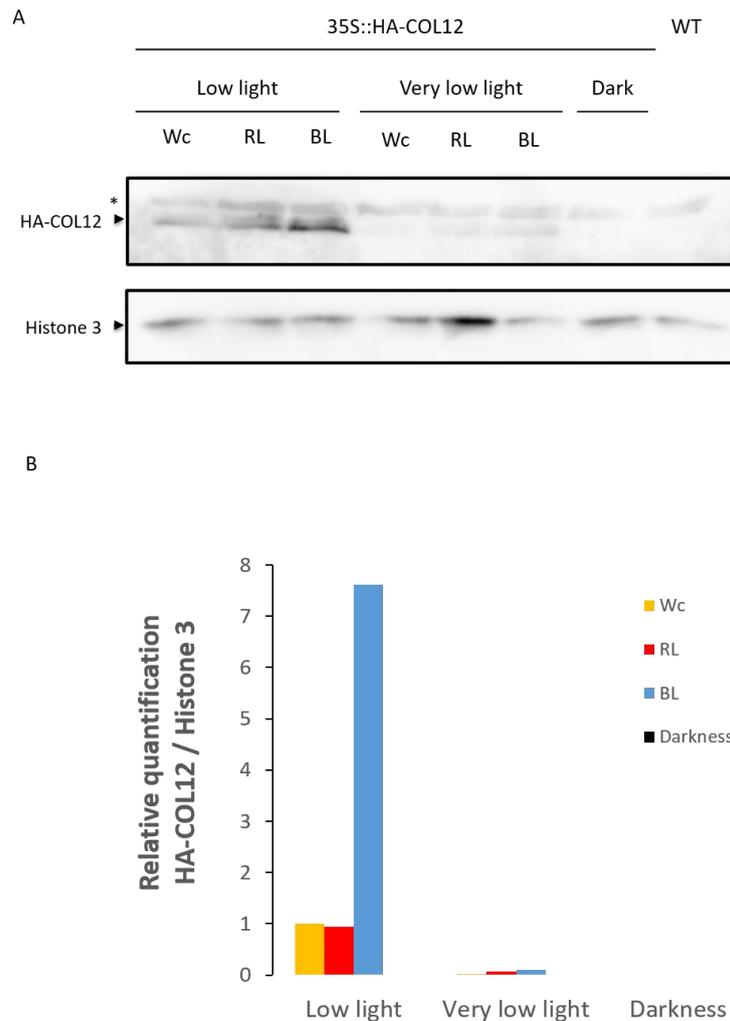
Figure 15. Monochromatic R and B light stabilize COL12 protein

 (A) Immunoblot shows the accumulation of COL12 protein after shifting experiments from White to Monochromatic light. 10-days-old seedlings were grown under constant white light (30 µmol m^{-2} s^{-1}). Then, shifted to low light (10 µmol m^{-2} s^{-1}) or very low light (1 µmol m^{-2} s^{-1}) of the following light qualities: Wc = white light, RL = red light, BL = blue light. * Indicates an unspecific band running at a similar size than HA-COL12. The arrow marks the specific HA-COL12 band. Prepared samples were separated on a 15 % acrylamide gel. Experiment was repeated three times.

(B) Relative protein quantification of HA-COL12 normalized to Histone 3 levels some with FIJI software (Robers, L 2015. Master Report).

3.1.10 Overexpression of COL12 downregulates mRNA levels of *FT* but does not alter *CO* mRNA levels

After establishing that COL12 interacts with CO, we aimed to elucidate whether COL12 plays a role in the transcriptional control of the main *Arabidopsis* floral transition regulators. We compared the transcript abundance of *CO*, *FT*, *SVP*, *SOC1*, *FLC* and *FUL* in the WT and two independent COL12 ox lines. Plants were grown under inductive photoperiod for 12 days and total rosette tissue harvested at ZT16, this is the developmental stage when important flowering induction events occur. Interestingly, overexpression of COL12 results in a significant reduction of *FT* transcript levels in both lines tested. On the other side, *CO* levels are unmodified by COL12 action. The transcriptional levels of the other aforementioned floral regulator genes were also not significantly affected by COL12 ox (Fig 16).

The timing of *CO* and *FT* mRNA expression is an essential component of the photoperiodic mechanism. Therefore, we examined the transcript abundance of *CO* and *FT* through the day in WT and COL12 ox lines growing in LD. In WT samples, *FT* expression raises from ZT12 to peak at dusk (ZT16), as expected. *FT* circadian pattern was unaffected by COL12, but the magnitude of the peak of expression in the end of the day (ZT16) and expression in the morning (ZT4) were significantly reduced in COL12 ox lines compared to WT (Fig 17). The *CO* expression in the WT is low in the morning hours (ZT 4-8) and rises to moderate levels at midday (ZT12) keeping high expression during the night until the beginning of the next day (ZT0). Both the circadian oscillation and the amplitude of *CO* mRNA expression were unaltered by COL12 (Fig 17). Subsequently, we examined whether the *COL12* mRNA expression oscillates through the day in WT plants grown in LD. There are no significant differences in the levels of *COL12* expression among the different time points of the day, despite a slight but no statistically significant increase of expression at midday (Fig 18). In summary, COL12 downregulates *FT* levels at the critical point of the day (ZT16) which positively correlates with the late-flowering of the overexpression lines.
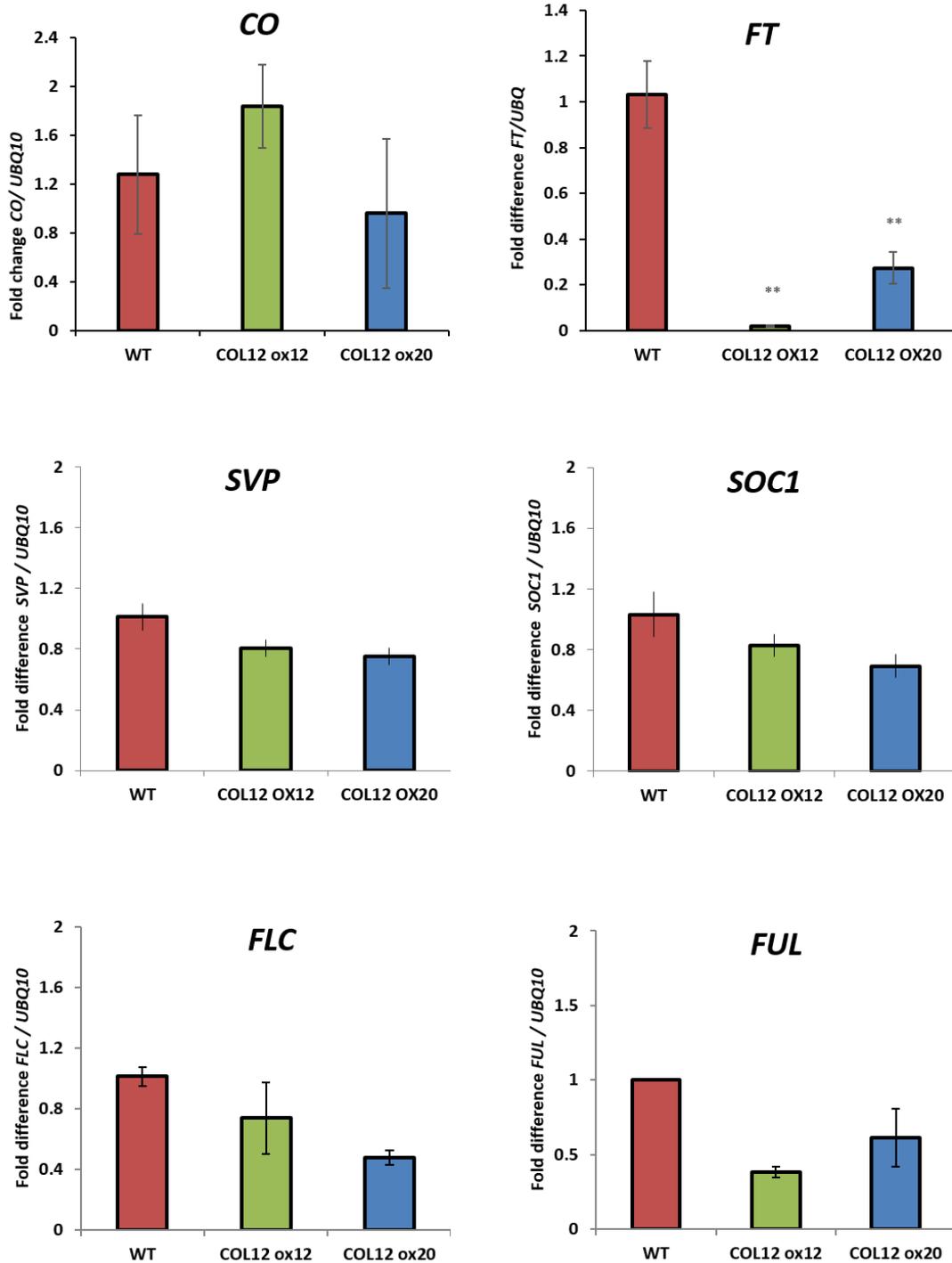
Figure 16. COL12 downregulates the mRNA expression of *FT* but not of other floral regulators

Changes in gene expression of main floral regulators tested by qRT-PCR. Two independent COL12 ox lines were compared to WT. 12 days-old seedlings growing in LD conditions, with a white light intensity of 200 µmol m^{-2} s^{-1}, were harvested at ZT16. Bars show the average fold change relative to *UBQ10* of 2 to 4 biological replicates ± SE. (** p value< 0,005). Three technical replicates on the plate were performed (Trimborn, L 2015. Bachelor Thesis).
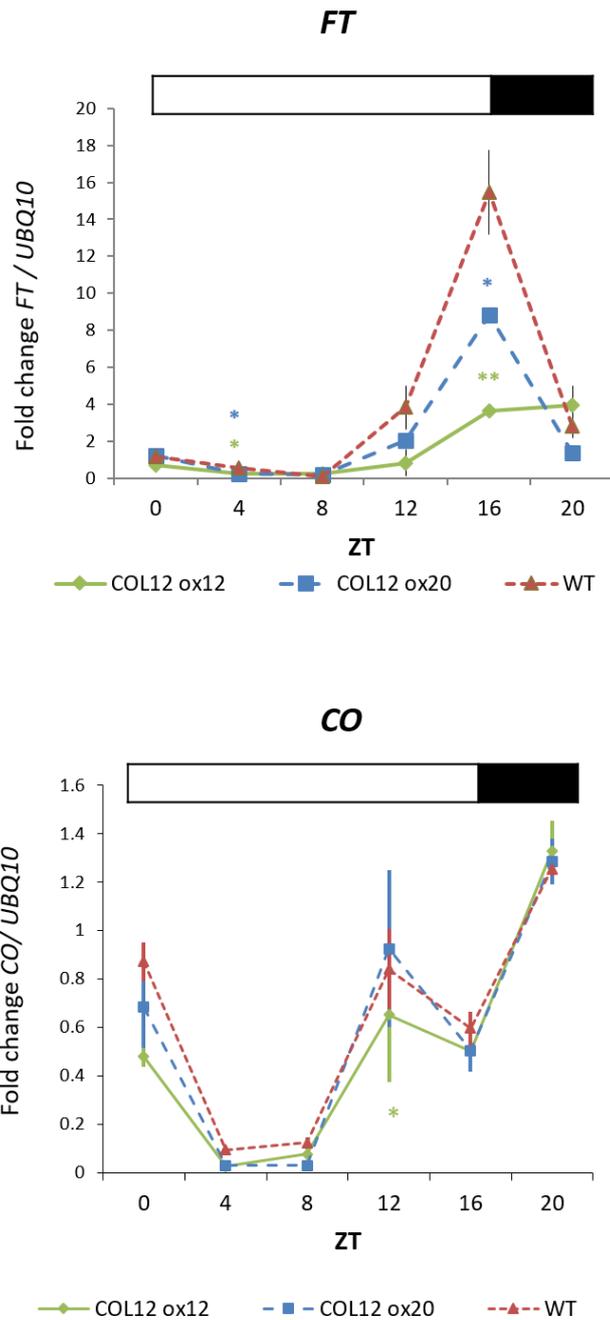
Figure 17. Overexpression of COL12 downregulates *FT* at ZT4 and ZT16 but does not alter *CO*

COL12 effects in *FT* and *CO* mRNA expression along the day, tissue samples from WT and two independent COL12 ox lines were harvested every four hours. Seedlings were grown on soil for 12 days in LD. Quantification was performed by qRT-PCR calculating the average fold change relative to *UBQ10* from 2 to 3 biological replicates ± SE. (* p value< 0,05, ** p value< 0,005 ANOVA with Tukey's post-hoc relative to ZT0). The experiment was repeated twice with similar results. (Trimborn, L 2015. Bachelor Thesis).
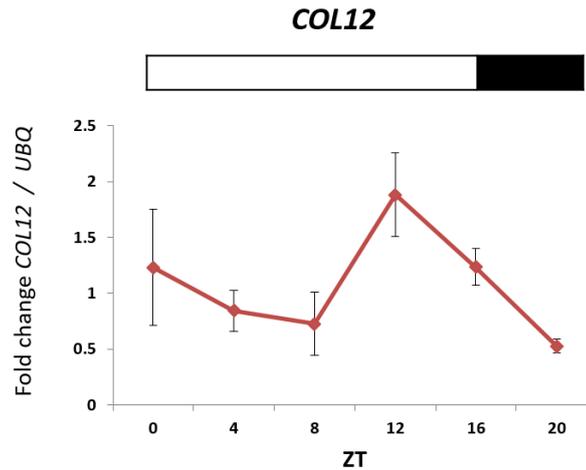
Figure 18. *COL12* **mRNA levels do not fluctuate along the day**

COL12 mRNA expression measured along the day by qRT-PCR. Experiment performed as in Fig 16. No significant changes in gene expression among ZTs were detected by ANOVA with Tukey's post-hoc. The experiment was repeated twice with a similar result.

3.1.11 Developmental time course of COL12 transcriptional expression

Understanding a gene function in plants also involves the analysis of tissue and developmental patterns of expression. With this purpose, we collected RNA samples at different stages of development and from different plant organs and analyzed the abundance of *COL12* and *COL11* transcripts. *COL11* was included, because it is the closest *COL12* homologous gene that might exhibit functional redundancy with *COL12*. The quantitative analysis shows that *COL12* transcripts are produced from early seedling development (5-days-old) and accumulate at similar levels throughout vegetative development (11 and 15 days-old). At reproductive stage, *COL12* expression increases in flowers and flower buds. In these organs, *COL11* transcript levels are also at maximum whereas its expression is undetectable in the vegetative samples and inflorescence stems (Fig 19).
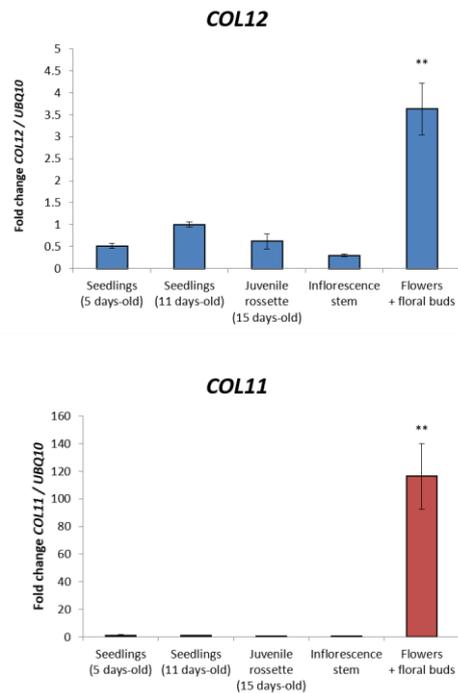
Figure 19. *COL12* **mRNA is expressed through vegetative development and increases in flowers and floral buds**

Tissue was harvested WT plants growing on LD at different points through development. 2-3 Biological replicates per experiment. mRNA expression of *COL12* and *COL11* was measured by qRT-PCR and statistical analysis performed with ANOVA post-hoc Tukey (** p value< 0,005). The experiment was repeated twice with similar results.

3.1.12 Genetic analysis of the interactions between COL12 and CO – FT

Our molecular analyses suggest that COL12 protein binds to CO and downregulates the expression levels of *FT* mRNA. We then performed genetic analysis to clarify the genetic interactions between the genes. The COL12 ox lines were crossed with *SUC::HA-CO* line, to obtain plants that express both genes at high levels, and flowering time was assessed. Protein expression was confirmed and analyzed in section 4.1.8 (Fig 14). As expected, plants that overexpress *CO* flower extremely early with an average of 4.13 leaves at bolting and COL12 ox significantly delays the flowering to 5.33 leaves (p-value 0.0024) (Fig 20A). This result indicates that COL12 counteracts the action of CO protein exerting an antagonizing role. Then we tested if *COL12* acts exclusively via *CO* and *FT* by obtaining the COL12 ox in the *co_SAIL (co_10)* (Laubinger *et al.*, 2006) and *ft-10* (Yoo *et al.*, 2005) mutant backgrounds, referred here as *co* and *ft* respectively. The flowering time of the *co* COL12 ox lines is not significantly different than that of the *co* single mutant. In a similar way, the *ft* COL12 ox lines flower as late as *ft* mutant plants (Fig 20B). The fact that COL12 ox does not exert additive effects on the already late flowering of *co* and *ft* indicates that *COL12* operates through the *CO - FT* module and does not interfere with other genetic pathways.

The genetic interactions of *COL12* with *CO* and *FT* in the control of inflorescence length and rosette branching were also analyzed. For plants grown in LD and measured at the end of

development, both *co* and *ft* mutants have a significantly lower number of rosette branches than the WT Col-0 plants. In contrast, COL12 ox plants develop more rosette branches than WT (Fig 21). The *co* COL12 ox lines exhibit high rosette branching, similar to the single COL12 ox lines. The *ft* COL12 ox double mutant develops few branches, resembling the single *ft* mutant. This analysis suggests that *FT* is required for *COL12* to modify rosette branching whereas *CO* is unnecessary. Alternatively, the result can also be explained by silencing of COL12 ox transgene in the double *ft* COL12 ox lines. We tested the latter hypothesis by performing protein extraction and immunoblot, replicated only once. COL12 protein levels in *ft* COL12 ox are lower than in COL12 ox (Fig S5), however, the lines are not completely silenced. The inflorescence length phenotype was also assessed in single and double mutant lines. COL12 ox are dwarfed, exhibiting significantly shorter inflorescences than WT. The *co* COL12 ox mutants are as dwarfed as COL12 ox, reflecting that this action of *COL12* is independent of *CO* (Fig 21). In the case of *FT* analysis, double mutants *ft* COL12 ox inflorescences grow as tall as single *ft.* This can be explained by an *FT*-dependent action of COL12 or transgene silencing as explained above.

A

Number of leaves at bolting

	Avg	StDev	n	P-value
SUC2:HA-CO	4.13	0.35	15	
SUC2:HA-CO x COL12 ox 16	5.33	0.90	15	0.0024

SUC2:HA-CO

SUC2:HA-CO
X
COL12 ox16

B
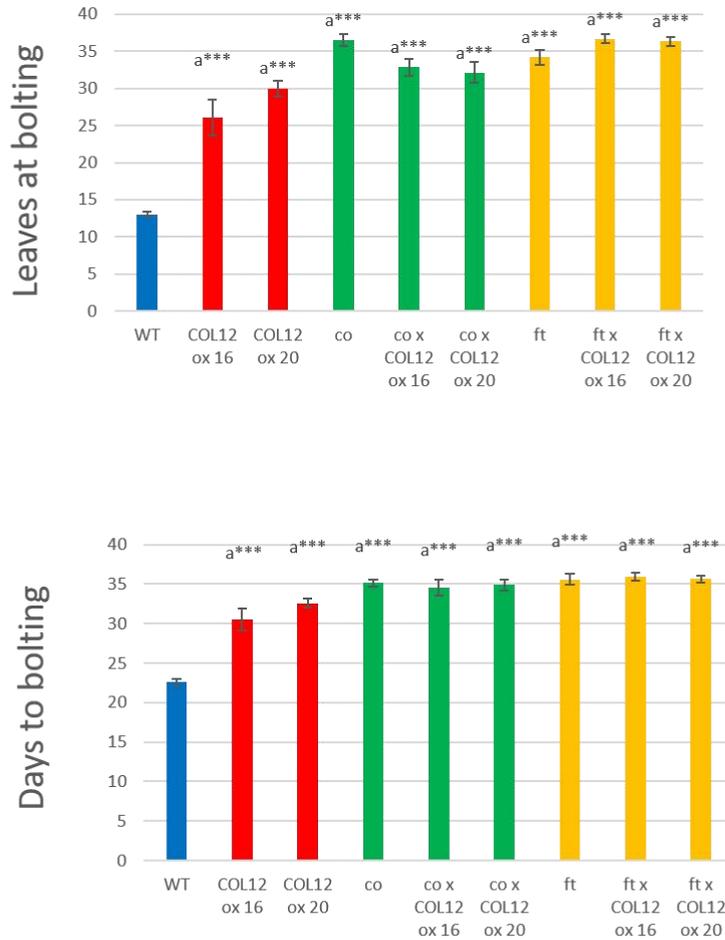
Figure 20. Genetic interactions of COL12 with CO and FT in the control of flowering time

(A) Overexpression of COL12 delays flowering of *SUC2::HA-CO* plants. Picture of 16-days-old plants grown on LD and quantification of the number of leaves at bolting. The quantification was performed once.

(B) COL12 acts exclusively through CO and FT to delay flowering time in LD. Flowering time of single and double mutant plants grown in LD, scored as days from seed sowing to bolting and number of leaves at bolting. Bars denote average ± SE (n= 8 – 16). Statistically significant differences tested by ANOVA one way with Tukey's post hoc: Groups were compared to the reference WT =a, *co* single = b and *ft* = c single mutants. (*** = p <0.001).
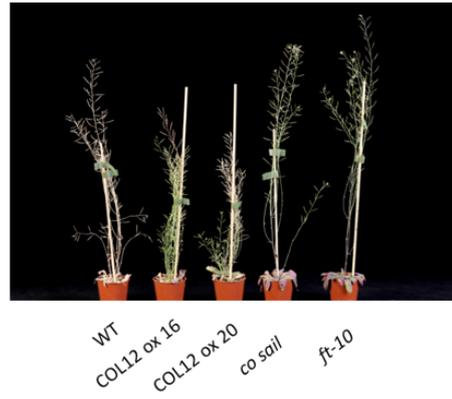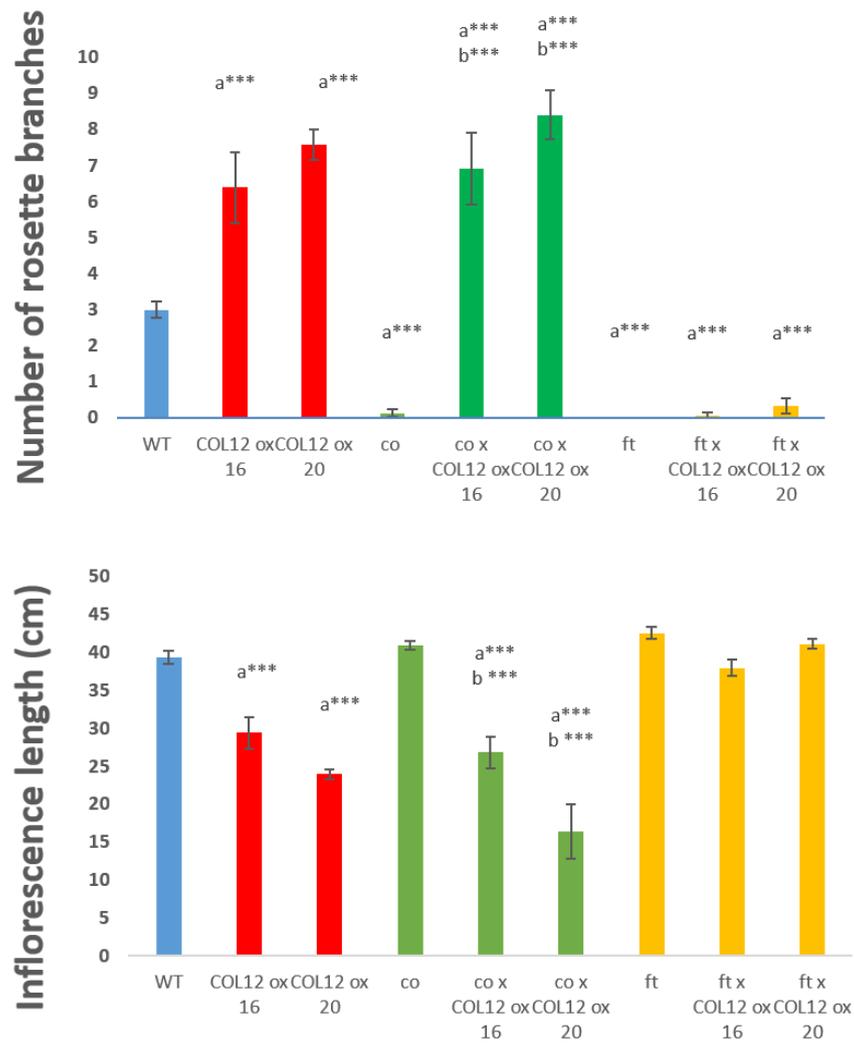
Figure 21. Genetic interactions of COL12 with CO and FT in control of plant architecture

Up, Picture from representative plants of indicated genotypes at full maturity. Middle and low: Number of rosette branches and length of inflorescence of single and double mutant plants grown in LD for 10 weeks. Bars denote average ± SE (n= 8 − 16). Statistically significant differences tested by ANOVA one way with Tukey's post hoc: Groups were compared to the reference WT =a, *co* single = b and *ft* = c single mutants. (*** = p <0.001).

3.2 PART II - Co-Action of COP1 and SPA during Arabidopsis post-embryonic development and photomorphogenesis

The COP1 and SPA proteins act in concert to convey light-signals into plant developmental responses. The function of COP1 is crucial for plant survival, as *cop1-5* mutants are unable to survive beyond the seedling stage. In contrast to plants that possess functional COP1 but lack the SPAs*, the spaQn mutant,* survive and complete its life cycle. Indicating that COP1 and the SPAs act partially redundantly. To test if the SPAs can function without COP1 at early developmental stages we isolated the quintuple *spaQn cop1-5* (Fig 22).
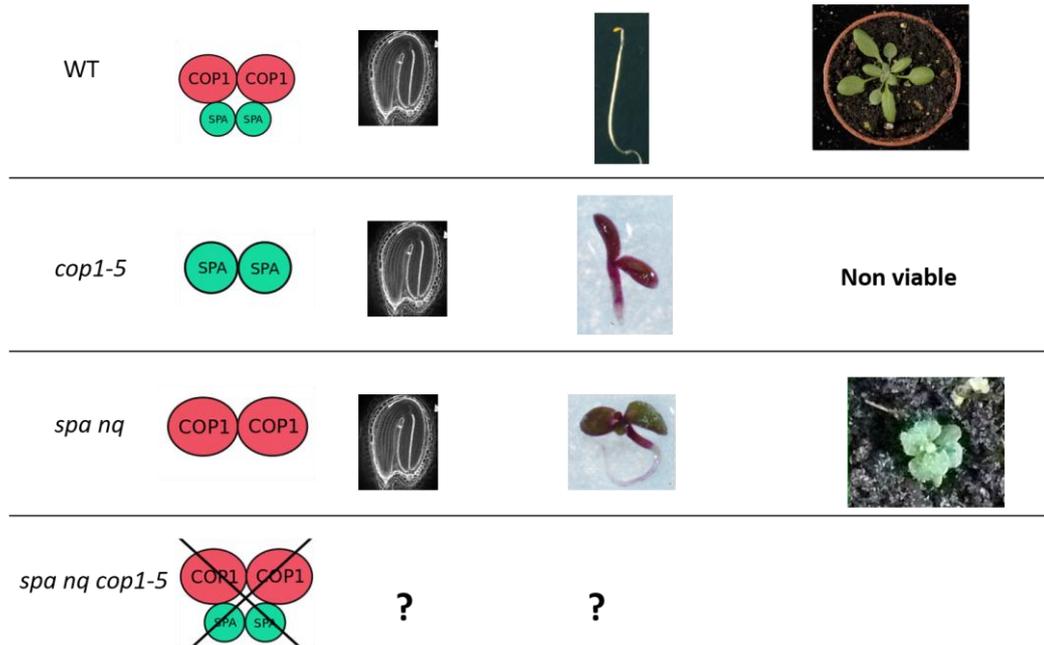
Figure 22. Research question addresses the co-action of COP1/SPA at early developmental phases

The *cop1-5* mutant undergoes normal embryogenesis and develops into a photomorphogenic seedling, afterwards it arrests the development and the adult plants are not viable. In contrast, the *spa* quadruple null mutant is capable for completing its life cycle. To investigate if the COP1/SPA complex is needed for embryo and seedling development we isolated the mutant plant that is devoid in *COP1* and the four members of the *SPA* family.

3.2.1 Design of molecular markers for the *cop1-5 allele*

A screening of a T-DNA mutagenized population for constitutive photomorphogenic seedlings identified the *cop1-5* null allele (Deng *et al.*, 1992). To monitor the presence of this allele by PCR, molecular markers were obtained. The original mutagenesis was performed by inserting the 3850:1003 Ti plasmid into the genome of Arabidopsis (Feldmann and Marks, 1987). This plasmid consists of a dual cassette of neomycin phosphotransferase II gene (NPTII) controlled by the TiAch5 promoter, which confers kanamycin resistance to plants as a selectable marker (Velten and Schell, 1985). A primer pair that amplifies a region that spans a part of the TiAch5 promoter

and the NPTII gene was proved to identify *cop1-5* and not mutant alleles present in *spaQn* (Table8) (Fig 23). In addition, to be able to distinguish *cop1-5* homozygous from heterozygous plants, primers flanking the T-DNA insertion site were generated (Table8). Using these primers, a PCR amplicon is produced from gDNA WT whereas is absent from *cop1-5* (-/-) (Fig 23). Thus, using the new pairs of primers it is possible to monitor the heterozygosity of the *cop1-5* allele.

a)

b)
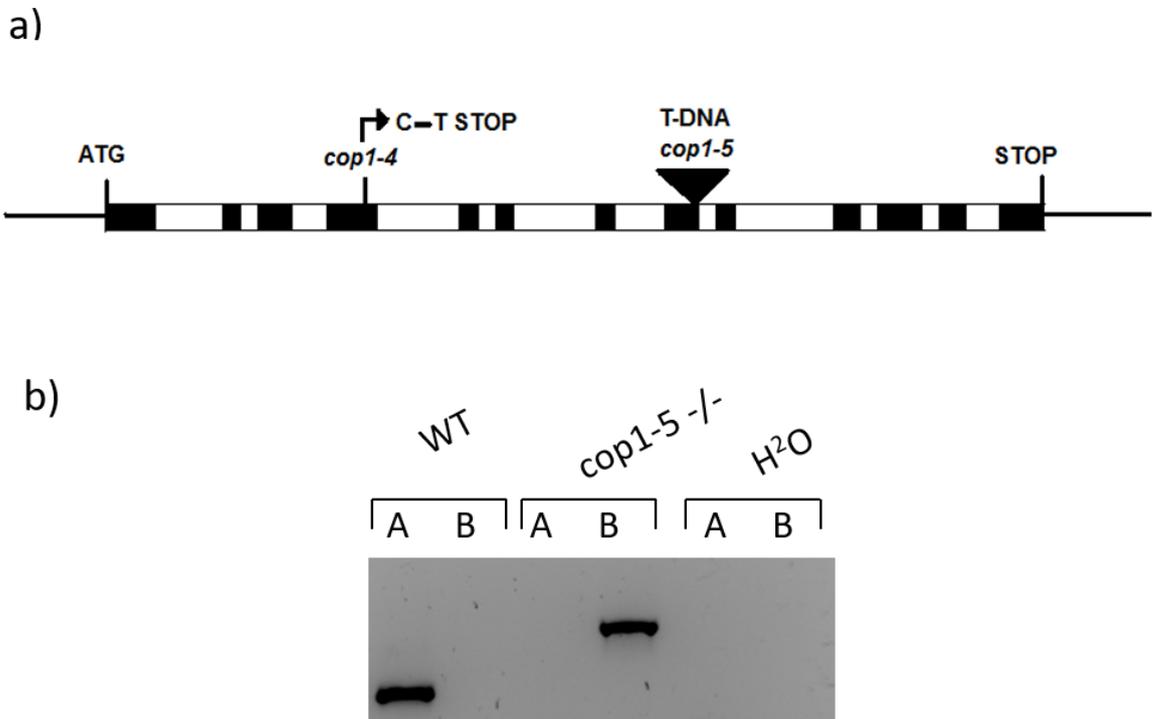
Figure 23. Molecular markers for *COP1* and *cop1-5* alleles

(A) Depiction of *COP1* gene indicating the positions of *cop1-4* and *cop1-5* alleles. Exons are indicated by black boxes.

(B) Molecular markers to distinguish WT from *cop1-5*; A = WT primers (cop1_3534 fwd + cop1_3840 rev, amplicon 302 bp), B= Mutant primers (pTiach5 promoter fwd + Kan2 Rev, amplicon 529 bp).

Lack of *cop1-5* germination is overcome by GA and manual removal of the seed coat

Seedlings that are homozygous for the *cop1-5* mutation do not survive, reflecting the absolute requirement for functional COP1 after the seedling stage. Moreover, *cop1-5* mutant seeds do not germinate under standard growth conditions. The *cop1-5* seeds visibly appear darker than WT seeds, which is indicative of a higher anthocyanin accumulation (Debeaujon *et al.*, 2000). The high concentration of pigments in the seed coats can limit water permeability and might impose a higher barrier for the induction of germination (Debeaujon and Koornneef, 2000). During seed germination, the phytohormone GA promotes the breakage of the resistance imposed by the seed envelopes facilitating the protrusion of the embryo radicle (Debeaujon and Koornneef, 2000). We attempted to rescue the non-germination phenotype of *cop1-5* seeds by adding exogenous GA to the MS medium at a concentration of 50 µM. The germination rate of *cop1-5* increased from 0% in media without GA to 18% with GA (Fig S6). The GA biosynthesis mutant *ga1-1* can be also rescued by manual removal of the seed envelopes (Debeaujon and Koornneef, 2000). This approach has the advantage that it preserves the natural growth of the plants from the treatment with exogenous hormones. We observed that manually removing the seed coats

effectively relieves the *cop1-5* germination constraints because following this procedure most of the embryos grew until the seedling stage. Therefore, this technical step was implemented into the subsequent comparative experiments.

3.2.2 The quintuple mutant *spaQn cop1-5* completes embryogenesis

To generate the quintuple mutant *spaQn cop1-5,* we first isolated the double segregating *spa123(-/-) spa4 (+/-) cop1-5 (+/-)* as described in the *Materials and Methods* section. These plants are able to grow and produce seeds. Then, the plants were selfed and the resulting progeny was subjected to genetic analysis on individual basis. Among the seeds from segregating progeny it was possible to distinguish three different types of seeds according to its pigmentation: Yellow, light brown and dark brown (Fig S7). After seed dissection and molecular genotyping, it was observed that the dark brown coloration of the seeds cosegregates with the *spaQn cop1-5 (-/-)* genotype. Importantly, this quintuple mutant grows until the cotyledon stage resembling the single *cop1-5* both in darkness and light (Fig 24). Therefore, the data demonstrate that the COP1/SPA complex in not necessary for embryogenesis. Furthermore, it shows that the *SPAs* do not act independently of *COP1*. The only detectable phenotypical difference is that the quintuple *spaQn cop1-5* seedlings appeared darker than *cop1-5* and *spqQn* mutants, indicative of higher pigment accumulation. Therefore, the anthocyanin contents were measured taking the same amount of seedlings for each sample. The colorimetric quantification shows that the *spaQn cop1-5* accumulates significantly higher levels of anthocyanins than the *cop1-5* and *spqQn* mutants (Fig 25). This suggests a possible COP1-independent function of SPA proteins in anthocyanin accumulation. However, since the *cop1-5* and the *spaQn* alleles were derived from different Arabidopsis accessions, we cannot exclude the possibility that these differences are due to the mixed genetic background in the quintuple null mutant.
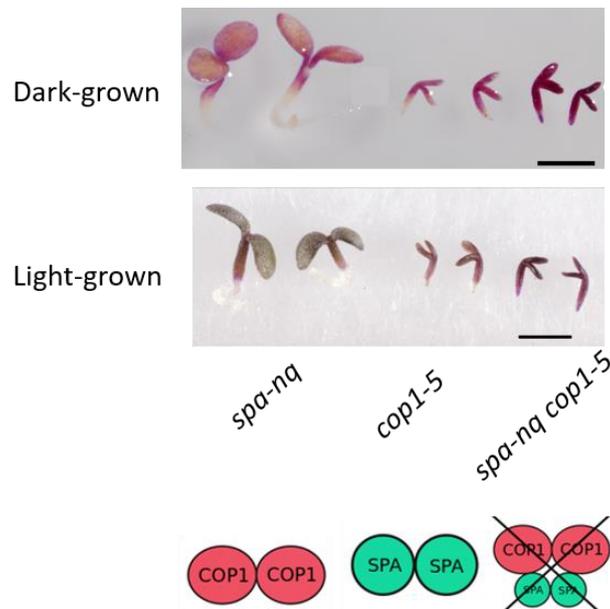
Figure 24. The COP1/SPA complex does not play a role in embryogenesis

Seedlings of indicated genotypes were grown on the top of filter paper for 4-days under complete darkness continuous white light (25 μmol m^{-2} s$^{-1)}$. Scale bar represents 1 mm.
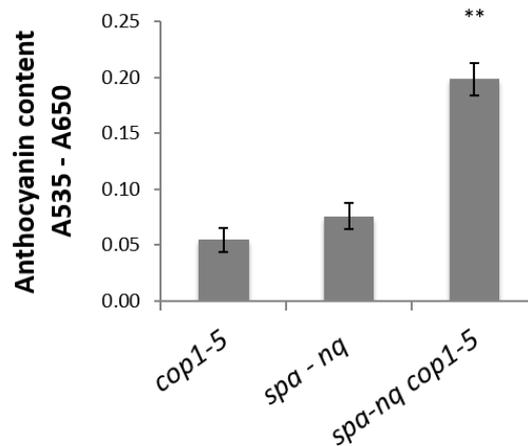
Figure 25. COP1 and the SPAs act synergistically to control anthocyanin accumulation

Anthocyanin content in 15 mature embryos of the indicated genotypes. Embryos were manually released from selected seeds. Anthocyanin contents are calculated as absorbance 535 nm – absorbance 650 nm. The data are representative of two experiments. Error bars represent ± StdDev (n=3) (**P< 0.001 Student's *t* test).

3.2.3 The WD-repeat domain of the SPAs can partially complement the function of the WD-repeat of COP1

In their C-termini, both COP1 and SPA carry a WD-repeat domain which mediates direct interactions with substrates and with DDB1 in the higher-order CUL4-DDB1$^{COP1/SPA}$ E3 ubiquitin ligase (Chen *et al.*, 2010, Huang *et al.*, 2014). In general, mutations in the respective WD-repeat domain abolish COP1 and SPA1 function(Hoecker and Quail, 2001, Saijo *et al.*, 2003, Zhu *et al.*, 2008). Nevertheless, the *cop1-4* mutant, which carries a premature STOP codon and therefore accumulates a truncated COP1 lacking all WD repeats, has only a partial loss-of-function phenotype (McNellis *et al.*, 1994). This mutant is viable and has a plant size intermediate between those of the *spa* quadruple mutant and the wild type. Hence, the COP1-4 protein is partially functional despite the missing WD-repeat domain. To investigate whether the SPA proteins are responsible for the observed residual COP1-4 activity, we generated *cop1-4 spaQn* quintuple mutants (Fig 26). The segregating *spa123(-/-) spa4 (+/-) cop1-4 (+/-)* were isolated and selfed. Subsequently, the individuals from the offspring were subjected to molecular genotyping. This quintuple mutant had a ''*fusca*''phenotype that was more severe than those of the *cop1-4* and *spaQn* mutants (Fig 27). Indeed, the *cop1-4 spaQn* quintuple mutant exhibited a seedling phenotype very similar to that of the *cop1-5* null mutant and failed to develop beyond the seedling stage. This result indicates that the COP1-4 protein does not retain any activity in the absence of SPA proteins. Hence, the WD-repeat domains provided by the SPA proteins can at least partially substitute for the lack of the COP1 WD-repeat domain in the COP1-4 protein.
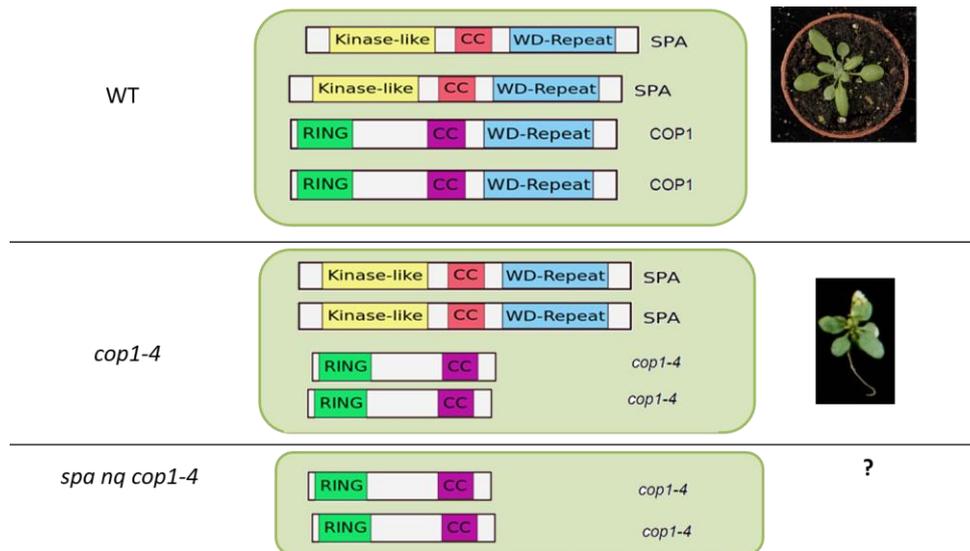
Figure 26. Research question addresses whether the WD-repeat domains of the SPAs are responsible for the residual COP1-4 activity

Schematic representation shows the domain structure of COP1 and SPA proteins. The *cop1-4* plants complete the lifecycle in contrast to null *cop1-5*. The residual activity of the complex in this mutant might occur due to redundancy at the WD-repeat domain. The isolated of the quintuple mutant *spaQn cop1-4,* devoid in WD-repeat, addresses this hypothesis.
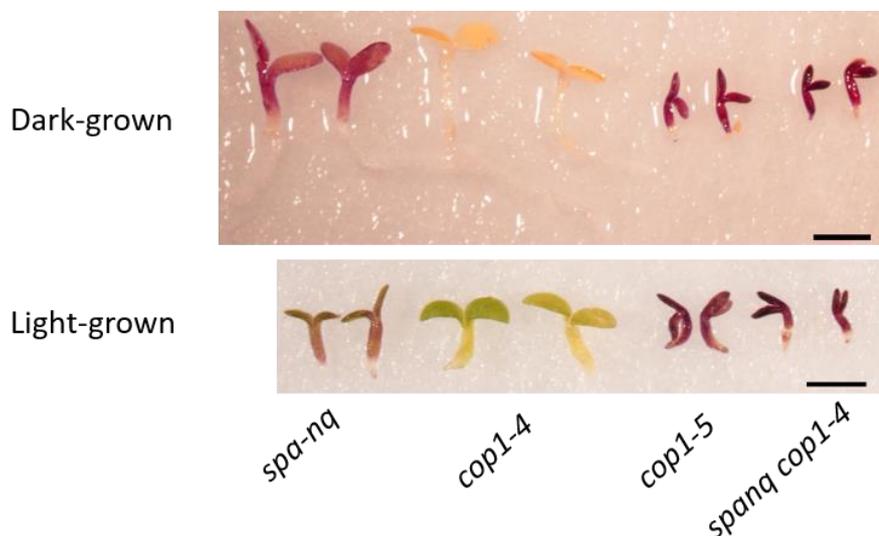
Figure 27. The WD-repeat domain is essential for COP1/SPA function

Seedlings of indicated genotypes grown on the top of filter for 4-days in either complete darkness or continuous white light (25 μmol m^{-2} s$^{-1)}$. Scale bar represents 1 mm. Embryos were manually released and placed on MS medium. Genotypes: *spa –nq cop1-4 (-/-), cop1-5 (-/-), spa –nq* and *cop1-4 (-/-).*

4 Discussion

4.1 PART I - COL12 is a COP1/SPA substrate that represses flowering in *Arabidopsis thaliana*

The light is a key environmental factor that drastically modifies the time at which plants flower (Andres and Coupland, 2012). The outcome is dependent on light parameters such as spectral quality, intensity, and duration of the exposure. The light acts in combination with the signals from the internal circadian oscillator to provide information about the length of the day-night cycles (Andres and Coupland, 2012). At the molecular level, the visible light inhibits the activity of the COP1/SPA complex, thereby preventing the degradation of its substrates (Hoecker, 2005). One of this targeted proteins, CO, is a B-box transcription factor that integrates the photoperiodic cues into the regulation of flowering time(Samach and Coupland, 2000, Laubinger *et al.*, 2006, Jang *et al.*, 2008). Accumulation of CO protein leads to the induction of *FT* transcription triggering molecular events that change the meristem fate (Samach *et al.*, 2000). The plants employ diverse molecular mechanisms to constrain the accumulation and action of such flowering promoter genes thereby preventing premature flowering (Boss *et al.*, 2004, Romera-Branchat *et al.*, 2014). In this study, we identified COL12 as a new repressor of flowering time that acts specifically in LD. This protein belongs to the COL family of transcription factors, sharing homology with CO and other 15 *Arabidopsis* proteins at three conserved domains. The COL12 protein physically interacts with CO and antagonizes its function. Hence, *FT* mRNA accumulation is reduced in *COL12 ox* plants compared to WT. Here, we demonstrate that the light exerts post-translational control on COL12 accumulation. The regulatory control of protein abundance is mediated by the COP1/SPA complex. Therefore, *COL12* might act as part of a fine-tuning mechanism by which the action of the visible light can reduce *CO* activity, thus adding plasticity to the flowering response.

4.1.1 *COL12* is a novel COP1/SPA substrate

Besides exhibiting constitutive de-etiolation at the seedling stage, the *cop1* and *spanQ* mutants exhibit aberrant adult features, like decreased rosette growth, petiole length, and leaf size as well as early flowering time in LD and SD (Deng *et al.*, 1992, Laubinger *et al.*, 2004, Ordonez-Herrera *et al.*, 2015). The COP1/SPA complex controls the protein turnover of several transcription factors thereby affecting numerous developmental processes (Lau and Deng, 2012). Some of the substrates have been identified and functionally linked to the processes that COP1/SPA controls, hence offering a direct mechanistic link between the E3 ligase and the phenotypical responses. However, not all the phenotypical aberrations of the *cop1-4* and *spanQ* mutants can be explained by the known targets, therefore we hypothesized that the COP1/SPA has more substrates that the ones described so far.

Known direct interactors of the COP1/SPA complex include several members of the BBX family of transcription factors, CONSTANS (BBX1), COL3 (BBX4), BBX20, BBX21 (STH2), BBX22, BBX24 and BBX25 (Holm *et al.*, 2001, Datta *et al.*, 2006, Laubinger *et al.*, 2006, Jang *et al.*, 2008, Fan *et al.*, 2012, Gangappa *et al.*, 2013, Xu *et al.*, 2016a). A previous study from our group indicated that a subgroup of BBX recombinant proteins are able to physically interact with COP1 and SPA1 *in vitro* (Adrian, 2005). This subgroup encompasses genes that harbor B-box and CCT domains, thus classified as COLs. Our study started with the confirmation of the physical interactions between members of COLs from subgroup III (Griffiths *et al.*, 2003) and the COP1/SPA complex. In the yeast-two hybrid system the interactions between SPA4 with COL15, COL13 and COL14 as well as SPA1 with COL15 were detected. Attempts to consistently detect interactions of COL12 with COP1/SPA members failed as yeast grew poorly in non-selective media. This is possibly due to toxicity of COL12 overexpression in yeast, similarly to what is reported for CO (Gil *et al.*, 2017). Thus, the yeast system further confirms the direct binding between SPA1 and COL15, which was suggested previously by the *in vitro* pulldown assay (Adrian, 2005). Moreover, it points to new SPA4 direct interactors, COL13 and COL14, that were not tested in the past experiments.

To validate the protein-protein interactions with a system *in planta*, we took advantage of the localization of COP1 and SPA1 into discrete NB and employed the co-localization analysis of fluorescent proteins. Remarkably, COL12 is recruited to NB by COP1 and SPA1. In addition, FRET-FLIM measurements detect that the lifetime of YFP-SPA1 is significantly reduced in presence of mCherry-COL12. This data suggests that COL12 physically interacts with SPA1 and COP1 *in planta*. In contrast, weaker or non-existing interactions were detected for the other tested COLs using the co-localization analysis: COL9, COL10, COL11 and COL15 are not mobilized into NB by neither SPA1 nor COP1 whereas COL13 and COL14 scarcely display partial co-localization with SPA1. Lack of recruitment for these COLs can occur due to steric hindrance imposed by the fluorescent tags, to rule out this possibility future experiments can employ alternative fluorescent tags at different positions of the chimeric proteins. Although interactions between COP1/SPA with all COLs cannot be excluded, the differences in recruitment to NB might reflect a degree of molecular specificity. The specificity of the interactions can be observed *in planta* whereas using *in vitro* pulldown or yeast the interactions with all the COLs are detectable. Then, it is likely that the recognition of non-recruited COL proteins by COP1 and SPA1 is repressed inn planta. For example, by attachment of repressor proteins. In synthesis, co-localization studies suggest that COP1/SPA exhibits specificity regarding the molecular choice of COLs, this is given by factors present in the plant system.

The physical interactions between COP1/SPA and COL proteins apparently arose early in evolution, as the ancestral *Physcomitrella patens* proteins PpCOP1 and PpSPAb physically interact with PpCOLs *in vivo* (Dickopf, 2015). The three ancestral *PpCOLs* are expressed in a light-regulated manner and therefore have been hypothesized to play roles in light signaling transduction. The unique *CrCOL* gene coordinates photoperiodic responses (Zobell *et al.*, 2005, Serrano *et al.*, 2009) . Within the land plants, the COL gene family evolved through expansion and action of selective pressures resulting in a high degree of protein-sequence divergence (Figure 5). The sequence modifications might have led to changes in the binding partners as well as in the affinities towards the E3 ligase components. The ability to interact with COP1/SPA is retained in many proteins of the family representing a module that confers light signaling properties.

The COLs are plant-specific proteins with recognizably conserved domains: B-box and CCT (Robson *et al.*, 2001). Here, we performed mapping of COL12-interacting domains with COP1 and SPA1 using co-localization and FRET-FLIM. Remarkably, the CCT domain of COL12 is critically important for the association with COP1, whereas it is not necessary for the interaction with SPA1. Indeed, the FRET-FLIM analysis suggests that the predominantly the B-box1 domain contribute to mediate the COL12 association with SPA1. Hence, COP1 and SPAs are directed towards differential portions, thus the proteins can work cooperatively to achieve binding. This hypothesis can be tested by yeast three-hybrid experiments and pulldown experiments. In addition, the distribution of interaction domains in COL12 is similar to what has been observed for CO and COP1 (Jang *et al.*, 2008) and to CO and SPA1 using *in vitro* pulldown experiments (Laubinger *et al.*, 2006). This opens the possibility that, CO and COL12 physically compete for binding to the COP1/SPA complex.

The analysis of COL12 interaction with SPA1 reveals that this requires the presence of the SPA1 WD-repeat domain (Fig 5). Similarly, the WD-repeat of SPA1 is essential for the recognition of HY5 and HFR1 (Yang and Wang, 2006). We did not test whether the N-terminal domain of SPA1 is also involved in the recognition of COL12, this possibility remains open. Recently, the N-terminal domain of SPA1 was shown to be essential for the regulation of flowering time, possibly because it enhances the interactions of SPA1 with CO (Holtkotte *et al.*, 2016). On the other hand, the analysis of COP1 substrates has revealed that a VP consensus motif in the substrate confers selectivity towards the WD-repeat (Holm *et al.*, 2001). Recent biochemical studies have confirmed that the VP motif is essential for establishing electrostatic interactions with the WD-repeat propeller structure (Uljon *et al.*, 2016). All the COLs tested here encode at least 1 VP sequence, particularly COL12 encodes two VP motifs in the middle region of the protein. For COL3, it is documented that both the VP motif located at the C-terminal as well as the B-Boxes are needed for the binding to COP1 (Datta *et al.*, 2006). Hence, it is likely that in addition to the conserved domains also the VP motifs contribute to COL12 -COP1/SPA interactions.

Consistently with the COL12-COP1/SPA physical interactions, here we demonstrated that in darkness the COP1/SPA complex targets COL12 for protein turnover. In WT plants, COL12 protein is stabilized by the white light whereas rapid degradation occurs in darkness (Fig 7). Proteolysis in darkness is overcome by the action of the protease inhibitor MG132 implicating that COL12 is degraded specifically at the 26 proteosome as part of ubiquitination pathway. In the light, COL12 protein degradation occurs at a minor degree, as MG132 stabilizes a small amount of the protein (Fig 8). The protein degradation in the light can be explained by the residual activity of the COP1/SPA complex, this action is important to fine-tune the light responses. Alternatively, other E3 ligases might target COL12 for a proteasome-dependent turnover. In *cop1-4* plants, COL12 protein degradation in darkness does not occur (Fig 8). Therefore, we conclude that COL12 is a COP1/SPA substrate, positively regulated by the light at the post-translational level.

4.1.2   Functional analysis of COL12 in Arabidopsis

A number of Arabidopsis BBX proteins have been functionally characterized, these play roles in the regulation of seedling de-etiolation, flowering transition, responses to abiotic stress and SAS (Gangappa and Botto, 2014). Besides the role of COL9 as a repressor of flowering (Cheng and

Wang, 2005), the functions of members of COLs group III are unknown. We addressed this problem by obtaining and analyzing the phenotypes of *Arabidopsis* transgenic lines that express the COLs at constitutively high levels (*35S::HA-COLs*) and T-DNA insertion mutants (when these were available). The phenotypical analysis presented here reveals that the overexpression of COL12 drastically delays flowering time in LD, it also leads to pleiotropic effects reducing the length of the main inflorescence stem and increasing rosette branching (Fig 10 and Fig 11). In the same experiments, the *col12-1* mutant line behaves like WT.

Given that COL12 participates in the light pathway, the pleiotropic effects of COL12 ox could be caused by general defects in the light perception. For example, mutations in the E3 ligase *HOS1* lead to early flowering, constitutive seed germination and reduced inhibition of hypocotyl elongation in R. These phenotypes are caused in part by the action of *HOS1* directly downstream of phyB in the red-light signaling pathway (Lazaro *et al.*, 2015). We analyzed the hypocotyl length in response to different doses of Wc and monochromatic light qualities (B, R, Fr) and found that the COL12 ox and *col12* mutants are not distinguishable from WT. Therefore, a general defect in the visible light signaling pathways does not seem to be the cause COL12 ox phenotypes.

In our hands, overexpression of COL9 delays flowering time in greenhouse conditions, as reported in the literature (Cheng and Wang, 2005). This is in contrast to the overexpression of COL10, COL11, and COL15 which did not lead to any observable flowering time effects. One way to explain the result is that the lines carrying COL10, COL11 and, COL15 do not express high levels of proteins that are needed to alter the responses. This technical scenario might apply for COL10 and COL11 since our attempts to detect the HA-tagged proteins failed. Another possible explanation is that there is molecular specificity in the protein sequences of COL9 and COL12 that confers flowering time control functions to these proteins. The functional specificity hypothesis is favored by recent reports showing that overexpression of COL16 and BBX24 do not lead to drastic effects on flowering time (Graeff *et al.*, 2016).

4.1.3 Positioning of COL12 into the molecular network that controls flowering time

Positioning the *COL12* gene within the known network that regulates flowering started with the assessment of the phenotype in SD and LD conditions. The COL12 ox delays flowering in LD but not in SD indicating that the gene participates as a repressor in the photoperiodic pathway. The behavior of *COL12* in LDs is different to *CO* and similar to the suppressors *COL9,* microProteins miP1a/b and *BBX19* (Cheng and Wang, 2005, Wang *et al.*, 2014, Graeff *et al.*, 2016). The close COL12 relative, COL9 acts at the transcriptional level reducing *CO* mRNA expression in LDs (Cheng and Wang, 2005). In contrast to BBX19 that acts on CO at a pot-translational level engaging the protein into inactive heterodimers, thus reducing the available pool of molecules that drive FT transcription (Wang *et al.*, 2014). The miP1a/b microProteins physically interact with CO and with the TPL/TPR transcriptional repressor complex impairing *FT* transcriptional activation (Graeff *et al.*, 2016). Our experiments revealed that, unlike COL9, COL12 does not influence *CO* at the transcriptional level (Fig 16). Conversely, COL12 acts on CO at the post-translational level by forming heterodimers (Fig 12), like BBX19 and miP1a/b. The mutational analysis of these proteins reported that both BBX19 and miP1a require a functional B-Box1 to heterodimerize with CO whereas the B-box2 of BBX19 is not essential for the interaction. Here, the FRET-FLIM analysis

evidenced that COL12 also requires the B-Box1 to bind to CO and that the B-Box2 is involved in the interaction (Fig 13). This group of BBX proteins, extended with COL12, stablishes a paradigm in the mode of action to inactivate CO by exploiting the dimerization ability of the B-box domain combined with reinforcing regions located adjacently. The dimerization property of the B-box domain also opens the possibility that a more complex interaction network within the members of the COLs exists.

Flowering time is not affected in the *col12-1* loss-of-function allele under the conditions tested. The lack of phenotypic effects might be explained by alternative hypotheses. First, COL12 can influence the flowering time when overexpressed by the dominant negative effect but it is not needed by *Arabidopsis* plants. The gene might function in other conditions than the ones that we tested, for example under different temperature regimes or physiological conditions. Second, the *col12-1* allele encoding the N-terminal region of COL12 possesses sufficient elements to maintain control over the flowering time. We presented evidence for this hypothesis showing that the *col12-1* allele is not null but encodes an N-terminal truncated transcript that lacks the CCT domain. Finally, the CCT-domain of COL12 is not needed for the physical interaction with CO. This scenario has been reported for the *bbx19* mutant alleles that encode functional B-boxes and the *BBX19* N-terminal overexpression lines that do not influence the flowering time (Wang *et al.*, 2014). Third, COL12 acts redundantly with other *Arabidopsis* genes, therefore higher order mutants are needed to deplete the plant from this function and observe the phenotype. We monitored the tissue and developmental expression pattern of *COL12* and *COL11*, the closest homolog, and found that this gene is not expressed through the vegetative stages (Fig 19). Hence, functional redundancy of *COL12* and *COL11* is not expected for the control of the flowering time. To address these hypotheses, additional *COL12* alleles or silencing lines must be obtained and analyzed in detail. Our attempts to generate silencing lines using amiRNA failed, so we are currently generating knock-out lines using targeted genome editing with the CRISPR-Cas system (Hyun *et al.*, 2015).

The CO protein levels integrate information from light, circadian clock and temperature cues (Valverde *et al.*, 2004, Song *et al.*, 2012, Fernandez *et al.*, 2016). The regulation of CO protein stability by the light constitutes a key part of the mechanism by which plants achieve photoperiodic flowering (Andres and Coupland, 2012). The proteolysis is instructed by at least two characterized E3 ligases: The COP1/SPA complex and HOS1 (Laubinger *et al.*, 2006, Jang *et al.*, 2008, Lazaro *et al.*, 2012). In addition, in the afternoon hours of LD, CO protein is stabilized by the direct interaction with FKF1 (Song *et al.*, 2012). Adaptor proteins that modify the assembly of the substrate with the E3 ligase complex can contribute to shape the protein accumulation. For example, BBX19 modulates the hypocotyl length by enhancing the interaction between ELF3 and COP1/SPA thereby promoting ELF3 destabilization (Wang *et al.*, 2015). Recent publications report that the inactive isoform of CO aid to recruit the active isoform of CO towards the E3 ligases, HOS1 and COP1/SPA, thus enhancing protein turnover (Gil *et al.*, 2017). Given that COL12 binds strongly to both the E3 ligase COP1/SPA and its substrate CO, we examined whether the protein stability of CO was targeted by COL12. Immunoblot analysis of double transgenic lines *35S::HA-COL12* x *SUC2::HA-CO* indicates that COL12 does not modify CO protein accumulation in seedlings grown in LD at ZT16 (Fig 14). This time of the day was chosen because it is the time of the day when COL12 and CO proteins are expected to accumulate at high levels and when the effects on FT expression are observed. We cannot rule out that regulation of the protein abundance occur at other moments of the day, for example at the early night ours when the pool of active COP1/SPA

is increasing and the concentration of the substrates is decreasing. Further protein stability experiments should consider different experimental conditions and time points during the day. Also, the formation of a ternary complex can be investigated employing the yeast three-hybrid system and pulldown assays.

We observed that CO and COL12 proteins act antagonistically in the control of the flowering time in LD. Because the double mutant *SUC2:HA-CO* x *35S::HA-COL12* flowers later than the single mutant *SUC2::HA-CO* (Fig 20). In this manner, the pool of CO protein available for FT transcription is controlled by the balancing action of the COL12 protein. It might be functional for the plants to alter the relative balance between the two proteins in response to particular conditions. Therefore, we tested whether different light qualities alter the accumulation of COL12 protein, which can possibly influence the balance between the two proteins and the outcome of the response. The immunoblot analysis revealed that COL12 protein is stabilized by white, blue and red light (Fig 14). The stabilization of COL12 by blue and red light treatments is consistent with the inactivation of the COP1/SPA complex by active phyB, CRY1, and CRY2. Here, treatments with monochromatic wavelengths of light were used in order to excite individual light pathways. To better establish the action of specific photoreceptors on COL12 protein levels, it is still necessary to monitor them in the corresponding mutant backgrounds. Interestingly, the behavior of COL12 in red light is distinct with the reported response of CO. We cannot rule out that the differential outcome of COL12 and CO reflects differences in the experimental set-up in our chambers as the control *SUC2::HA-CO* was not included in the experiment because of insufficient plant material. The net effect of red light on CO protein levels is destabilizing, although dual effects of phyB on CO occur depending on the time of the day (Valverde *et al.*, 2004, Hajdu *et al.*, 2015). The behavior of COL12 protein in red light does not suggest that PHYB intervenes to destabilize COL12 through HOS1 or other protein turnover branches. The differential effects of the red light on CO and COL12 protein accumulation might favor the formation of inactive heterodimers in the morning hours, reinforcing CO inactivation at this critical period of the day. Moreover, phyB is the major photoreceptor involved in the perception of SAS, thus *phyB* mutants exhibit a constitutive acceleration of flowering (Halliday *et al.*, 2003). The flowering response to SAS is also dependent on *CO* and *GI* (Wollenberg *et al.*, 2008). However, the molecular mechanisms thereby phyB acts on CO to accelerate flowering in response to SAS remain unveiled. Presumably, the phyB action includes the modulation of CO activity, mediated by repressors such as COL12.

The regulatory role of CO relies on its ability to induce the transcription of the florigen integrator genes *FT* and *SOC1* (Samach *et al.*, 2000). The transcriptional activity of CO is executed through a combination of direct and indirect associations with the *FT* promoter (Cao *et al.*, 2014). For the indirect association, CO partners with the NFY-complex that is recruited to the CCAAT *cis* elements (Ben-Naim *et al.*, 2006, Wenkel *et al.*, 2006). This protein-protein interaction requires the functional CCT domain of CO (Ben-Naim *et al.*, 2006). The direct CO chromatin binding occurs at the CORE elements located at the proximal part of the FT promoter (Tiwari *et al.*, 2010). Interestingly, not only CO but also COL9 and COL15 activate the transcription of CORE elements in transactivation assays (Tiwari *et al.*, 2010). Here, we showed that CO forms dimers with COL12 and that the action of COL12 lowers the FT transcriptional amplitude in LD. Hence, the heterodimerization might interfere with CO activity. Further experiments are needed to test whether the dimerization of CO with COL12 interferes with its DNA-binding capacity and transcriptional activity on the *FT* promoter. For instance, COL12 might be able to physically interact with the NFY complex through the conserved CCT domain or the dimerization could

induce conformational changes that alter the direct recognition of *cis* elements. In addition, it remains to be tested whether COL12 binds directly to the *FT* promoter. This mechanism might be employed by COL12 for the control of plant architecture, given that the genetic interaction experiments support a CO-independent and FT-dependent mode of action. However, direct binding of COL12 to the *FT* promoter might not be employed in the control of flowering time, since this regulatory function is completely dependent on CO. These aspects of the molecular mechanisms of COL12 can be tested in the future, using *FT*-promoter transactivation assays, chromatin immunoprecipitation, and EMSA experiments.

The molecular network that controls Arabidopsis flowering time converges in a small number of floral integrator genes that contribute dramatically to the outcome (Boss *et al.*, 2004, Andres and Coupland, 2012). The floral inducer genes include *CO, FT, TSF* and *SOC1* are involved in the early events of the floral induction. The transcriptional cascade is followed by upregulation of genes that change the meristem fate, including *FUL*, *LFY*, and *AP1*. Another group of genes encompasses the repressors of the floral program that function to enable the flowering response (Boss *et al.*, 2004). This group of genes includes *FLC*, *SVP*, *TFL*, *TOE1-2,* and *TEM*. In this study, we monitored the effects of COL12 ox on the transcriptional levels of some flowering regulators genes. As mentioned previously, COL12 does not alter the *CO* mRNA transcriptional levels but leads to a reduction in *FT* mRNA levels. Although *SOC1* and *FUL* are transcriptional targets of *CO* and *FT* (Samach *et al.*, 2000, Wigge *et al.*, 2005), COL12 does not significantly modify the mRNA levels of these genes. It is possible that transcriptional changes occur later in the floral induction process, therefore major changes are not detected by our one-point analysis. Our attempts to amplify *LFY* and *SPL4* from our WT cDNA samples failed, probably due to the same reason. The MADS box transcriptional regulators, *SVP* and *FLC*, prevent flowering under LD and SD (Michaels and Amasino, 1999, Sheldon *et al.*, 1999, Hartmann *et al.*, 2000). The lack of effects of COL12 ox on *FLC* and *SVP* transcriptional levels is consistent with the absence of a flowering phenotype in SD.

The day-length sensing mechanism confers circadian rhythmicity to the *FT* mRNA expression. Both, the pattern and the amplitude of *FT* expression encode information that impacts the flowering response (Krzymuski *et al.*, 2015). In LD, *FT* mRNA levels rise dramatically at the end of the day and may increase slightly in the morning hours. The morning peak arises under certain growth conditions like illumination with low R:Fr (Kim *et al.*, 2008, Wollenberg *et al.*, 2008). However, the plants respond more effectively when *FT* rises at the end of the day, due to a gating effect by the circadian clock (Krzymuski *et al.*, 2015). Both peaks of expression are dependent on the presence of CO (Wollenberg *et al.*, 2008, Zhang *et al.*, 2015). Indeed, CO protein accumulates in the early morning and at the end of the day. However, its action is more effective in the evening hours. Mathematical models predict the existence of signals that attenuate CO actions in the morning (Salazar *et al.*, 2009). Experimentally, it was shown that repressors like the TOE proteins are necessary to counteract CO activity in the mornings, hence the *toe* mutants display higher FT expression in the morning hours (Zhang *et al.*, 2015). In this thesis, we show that the overexpression of COL12 leads to a significant reduction of *FT* levels in both the morning hours (ZT4) and the end of the day (ZT16) of LD (Fig 17). These transcriptional effects agree with a CO-dependent mechanism. However, it remains to be tested whether *col12* null alleles display higher FT mRNA levels and when are the effects more prominent. The *COL12* diurnal pattern of mRNA expression is uniform, thus it does not point toward preferential accumulation at a particular time of the day. Further experiments are needed to determine whether the regulation at the post-transcriptional level imparts circadian rhythmicity to COL12 accumulation.

The functional role of the genes is dependent on its protein sequence as well as on its pattern of expression. Therefore, as part of the functional characterization of *COL12*, we monitored its expression levels at different stages of development. Importantly, the gene is expressed steadily through the vegetative development and is maintained after the floral transition in leaves, flowers and floral buds. This data agrees with the RNAseq developmental analysis published by Genevestigator database (Clough and Bent, 1998). The pattern of expression of *COL12* overlaps with that of *CO* (Schmid *et al.*, 2005)*,* supporting the functional dependence of *COL12* on *CO*. The fact that during the vegetative period, the *COL12* mRNA expression does not change with age, implicates that it is unlikely that *COL12* takes part of an age regulatory mechanism that limits flowering. Developmental control is being observed for the transcription of FT repressive factors like TEM and TOE proteins (Castillejo and Pelaz, 2008, Zhang *et al.*, 2015). In parallel with COL12 mRNA levels analysis, we monitored COL11 levels, to evaluate possible functional redundancy. *COL11* is the putative paralogue of COL12 that shares homology at 58% of the protein sequence. The relative mRNA quantification points out that *COL11* expression is restricted to the flowers and buds sample. Therefore, *COL11* might not contribute to the flowering time control in *Arabidopsis*. Nevertheless, it is possible that *COL11* and *COL12* share a role in the reproductive structures.

In addition to delayed flowering, overexpression of COL12 acts positively on rosette branching and negatively on inflorescence length. Interestingly, both CO and FT exert pleiotropic effects on plant architecture. Particularly, FT and TSF positively regulate the onset and speed of growth of lateral cauline branches, acting more prominently in LD and SD respectively (Hiraoka *et al.*, 2013, Huang *et al.*, 2013a). It was clarified that the FT produced in subtending leaves can move to the axillary buds to modify its differentiation, including shoot outgrowth and floral transition at the axillary meristems (Hiraoka *et al.*, 2013, Niwa *et al.*, 2013). Hence the behavior of the dormant buds is modified by both the floral changes at the SAM as well as by FT direct transcriptional activity. Our own measurements in LD show that both CO and FT positively influence the number of rosette branches at the end of development (Fig 21). Oppositely, the outgrowth of rosette branches in COL12 ox is significantly higher than WT, although COL12 ox flowers nearly at the same time as co-*SAIL* and *ft-10*. Strikingly, *ft-10* is epistatic to COL12 ox with respect to branching (Fig 2). Thus, COL12 needs *FT* to change the behavior of axillary buds. In COL12 ox lines, the effects of flowering time and branching are uncoupled suggesting that the main mechanism thereby COL12 influences branching is the modulation of *FT* direct effects. Further experiments are needed to test whether COL12 positively regulate *FT* mRNA after the floral transition. Moreover, the genetic analysis shows that the COL12 ox operates independently of CO in the regulation of branching. Pointing towards developmental-stage specific mechanisms, in vegetative development *COL12* partners with CO to repress *FT* mRNA whereas after flowering it acts independently, presumably to upregulate *FT*. Importantly, the elucidation of the *COL12* niche in Arabidopsis plants awaits for the isolation of more mutant alleles.

It has been proposed that the dual actions of FT on the SAM and the axillary meristems might have functional implications. As the plants gain plasticity by uncoupling flowering and branching in certain conditions like the shade (Hiraoka *et al.*, 2013, Niwa *et al.*, 2013). For example, BRANCHED1 (BCR1) negatively modulates *FT* expression specifically at the axillary meristems limiting lateral bud outgrowth (Niwa *et al.*, 2013). Because this gene is upregulated in the shade,

then branching is reduced even when flowering is accelerated (Aguilar-Martínez *et al.*, 2007, Niwa *et al.*, 2013). Since *COL12* is expressed after flowering, it is possible that the gene integrates light signals into the plant architecture response. This can be tested by comparing the outcome of the *COL12 ox* and *col12* lines to WT in normal R:Fr and reduced R:Fr. The light modifies plant architecture, acting through the main hubs COP1 and the PIFs to modulate auxin biosynthesis and GA sensitivity, among others (Casal, 2013). Here we observed that besides higher branching, *COL12 ox* lines display shorter inflorescence stems in an *FT*-dependent manner (Fig 21). The perturbations in stem elongation and branching can be a consequence of aberrant hormonal levels or sensitivity. In particular, the opposing actions of the phytohormones auxin and strigolactones are important determinants of branching and internode elongation (Domagalska and Leyser, 2011). Thus, it remains to be tested whether COL12 perturbs hormonal levels or sensitivity as part of the plant branching response.

In summary, our findings identify *COL12* as a novel gene that can act as a repressor of photoperiodic the flowering time. A model for the COL12 molecular mechanism is presented in figure 27. At the molecular level, COL12 physically interacts with CO leading to reduced transcriptional activation of *FT* mRNA. It is unlikely that *COL12* represent an output of age or circadian clock pathways. Interestingly, the protein can convey the light signals. Compiling evidence presented here indicates that the protein stability of COL12 is controlled by the light through the activity of the COP1/SPA complex. The visible light signals are pivotal for the photoperiodic control of flowering, acting to regulate *CO* mRNA and protein accumulation (Andres and Coupland, 2012) . Additional post-translational mechanisms might contribute to fine-tuning the responses. For example, COL12 is a light-switchable protein that represses CO activity. The regulatory effects of the photoreceptors phyA, CRY1, and CRY2 on shaping the *CO* mRNA accumulation in LD are completely dependent on COP1 (Sarid-Krebs *et al.*, 2015). COP1/SPA achieves this control by inducing selective degradation of GI and ELF3. At the same time, the COP1/SPA hub is central for integrating light signals into the accumulation pattern of CO protein (Laubinger *et al.*, 2006, Jang *et al.*, 2008). The *cop1-4* mutation is completely epistatic to the triple photoreceptor mutant *phyA cry1 cry2* with respect to CO protein accumulation (Sarid-Krebs *et al.*, 2015). The combined action of phyA CRY1 and CRY2 drives CO protein degradation during the night and at certain windows during the day. Reflecting that during the day, COP1/SPA action is important and operate at different rates depending on the time of the day. This can be explained in part by the effects of the circadian clock on the accumulation of SPA1 (Fittinghoff *et al.*, 2006, Jang *et al.*, 2008). It is also possible that modulator proteins fine-tune the activity of COP1/SPA towards specific factors at specific periods during the day. We tested whether COL12 influences CO protein stability at ZT16 and did not find any effects. To clarify the biological importance of the COP1/SPA regulation on COL12, it is still necessary to convey a detailed epistasis analysis.

White light drastically stabilizes COL12, this combined with a steady mRNA transcription pattern along the day in LD might result into protein accumulation along the days and not during the night. For CO, the protein destabilizing action of PHYB in the mornings and COP1/SPA destabilizing at night limit the protein accumulation to the end of the day. Oppositely to CO, COL12 is stabilized by the red light. Hence during the day hours, the balance between CO and COL12 can be modulated by the red light. Consequently, COL12 might constitute a mechanism to fine-tune CO activity depending on the light conditions. Under the blue light, high levels of both CO and COL12 proteins accumulate, hence the intervention of COL12 can lead to attenuation of

the response. Whereas in the red light, protein levels of CO are lowered and COL12 accumulates, thus activity on COL12 reinforces the repression of flowering.

Because the loss-of-function allele of *col12* does not lead to a perturbation in the plant phenotype. We cannot unequivocally determine the biological role of the gene in *Arabidopsis* plants. The possible reasons for the lack of phenotype have been discussed. The analysis of overexpression lines points to roles in the control of the flowering time as well as plant architecture. One immediate aim is the isolation of more mutant alleles and higher degree mutants which is required to address this point.
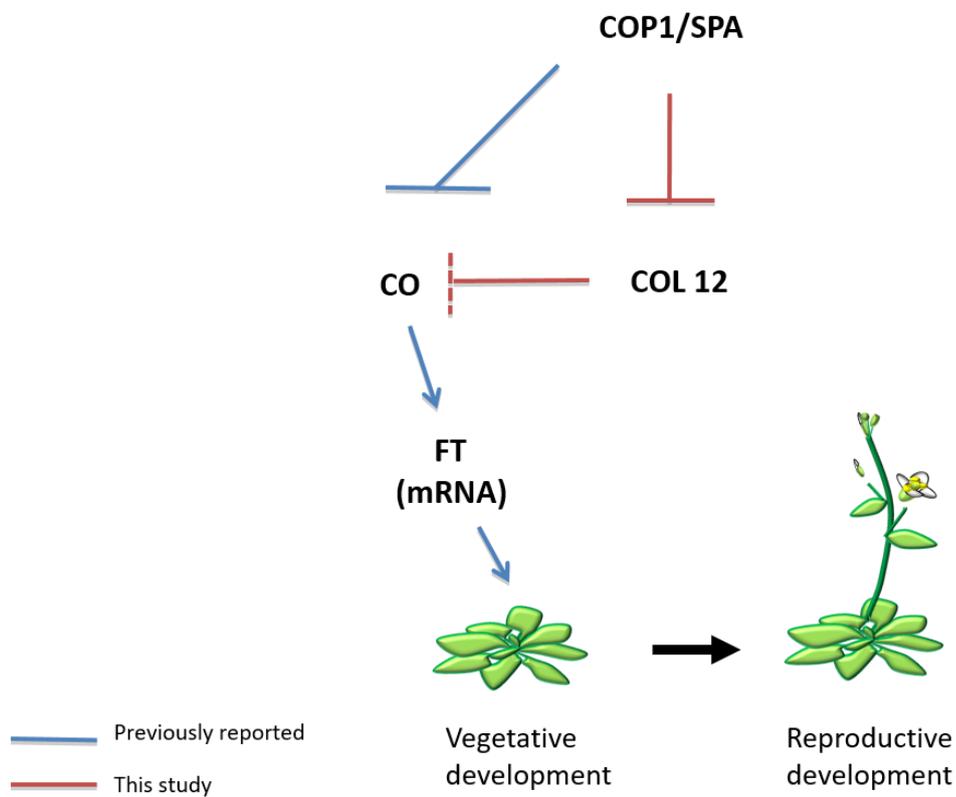

Figure 27 Model for the action of COL12 in the control of flowering time

4.2 PART II - Co-Action of COP1 and SPA during Arabidopsis post-embryonic development and photomorphogenesis

The COP1 and SPA proteins act in concert to control plant responses to the visible light (Laubinger *et al.*, 2004, Hoecker, 2005). The completion of the plant life-cycle requires the presence of a functional COP1, as indicated by the *cop1-5* seedling lethal phenotype. However, an open possibility was that before the seedling stage, the SPA proteins acting independently of COP1 sustain early development. To address this hypothesis, we isolated the *spaQn cop1-5* mutant, that is devoid in both COP1 and SPA. The data presented here provide evidence that the *spaQn cop1-5* develops until the seedling stage resembling *cop1-5*. Therefore, the SPAs do not have significant activity in the absence of COP1. The COP1/SPA complex is part of a higher order E3 ligase together with DDB1 and CUL4 (Chen *et al.*, 2010, Huang *et al.*, 2014). Both COP1 and SPA proteins establish interactions with DDB1-CUL4 *in planta* (Huang *et al.*, 2013b). Our data dismisses the possibility that without COP1, a DDB1-CUL4-SPAs complex has E3 functional activity during early plant development. The only detectable phenotype in which SPA activity might be independent of COP1 is the accumulation of Anthocyanins. Because the *spaQn cop1-5* quintuple displays significantly higher Anthocyanin levels than the controls. Alternatively, this can be explained by the synergistic action of COP1 and SPAs to regulate the biosynthesis of this pigment. This can be achieved by cooperative recruitment of specific targets, i.e. HY5 and PAP proteins.

Here, we show that the COP1/SPA complex is not required for embryogenesis. The orthologue of COP1 in mammals plays a role in DNA-damage repair process and progression of the cell cycle (Dornan *et al.*, 2004). In plants, the existence of *cop1 spanQ* null embryos implies that fundamental cellular processes can proceed in the absence of COP1/SPA activity. Major disturbances specifically in meristem function of *cop1* and *cop1 spa* null mutants are likely responsible for the growth arrest at the seedling stage (Yoshida *et al.*, 2011).

The COP1 and SPA proteins exhibit structural similarities, both encoding a coil-coiled and a WD-repeat domain. The sequence resemblance provides a plausible explanation for the partial functional redundancy of both entities. Here we addressed whether the SPAs WD-repeat domains can replace the functions of the WD-repeat domain of COP1 isolating the *spaQn cop1-4* quintuple mutant, which completely lacks WD-repeats. The phenotypical analysis reveals that the *spaQn cop1-4* behaves like the *cop1-5* mutant in darkness and light. Indicating that in the *cop1-4* mutant, the residual activity of COP1-4 is sustained by the functional SPAs. Our data implies that the WD-repeat domain is absolutely required for the function of the COP1/SPA complex. This domain is pivotal for the recognition of the substrates and interactions with DDB1 E3 ligase adaptor (Holm *et al.*, 2001, Saijo *et al.*, 2003, Chen *et al.*, 2010, Maier *et al.*, 2013). It remains to be assessed what is the functional importance of the DDB1 binding for COP1/SPA complex, this can be done by mutating specific amino acids within the WD-repeat that disrupt these interactions and assessing its functional capabilities. The COP1/SPA interacts with UVR8 acting as a substrate receptor that promotes protein stabilization instead of an E3 ligase function (Huang *et al.*, 2014). Upon UV-B light exposure, UVR8 competes with DDB1-CUL4 for binding with COP1/SPA. Thus,

changes in the COP1/SPA affinity for DDB1-CUL4 or UVR8 might impact dramatically the outcome of the photomorphogenic response. Such differences in binding affinity for DDB1 might be fine-tuned by the different contributors of WD-repeat domains.

Moreover, the recognition of the substrates requires information that is redundantly encoded by the SPAs and COP1. It is likely that the WD-repeat domains of the SPAs enhance the affinity of COP1 for the targets, this can be tested using yeast three-hybrid and pulldown assays. It has been suggested that the composition of the complex, in terms of SPA proteins, can vary the molecular specificity for the substrates thereby regulating specific aspects of the light response (Laubinger *et al.*, 2004, Fackendahl, 2012). Thus, the functional divergence of the WD-repeat together with combinatorial use can be used by plants to enhance plasticity in the control of light responses (Menon *et al.*, 2016).

The WD-repeat domains are pivotal for the COP1/SPA E3 function as well as contribute to the sensitivity towards the light. The WD-repeat of SPA1 mediates the inhibitory interaction with the photoreceptor CRY1 (Lian *et al.*, 2011, Liu *et al.*, 2011). It has been proposed that other photoreceptors, CRY2 and PhyA, bind to the N-terminus portion of SPA1 (Zuo *et al.*, 2011, Sheerin *et al.*, 2015). However, the deletion of the SPA1 N-terminus did not lead to differences in monochromatic light sensitivity raising the possibility that the WD-repeat domains contribute to mediate the interactions with these photoreceptors (Holtkotte *et al.*, 2016). These new findings point to the existence novel regulatory roles of the WD-repeat domain in the COP1/SPA complex that add complexity to the system. These novel aspects await to be unveiled in the future.

5 Materials and methods

5.1 Materials

5.1.1 Chemicals

The chemicals employed in these experiments were purchased from: AppliChem GmbH (Darmstadt, Germany), BD Biosciences (Heidelberg, Germany), Bio-Rad Laboratories GmbH (Munich, Germany), Calbiochem (Darmstadt, Germany), Carl Roth GmbH (Karlsruhe, Germany), Duchefa Biochemie B.V. (Haarlem, Netherlands), Honeywell Riedel-de-Haen Specialty Chemicals Seelze GmbH (Seelze, Germany), Life Technologies, GmbH (Karlsruhe, Germany), Merck KGaA (Darmstadt, Germany), Miltenyi Biotec, (Bergisch Gladbach, Germany), p.j.k GmbH (Kleinblittersdorf, Germany), Promega (Mannheim, Germany), Roche Diagnostics GmbH (Mannheim, Germany), SERVA Electrophoresis, GmbH (Heidelberg, Germany), Sigma-Aldrich Chemie GmbH (Munich, Germany), ThermoFisher Scientific (Schwerte, Germany) and VWR International GmbH (Darmstadt, Germany).

5.1.2 Antibiotics

The antibiotics listed in table 1 were employed in the preparation of selective media. The stock solutions were stored at -20°C otherwise stated.

Table 1. List of antibiotics used for selection of genetically transformed organisms.

Antibiotic	Working concentration	Manufacturer
Ampicillin (Amp)	100 µg/ml	Duchefa Biochemie B.V. (Haarlem, Neth.)
Chloramphenicol[a] (Chlo)	75 µg/ml	Duchefa Biochemie B.V. (Haarlem, Neth.)
Gentamycin (Gen)	25 µg/ml	Duchefa Biochemie B.V. (Haarlem, Neth.)
Kanamycin (Kan)	50 µg/ml Bacteria 50 mg/ml Plants	Duchefa Biochemie B.V. (Haarlem, Neth.)
Rifampicin[a] (Rif)	25 µg/ml	Duchefa Biochemie B.V. (Haarlem, Neth.)
Spectinomycin (Spec)	10 µg/ml	Duchefa Biochemie B.V. (Haarlem, Neth.)
Carbenicillin[b] (Carb)	100 ug/ml *Agrobacterium*	AppliChem GmbH (Darmstadt, Germany)

a Stock solution stored at room temperature.

b Degraded after 5 days at 4°C.

5.1.3   Kits and enzymes for molecular biology procedures

The commercial kits in table 2 were used for nucleic acid isolations and cloning.

Table 2. List of kits employed in Molecular biology procedures

Commercial kit	Manufacturer
Nucleospin Plasmid Purification	(Macherey Nagel, Düren, Germany)
High Pure PCR Product Purification	(Roche Diagnostics (Mannheim, Germany)
Plasmid Plus Midi Kit	(QIAGEN GmbH, Hilden, Germany)
RNeasy Plant Mini Kit	(QIAGEN GmbH, Hilden, Germany)
CloneJET PCR Cloning	(Thermo Fisher Scientific, Schwerte, Germany)
Gateway® LR Clonase® Enzyme mix	(Thermo Fisher Scientific, Schwerte, Germany)
Gateway® BP Clonase® Enzyme mix	(Thermo Fisher Scientific, Schwerte, Germany)
Oligo(dT) 18 primers	(Thermo Fisher Scientific, Schwerte, Germany)
RevertAid H Minus Reverse Transcriptase	(Thermo Fisher Scientific, Schwerte, Germany)
dNTPs mix	(Thermo Fisher Scientific, Schwerte, Germany)

The enzymes in table 3 were employed for cloning, PCR, and qPCR.

Table 3. List of enzymes used in Molecular biology procedures

Enzyme	Manufacturer
Pfu DNA Polymerase	Thermo Fisher Scientific (Schwerte, Germany)
Q5 High-Fidelity DNA Polymerase	New England Biolabs GmbH (Frankfurt am Main, Germany)
Restriction endonucleases	Thermo Fisher Scientific (Schwerte, Germany)
T4 DNA Ligase	Thermo Fisher Scientific (Schwerte, Germany)
FastAP Thermosensitive Alkaline Phosphatase	Thermo Fisher Scientific (Schwerte, Germany)
Taq DNA Polymerase	Home-made
DreamTaq DNA Polymerase	Thermo Fisher Scientific (Schwerte, Germany)
SYBR Green	KappaBiosystems (Wilmington, MA, USA)
DNAse I	Thermo Fisher Scientific (Schwerte, Germany)

The kits used for immunoprecipitation and immunoblot are listed in table 4.

Table 4. List of commercial kits used for biochemical procedures

Commercial kits	Manufacturer
µMACS Epitope Tag protein Isolation Kits	(Miltenyi Biotec, Germany)
West Femto Maximum Sensitivity kit	(ThermoScientific)

5.1.4   Antibodies

The antibodies in table 5 were used for protein detection by immunoblot analysis. Primary antibodies were diluted in a solution containing 2.5 % non-fat milk powder in TBS (20 mM Tris/HCl pH 7.5, 137 mM NaCl). Diluted solutions were kept at 4°C and re-used until a signal was detected. Secondary antibodies were prepared in a solution containing 5 % non-fat milk powder in TBS.

Table 5. List of antibodies used for protein immunodetection

Antibody	Animal source	Dilution	Manufacturer
α-HA-HRP	Rat	1:1000	Roche Diagnostics (Mannheim, Germany)
α-Histone H3	Rabbit	1:5000	Abcam (Cambridge, MA, USA)
α-rabbit IgG-HRP	Goat	1:80000	Sigma-Aldrich (Munich, Germany)
α-mouse IgG-HRP	Goat	1:50000	Sigma-Aldrich (Munich, Germany)
anti-GFP	Mouse	1:1000	Roche Diagnostics (Mannheim, Germany)

5.1.5   Growth media

Growth media for bacteria, plant seedlings, yeast and mammalian cell line HEK293TN are described below. Solid LB media contain 1.5% while yeast media contains 2% agar.
Plant media contain 1% agar high gel-strength.

Table 6. List and description of media used for growth of living organisms

Media	Purpose	Composition
Dulbeccos modified Eagle medium (DMEM)	Mammalian cell culture	DMEM with Glutamax 1 x Pyruvate 1 x Non-essential amino acids 1% (v/v) Penicillin-Streptomycin solution 10 g/L Fetal bovine serum
Luria-Bertani (LB) broth media	*E.coli* *A. tumefaciens*	1% (w/v) Tryptone 0.5 % (w/v) Yeast extract 1 % (w/v) NaCl
YEB media	*A. tumefaciens*	1% (w/v) Yeast extract 1% (w/v) Tryptone 0.5% (w/v) NaCl pH adjusted to 7.0
Murashige & Skoog medium	Plant seedlings	4.44 g/L MS salts pH adjusted to 5.8
YAPD medium	Yeast	20 g/L Difco-peptone 10 g/L Yeast extract

		100 mg/L Adenine hemisulfate pH adjusted to 5.8 20 g/L Glucose
Yeast-two-hybrid drop-out medium	Yeast	6.7 g/L Nitrogen base without amino acids 40 mg/L Adenine hemisulfate x g/L Drop-out pH adjusted to 5.8 (Clonetech, Palo Alto, USA) 20 g/L Glucose

5.1.6 Buffers and solutions

The buffers and solutions used in the experiments are described below.

Table 7. List and description of buffers and solutions

Purpose	Buffer/Solution	Composition
DNA extraction	Thompson DNA extraction buffer	200 mM Tris-HCl pH 7.5 250 mM NaCl 25 mM EDTA 0.5% (w/v) SDS
DNA electrophoresis	DNA loading dye	0.25% (w/v) Bromophenol Blue 30% (v/v) glycerol
	10 x TBE buffer	890 mM Tris 890 mM Boric acid 20 mM EDTA
PCR	PCR reaction buffer	100 mM Tris-HCl pH 9.0 500 mM KCl 15 mM MgCl$_2$
Yeast-two-hybrid	10 x TE buffer	0.1 M Tris/HCl 10 mM EDTA pH adjusted to 7.5
Tobacco agroinfiltration	10 x Agromix	100mM MgCl$_2$·H2O 100mM MES pH adjusted to 5.6 150 μM Acetosyringone (Stock dissolved into Ethanol) [a]
Protein extraction	Nuclear enrichment buffer	20% (v/v) TRIS 1M pH 6.8 5% (w/v) Sucrose 400 ml/L Glycerol 1.6 % Triton X100 20 mM MgCl$_2$ 0.8% (v/v) β-Mercaptoethanol 2% (v/v) Protease inhibitor cocktail [a] (Sigma-Aldrich, Munich, Germany) 1 mM DTT [a] 2 mM Phenylmethanesulfonyl fluoride (PMSF) [a]
	2 x Lämmli buffer	65.8 mM Tris-HCl pH 6.8

		2.1% (w/v) SDS 26.3% (w/v) Glycerol 0.01% Bromophenol blue
Protein electrophoresis and Immunoblot	SDS-PAGE resolving gel	7.5-15% (w/v) Acrylamide 375 mM Tris-HCl pH 8.8 0.1% (w/v) SDS 0.08 % (w/v) APS 0.08 % (v/v) TEMED
	SDS-PAGE stacking gel	5% (w/v) Acrylamide 125 mM Tris-HCl pH 6.8 0.1% (w/v) SDS 0.05 % (w/v) APS 0.1 % (v/v) TEMED
	10 x SDS running buffer	1.9 M Glycine 240 mM Tris 1% (w/v) SDS
	10 x Carbonate blotting buffer	0.31 % (w/v) $NaCO_3$ 0.84 % (w/v) $NaHCO_3$ 0.08 % (w/v) SDS
	10 x TBS buffer	200 mM Tris-HCl pH 7.5 1.5 M NaCl
	TBS-T buffer	Tween-20 in 1 x TBS
Immunoprecipitation	Nuclear isolation buffer	50 mM TRIS-HCl 1M pH 7.4 5% (w/v) Sucrose 400 ml/L Glycerol 0.5 % (v/v) NP-40 10 mM $MgCl_2$ 0.8% (v/v) β-Mercaptoethanol 2% (v/v) Protease inhibitor cocktail [a] (Sigma-Aldrich, Munich, Germany) 1mM DTT [a] 2 mM PMSF [a]
	Sonication buffer	50 mM TRIS-HCl 1M pH 7.4 0.5 % (v/v) NP-40 50 mM NaCl 2% Protease inhibitor cocktail [a] (Sigma-Aldrich, Munich, Germany) 1mM DTT [a] 2 mM PMSF [a]
	Washing Buffer	50 mM TRIS-HCl 1M pH 7.4 0.5 % (v/v) NP-40 150 mM NaCl
LUMIER assay	Lysis buffer	50 mM Tris-HCl pH 7.5 150 mM NaCl 1 mM EDTA 0.5 % Triton X-100 10 % Glycerol 4.45 % Protease inhibitor cocktail [a] (Roche Diagnostics, Mannheim, Germany)
	K_xPO_4 buffer	1 M KH_2PO_4 1 M K_2HPO_4

		Mix the solutions to pH 5.1
	10 x PBS	80 g/L NaCl 2g/L KCl 17.8g/L $Na_2HPO_4.2H_2O$ 2.7 g/L KH_2PO_4 pH adjusted to 7.4
	Renilla buffer	2.2 mM EDTA 200 mM K_xPO4 1.1 M NaCl 0.44 mg/ml BSA [a] 2.5 µM Coelenterazine
Anthocyanins extraction	Anthocyanins extraction buffer	1.8 % (v/v) 1-Propanol 1% HCl

[a] Added freshly before use

5.1.7   Primers

Primers were produced by Life Technologies (Karlsruhe, Germany) and Sigma-Aldrich (Munich, Germany).

Table 8. List and description of primers used for molecular genotyping

Name	Sequence 5' to 3'	Reference
co-SAIL F	ACGACATAGGTAGTGGAGAGAACAAC	(Fackendahl, 2012)
co-SAIL R	ATCCACAAGGTTTAGATACTCATCAC	(Fackendahl, 2012)
JH2295 (FT-R1)	TAAGCTCAATGATATTCCCGTACA	(Yoo *et al.*, 2005)
JH2296 (FT-F1)	CAGGTTCAAAACAAGCCAAGA	(Yoo *et al.*, 2005)
Gabi-LB	CCCATTTGGACGTGAATGTAGACAC	(Fackendahl, 2012)
COP1-Seq F5	TTCCTGCGTTCATACTTAGAC	(Fackendahl, 2012)
cop1-4-seq	ATAAATGCCGTTGAGAGAC	(Fackendahl, 2012)
spa1-100 WT F1	CATTCATAATACTATTCTCACCAGC	(Fackendahl, 2012)
spa1-100 WT R1	GATTTAAGGTATGGAGGCTGTAG	(Fackendahl, 2012)
SPA2 geno F2	GGGAAAATGTCTTTGCCTGA	(Fackendahl, 2012)
SPA2 geno R2	AGCACGGCAAACCATCATA	(Fackendahl, 2012)
SPA3-F2	TTCGGACTCTGGCTCTGATTCCTTG	(Fackendahl, 2012)
SPA3-R4	GTCCTCATTGATGGTCGACAAGTT	(Fackendahl, 2012)
SPA4 geno F1	GGTCAAGAAGCTTCCTCGTG	(Fackendahl, 2012)
SPA4 geno R1	TCATCATCAAGTCCTCCCAAG	(Fackendahl, 2012)
SALK-LBb1.3	ATTTTGCCGATTTCGGAAC	(Fackendahl, 2012)
FISH geno1	CTGGGAATGGCGAAATCAAG	(Fackendahl, 2012)
N862394 RP2	AGACAAGGCTCTAGAGGTCTC	This study
N862394 LP	ATTGGTTCTAAACCAGTGGGG	This study
LB-SAIL	TAGCATCTGAATTTCATAACCA	(Fackendahl, 2012)
cop1_3534 fwd	TCGGTCTAAACTTAGTTGCTTGA	(Ordonez-Herrera *et al.*, 2015)
cop1_3840 rev	CCTTGCAGTCGTCACTACCA	(Ordonez-Herrera *et al.*, 2015)
pTiach5	CTACACGCCGAAATAAACGACCAA	(Ordonez-Herrera *et al.*, 2015)
Kan2 rev	ATACTTTCTCGGCAGGAGCA	(Ordonez-Herrera *et al.*, 2015)

LB1.3	ATTTTGCCGATTTCGGAAC	SIGnal,Salk http://signal.salk.edu/

Table 9. List and description of primers used for cloning

Primer name	Primer sequence 5' to 3'	Reference
COL12 CDS Gtway Fwd 1-20	GGGGACAAGTTTGTACAAAAAAGCAGGCTCGATGCCTAAGAAGAAGAGAAAGGTTGGAGAGCCAAAGTGTGACCA	(Menje, 2016)
COL12 CDS gtway Rev 1092-1073	GGGGACCACTTTGTACAAGAAAGCTGGGTCATTGTTCGTCGTCGGTGAT	(Menje, 2016)
COL12 CDS Gtway Fwd 127 - 147	GGGGACAAGTTTGTACAAAAAAGCAGGCTCGATGCCTAAGAAGAAGAGAAAGGTTGGAATACGCTCTTTGATCTGCGA	(Menje, 2016)
COL12 CDS gtway Rev 920 - 901	GGGGACCACTTTGTACAAGAAAGCTGGGTCCTTGCTTGTGGACAACTAAC	(Menje, 2016)
COL12 rev overlapp 277-290 / 113-126	GGAGAAGGACAACCGTGCCTGTGAGACA	(Menje, 2016)
COL12 fwd overlapp 113-126/ 277-290	TGTCTCACAGGCACGGTTGTCCTTCTCC	(Menje, 2016)
COL12 Gtway fwd NLS 277 - 296	GGGGACAAGTTTGTACAAAAAAGCAGGCTCGATGCCTAAGAAGAAGAGAAAGGTTGGAGGTTGTCCTTCTCCTACAGA	(Menje, 2016)
SPA1 SalI For	TGTCGTCGACAATGCCTGTTATGGAAAGAGTAGCTGAAG	(Holtkotte *et al.*, 2016)
SPA1 Delta WD XhoI rev (2088)	TACTCGAGAGCAAATTTGCACAACCCCTCGAA	This study
Gateway Fwd COL13	GGGGACAAGTTTGTACAAAAAAGCAGGCTCGATGGAAGCAGAAGAAGGTCATC	This study
Gateway Rev COL13	GGGGACCACTTTGTACAAGAAAGCTGGGTCTGGATCTGCTGCCTTGGCGAAAC	This study
EcoRI Fwd COL14	ATCCGAATTCATGGGTACTTCTACTACAGAGAGTG	This study
EcoRI rev COL14	CGTAGAATTCAGGATCTGTAGCTTTCACAAATCTG	This study

Table 10. List and description of primers used for sequencing of plasmids

Primer name	Primer sequence 5' to 3'	Construct name
pTREX_dest30_ProtA_GW F	GGATCCTCTAAACTCGAGCCCATC	pTREX_dest30_ProtA_GW
pTREX_dest30_ProtA_GW R	CTTACGCGTGCATGCGACGTCATG	pTREX_dest30_ProtA_GW
Primer cDNA Rluc F	GCGAGCTCTCGAGACAAGTTTG	pcDNA-RLuc
Primer cDNA Rluc R	CAGCGAGCTCTAGCATTTAGGTGAC	pcDNA-RLuc

CFP/YFP fwd	AGCTTATAATGGTGAGCAAGGGC	pENSG-YFP pENSG-CFP
pdNR207 Fwd primer	TCGCGTTAACGCTAGCATGGATCTC	pDNR207
pdNR207 Rev primer	GTAACATCAGAGATTTTGAGACAC	pDNR207
caMV_35S Fwd pEarly201	CGCACAATCCCACTATCCTT	pEarlygate201
pDEst17 fwd	CCGCGAAATTAATACGACTCACT	pDEST17
mCherry fwd	GCCCCGTAATGCAGAAGAAG	pAMARENA
pDNR221 Fwd	GTAAAACGACGGCCAG	pDNR221

Table 11. List and description of primers used for qRT-PCR and transgenic line characterization

Primer name	Primer sequence 5' to 3'	Reference
CO_Fwd_qPCR	CAACAGCTTCACACCCAAGAACG	(Wang *et al.*, 2014)
CO_Rev_qPCR	TTGCAGGGTCAGGTTGTTGCTC	(Wang *et al.*, 2014)
FT_Fwd_qPCR	GCTACAACTGGAACAACCTTTGGC	(Wang *et al.*, 2014)
FT_Rev_qPCR	TGAATTCCTGCAGTGGGACTTGG	(Wang *et al.*, 2014)
FLC_Fwd_qprc	TGTTCAACTGGAGGAACACCTTG	(Wang *et al.*, 2014)
FLC_Rev_qprc	AGCTTCAACATGAGTTCGGTCTTC	(Wang *et al.*, 2014)
SVP_Fwd_qprc	AACGCTGCTGTGTACGAGGAAG	(Wang *et al.*, 2014)
SVP_Rev_qprc	TCTCTAACCACCATACGGTAAGCC	(Wang *et al.*, 2014)
FUL_Fwd_qPCR	TCGAATATTCCACCGACTCTTGC	(Wang *et al.*, 2014)
FUL_Rev_qPCR	TTTGTGAAACGTCTCGGCCAAC	(Wang *et al.*, 2014)
SOC1_Fwd_qPCR	TTCGCCAGCTCCAATATGCAAG	(Wang *et al.*, 2014)
SOC1_Rev_qPCR	TGCTGACTCGATCCTTAGTATGCC	(Wang *et al.*, 2014)
COL12_qpcr4_fwd	CCATGGGAAACGAATTTTGA	(Trimborn, 2015)
COL12_qpcr4_rev	TCGTGTCAGCTCTTGCTTTG	(Trimborn, 2015)
COL12_qpcr6_fwd	GTGTGACCATTGTGCAACCT	(Trimborn, 2015)
COL12_qpcr6_rev	ACAGTTGCTTTCGTGCCAAT	(Trimborn, 2015)
COL11_qpcr1_fwd	TTACAACCCACGGCAGTACA	This study
COL11_qpcr1_rev	ATCTTGCCGAAATCTGATGG	This study
UBQ10_fwd	CACACTCCACTTGGTCTTGCGT	(Balcerowicz *et al.*, 2011)
UBQ10_rev	TGGTCTTTCCGGTGAGAGTCTTCA	(Balcerowicz *et al.*, 2011)

5.1.8 Plasmids

Plasmids that were employed for a variety of purposes along this study are shown in table 12.

Table 12. List and description of plasmids

Plasmid name	Description	Reference
pDNR221	Gateway cassette flanked by recombination attP sites. Kan^r	(Lifetechnologies, Thermofisher)
pENTR221_COL12	Contains the *COL12* CDS flanked by gateway recombination sites.	(Henschel, 2014)
pENTR221_COL15	Contains the *COL15* CDS flanked by gateway recombination sites.	(Henschel, 2014)
pENTR221_COL13	Contains the COL13 CDS flanked by gateway	This study

	recombination sites.	
pDNR207	Gateway cassette flanked by recombination attP sites. Amp^r	(Lifetechnologies, Thermofisher)
pENTR207_COL9	Contains the *COL9* CDS flanked by gateway recombination sites.	(Henschel, 2014)
pENTR207_COL10	Contains the *COL10* CDS flanked by gateway recombination sites.	(Henschel, 2014)
pENTR207_COL11	Contains the *COL11* CDS flanked by gateway recombination sites.	(Henschel, 2014)
pENTR 3C	Gateway cassette flanked by recombination attP sites and restriction sites. Kan^r	(Lifetechnologies, Thermofisher)
pENTR SPA1 ΔWD	Contains the *SPA1* CDS (1 – 2088) flanked by SalI and XhoI sites. SalI-SPA1 ΔWD - XhoI	This study
pENTR 3C COL14	Contains the *COL14* CDS flanked by EcoRI restriction sites and gateway recombination sites.	This study
pENTR_221_COL12 Δbbx1	Contains the *COL12* CDS 127 – 1073 flanked by gateway recombination sites.	(Menje, 2016)
pENTR_221_COL12 Δbbx2	Contains the *COL12* CDS 1 – 126 + 277 -1073 flanked by gateway recombination sites.	(Menje, 2016)
pENTR_221_COL12 Δbbx1 bbx2	Contains the *COL12* CDS 277 -1073 flanked by gateway recombination sites.	(Menje, 2016)
pENTR_221_COL12 Δcct	Contains the *COL12* CDS 1 – 920 flanked by gateway recombination sites.	(Menje, 2016)
pEarly Gate 201_COL9	*35S::HA-COL9*	(Henschel, 2014)
pEarly Gate 201_COL10	*35S::HA-COL10*	(Henschel, 2014)
pEarly Gate 201_COL11	*35S::HA-COL11*	(Henschel, 2014)
pEarly Gate 201_COL12	*35S::HA-COL12*	(Henschel, 2014)
pEarly Gate 201_COL15	*35S::HA-COL15*	(Henschel, 2014)
pENSG_CFP	Binary Gateway destination vector; 35S::CFP-Gateway. Amp^r	(Laubinger *et al.*, 2006)
pENSG_CFP_COL9	*35S::CFP-COL9*	(Henschel, 2014)
pENSG_CFP _COL10	*35S:: CFP -COL10*	(Henschel, 2014)
pENSG_CFP _COL11	*35S:: CFP -COL11*	(Henschel, 2014)
pENSG_CFP _COL12	*35S:: CFP -COL12*	(Henschel, 2014)
pENSG_CFP _COL15	*35S:: CFP -COL15*	(Henschel, 2014)
pENSG_YFP	Binary Gateway destination vector; 35S::YFP-Gateway. Amp^r	(Laubinger *et al.*, 2006)
pENSG_YFP_SPA1	*35S::YFP-SPA1*	(Holtkotte *et al.*, 2016)
pENSG_YFP_COP1	*35S::YFP-COP1*	(Holtkotte *et al.*, 2016)
35S::Gateway-YFP	*35S:: CO-YFP*	(Fernandez *et al.*, 2016)
pAMARENA	Binary Gateway destination vector; 35S::mChery-Gateway. Amp^r	M. Jakoby, GenBank ID: FR695418

pAMARENA_COL12	35S::mChery-*COL12* (CDS 1 – 1073)	This study
pAMARENA_COL12 Δbbx1	35S::mChery-*COL12 Δbbx1* (CDS 127 – 1073)	This study
pAMARENA_COL12 Δbbx2	35S::mChery-*COL12 Δbbx2* (CDS 1 – 126 + 277 -1073)	This study
pAMARENA_COL12 Δbbx1 bbx2	35S::mChery-*COL12 Δbbx1bbx2* (CDS 277 -1073)	This study
pAMARENA_COL12 Δcct	35S::mChery-*COL12 Δcct* (CDS 1 – 920)	This study
pcDNA-RLuc	Destination vector for expression in mammal cells. Contains SV40 promoter and the *R. reniformis* luciferase. SV40::RLuc-Gateway Amp[r]	(Barrios-Rodiles *et al.*, 2005)
pcDNA-RLuc-COP1	SV40::RLuc-*COP1*	(Kokkelink L, unpublished)
pcDNA-RLuc-COL12	SV40::RLuc-*COL12*	This study
pTREX-dest30-Prot A	Destination vector for expression in mammal cells. Contains SV40 promoter controlling the protA fusion. SV40::ProtA-Gateway. Amp[r]	(Barrios-Rodiles *et al.*, 2005)
pTREX-dest30-Prot A-CO	SV40::ProtA-*CO*	(Holtkotte *et al.*, 2016)
pDest17_COL9	Destination vector for expression in bacteria. T7::*COL9* Amp[r]	(Adrian, 2005)
pDest17_COL10	Destination vector for expression in bacteria. T7::*COL10* Amp[r]	(Adrian, 2005)
pDest17_COL11	Destination vector for expression in bacteria. T7::*COL11* Amp[r]	(Adrian, 2005)
pDest17_COL12	Destination vector for expression in bacteria. T7::*COL12* Amp[r]	(Adrian, 2005)
pDest17_COL15	Destination vector for expression in bacteria. T7::*COL15* Amp[r]	(Adrian, 2005)
pACT	Gateway destination vector for Y2H. Contains the GAL4 transcription activation domain (AD)	(Hülskamp, M, unpublished)
pAS	Gateway destination vector for Y2H. Contains the GAL4 DNA-binding domain (BD).	(Hülskamp, M, unpublished)
pACT_COL12	AD-COL12	This study
pACT_COL15	AD-COL15	This study
pACT_COL13	AD-COL13	This study
pCT_COL14	AD-COL14	This study
pAS_SPA1	BD-SPA1	(Kokkelink, unpublished)
pAS_SPA4	BD-SPA4	This study
pGBKT7 COP1	Vector used for Y2H. Contains the GAL4 DNA-binding domain (BD) fused to *COP1*.	(Maier *et al.*, 2013)

5.1.9   Plant materials

The *A. thaliana* transgenic lines and mutants subjected to analysis are listed in table 13.

Table 13. List of transgenic lines and mutants

Mutant/ transgenic line	Background	Reference
WT	Col-0	
cop1-4	Col-0	(McNellis *et al.*, 1994)
cop1-5	Wassilevskija (Ws)	(Deng *et al.*, 1992)
spa1 spa2 spa3 spa4 spaQn	Col-0	(Fackendahl, 2012)
co-SAIL (co-10)	Col-0	(Laubinger *et al.*, 2006)
ft-10	Col-0	(Yoo *et al.*, 2005)
SUC2::HA-CO co-SAIL	Col-0	(Jang *et al.*, 2009)
col12-1 (N862394)	Col-0	This study
35S::HA-COL12	Col-0	This study

5.1.10 Bacterial and yeast strains

The *Escherichia coli* strain DH5α was used for cloning of Gateway recombinant vectors. The *E. coli* strain DB3.1 was employed for cloning of empty vectors carrying the gateway cassette. The *Agrobacterium tumefaciens* strain GV3101::pMP90 (Chlo[r]/Rif[r]) was used for stable transformation of *A. thaliana* and transient transformation of *N. benthamiana*. The *Saccharomyces cerevisiae* strain AH109 was used for yeast-two-hybrid experiments.

5.2 Methods

5.2.1 Methods for plant growth

For growing plants on plates, sterile seeds were placed on MS solid medium. Seed sterilization was achieved incubating seeds with chlorine gas for 2-3 hours into a desiccator jar. Chlorine gas was generated by mixing 80 mL of Sodium hypochlorite with 2.5 mL of 37% HCl. Subsequently, the seeds were ventilated at a laminar flow chamber and placed on the top of the solid MS medium. Seed stratification was achieved by placing the plates at 4°C for 2-3 days. Then plates were kept into a growth chamber (CLF Plant Climatics, Wertingen, Germany) settled to at 21°C and continuous white light at the indicated fluence rates. Fluora L58W/77 fluorescent tubes (Osram, Munich, Germany) were used to produce white light. For switch experiments into different monochromatic light treatments R and B, LED light sources were used (Quantum Devices, Barneveld, WI, USA). Plant material was harvested using a green lamp.

For growing *A. thaliana* plants on soil, the seeds were incubated in 0.1 % agarose at 4°C for 3 days. Then, they were sown on soil that was prepared as a mixture of three parts soil and one part vermiculite. The plants were grown in walk-in growth chambers (Johnson Controls, Milwaukee, WI, USA) settled with 21°C and 60% humidity. Light cycles were programmed to either short day (8 h light/ 16 h darkness) or long day conditions (16 h light, 8 h dark). Plants were exposed to light generated by Lumilux L36W/840 cool white fluorescent tubes Osram, Munich, Germany) at light intensities of approximately 150-180 µmol m^{-2}s^{-1}.

5.2.2 Stable transformation and selection of transgenic plants

Arabidopsis thaliana plants were transformed using *Agrobacterium tumefaciens* by the floral dip method (Clough and Bent, 1998). *A. tumefaciens* was transformed by electroporation of competent cells. Transformed bacteria colonies were plated on LB medium containing antibiotics and allowed to regenerate for 3 days at 28°C. Afterward, individual colonies were inoculated into 5 ml of YEP containing antibiotics and incubated at 28°C, with mild shaking overnight. The pre-culture was used to start a 250 ml YEP culture incubated for 8-10 h. This culture was centrifuged at 4000 g for 15 min at 4 °C, the pelleted bacteria was re-suspended in ice-cold 5 % (w/v) sucrose to an $O.D._{600}$ of 0.8. The surfactant Silwet L-77 was added to a final concentration of 0.05 % (v/v) to facilitate the attachments of the bacteria to the plants. Plants at the reproductive stage were selected and maturing siliques removed manually. Next, the inflorescences of the plants were dipped into the *A. tumefaciens* solution for 1 min. Plants were then kept under low light and high humidity for 24 h.

Plants transformed with the pEarlyGate 201-derived plasmids were selected with Basta (Glufosinate-Ammonium, stock solution 18,5% (w/v)). Selection with Basta on soil was performed as follows. Seeds were sown on big trays and stratified for 2-3 days. When seedlings reached the cotyledon stage (approximately 8-10 days), they were sprayed with a solution containing 0,01% (v/v) Basta, 0.1% (v/v) Tween. Seedlings were repeatedly exposed to Basta, every second day during 6-8 days. Resistant plants were transferred to new pots and allowed to grow. For assessment of segregation ratio, transgenic plants were selected with Basta in a concentration of 185 mg/L on MS. Resistant plants were distinguished after 10 days of growth.

Selection of plants carrying the *SUC2::HA-CO* transgene were selected based on the presence of a fluorescent signal reflected by the seed coat monitored at a fluorescence stereoscope.

5.2.3 Isolation of *spa cop1* quintuple mutants

First, *spa1-100*, *spa2-2*, *spa3-1* and *spa4-3 (+/-)* quadruple mutant plants were crossed with plants heterozygous for *cop1-5*. F_1 seedlings were grown for 15 days on Murashige & Skoog medium (MS) supplemented with kanamycin (50 mg/ml) which selects for individuals carrying the *cop1-5* allele. Resistant seedlings were transferred to soil and the molecular genotype at *SP4* determined, thereby we isolated plants segregating for *spa1234* and *cop1-5* that were grown to maturation and selfed. Next, F_2 progeny was grown in darkness for 6 days, seedlings exhibiting a short hypocotyl and open cotyledons were transferred to MS solid medium with 2% sucrose and then to soil. The molecular genotype of mature plants at the 4 *SPA*s and *COP1* loci was determined using PCR-based markers, in order to identify *spa123 (-/-) spa4 (+/-) cop1-5 (+/-)* plants that were selected for further self-cross. We observed that F_3 seeds can be classified according to its testa color into black, brown or yellow seeds, among which black seeds are non-germinating mutant seeds. To circumvent the germination problem, embryos were manually released under a stereomicroscope (SMZ1000, Nikon, Japan) as described previously (Telfer *et al.*, 1997), subsequently placed on filter paper (n° 413, VWR International, France) or MS solid medium and allowed to grow for 4 days. To identify the quintuple *spa-nq cop1-5* mutant, we

analyzed the segregation of the phenotype and the *cop1-5 spa4* WT and mutant alleles in 40 individual members of the F$_3$ population. Genomic DNA from individual seedlings was isolated as described in (Edwards *et al.*, 1991) with the following modifications: Each embryo was disrupted and mixed with 100 μl of lysis buffer, Isopropanol was added to this mixture in a 1:1 ratio and the dried pellet was resuspended into 30 μl of TE.

A similar approach was undertaken for the isolation of *spa-nq cop1-4* quintuple mutant with the following modifications: Kanamycin selection was not performed and the presence of the *cop1-4* point mutation was determined using sequencing of a purified PCR product (COP1-SeqF5 + COP1-geno_R1) (High pure DNA purification kit, Roche, Manheim, Germany).

5.2.4 Isolation of genotypes of A. thaliana for molecular analysis of COL12

To test whether the COP1/SPA complex controls the protein stability of COL12, mutant plants *35S::HA-COL12 cop1-4* were obtained. To this end, we crossed *35S:HA-COL12* line # 8 with the *cop1-4* mutant, and selected at the F$_2$ generation with Basta on soil as well as resemblance to *cop1-4* adults. F$_3$ individual seed batches were collected and confirmed to be homozygous for *cop1-4*, by analysis of growth in darkness. For these batches, the expression of HA-COL12 was tested by protein detection. Seedlings expressing *35S:HA-COL12* in the cop1-4 background were compared to the control in WT background.

To test whether the protein stability of CO is altered by COL12 overexpression, plants that carried both *SUC2::HA-CO* and *35S::HA-COL12* transgenes were obtained. To this end, the *SUC2::HA-CO* co-SAIL line and *35S::HA-COL12* (lines # 16 and 20) were crossed and the F$_1$ plants selfed. The F$_2$ plants were propagated individually and at F$_3$ seed batches segregation analysis performed. The presence of *SUC2::HA-CO* was scored by the presence of the selectable marker, GFP signal in the seed coat. Seed batches with 100% fluorescent seeds were analyzed by protein detection using the anti-HA antibody.

5.2.5 *Nicotiana benthamiana* agroinfiltration

For transient expression of proteins in *N. benthamiana* plants, the leaves of mature plants were infiltrated with *A. tumefaciens* carrying the binary vectors. First, *A. tumefaciens* strain GV3101 was transformed with the vectors using electroporation. Bacteria was plated on YEB solid medium supplemented with antibiotics and grown for 2-3 days at 28°C. In parallel, the anti-silencing strain RK19 (Rif^r/Kan^r), which facilitates protein expression, was also grown. Regenerated colonies were cultured in 5 ml of YEB and incubated overnight at 28°C with mild shaking. Cell cultures were centrifuged at 4000 rpm (3200 g) for 15 min and re-suspended into 1 x Agromix buffer to a final OD$_{600}$ of 1. Equal amounts of RK19 and vector-transformed *A. tumefasiens* were mixed together with acetosyringone (150 μM). Cell suspensions were kept at room temperature for 3 h. In parallel, tobacco plants were kept for 1 h in low light and high humidity ambient. Next, 3-4 leaves were infiltrated using syringes without needles. Plants were kept in the greenhouse for 3 days.

5.2.6 Phenotypical analysis

5.2.6.1 Flowering time assessment

Plants were grown in soil under controlled conditions in either long day or short day conditions. Flowering time was measured by counting the total number of leaves at plant bolting, defined as the moment when the first floral bud is visible, and the number of days from seed transfer to the light chamber to bolting. In each experiment, 8-16 plants per genotype were assessed and each experiment was repeated twice. Differences between WT and other genotypes were estimated using ANOVA followed by Tukey's Post hoc Tukey test performed with R statistic package (R Development Core Team, 2005).

5.2.6.2 Rosette branching and inflorescence length

Plants were grown in LD conditions on soil as described in section 5.2.1. They were grown for 10 weeks when they start to dry and have reached their final size. The length of the main inflorescence stem, as well as the number of branches emerging from the rosette, were measured. In each experiment, 8-16 plants per genotype were assessed and each experiment was repeated twice. Differences between WT and other genotypes were estimated using ANOVA followed by Tukey's Post hoc Tukey test performed with R statistic package (R Development Core Team, 2005).

5.2.6.3 Hypocotyl length

To measure the seedlings hypocotyl length, seedlings were grown for 4 days as described in section 5.2.1. All genotypes for a specific light condition were grown on the same plate. Thereafter, seedlings were flattened on the MS plates and photographed using a digital camera. The images were used for length quantification using IMAJE J software (Wayne Rasband, NIH Image Software; Bethesda, USA). Statistical comparison was performed with ANOVA test.

5.2.6.4 Embryo dissection

Embryos were manually released under a stereomicroscope (SMZ1000, Nikon, Japan) as described previously (Telfer *et al.*, 1997). Seeds were placed on filter paper (n° 413, VWR International, France) and embedded in sterile water overnight. Afterward, microdissection tweezers were employed to remove the seed envelopes.

5.2.6.5 Comparison of *spa cop1* quintuple mutants

For the experimental comparisons of the quintuple spa cop1 mutants, a batch of plants corresponding to the following genotypes were grown in the greenhouse under the same environmental conditions: WT (Col), *cop1-4 (-/-),cop1-5 (+/-), spa123 (-/-) spa4 (+/-),spa123 (-/-) spa4 (+/-) cop1-5 (+/-)* and *spa123 (-/-) spa4 (+/-) cop1-4 (+/-)*.Seeds were classified according to its color because we observed that this trait can be correlated with the embryo's genotype. Thus, *spa-nq, cop1-5* (-/-) and *spa-nq cop1-4* (-/-) embryos were obtained from brown seeds among the offspring of the segregating parental *spa123 (-/-) spa4 (+/-), cop1-5 (+/-)* and *spa123 (-/-) spa4 (+/-) cop1-4 (+/-)* respectively. In contrast, the quintuple *spa-nq cop1-5* (-/-) embryos come from black seeds generated from the corresponding segregating parental.

Selected embryos were manually released as described in section 5.2.5.4 and exposed to either complete darkness or continuous white light (25 μmol m^{-2} s^{-1}) for 4 days.

5.2.6.6   Anthocyanin quantification

Seeds were placed on filter paper and embedded in sterile water overnight. On the next day, 15 mature embryos were manually released from selected seeds and mixed with 200 μl of extraction buffer. The mixture was boiled for 4 min and allowed to cooled for 1 h. Next, the samples were centrifuged at maximum speed for 15 minutes and 150 μl of the supernatant was transferred to a 96-well microtiter plate. The absorbance at 535 nm and 650 nm was measured using a Tecan Infinite 200 plate reader (Tecan, Männedorf, Switzerland). The Anthocyanin content was calculated as the difference between the sample's absorbance at 535 nm and A650 nm, after subtraction of the blank absorbance (Extraction buffer). Three biological replicates per genotype were used and the experiment was repeated twice.

5.2.7   Molecular biology methods

5.2.7.1   **Genomic DNA isolation from plants**

Genomic DNA from was isolated as described in (Edwards *et al.*, 1991). Thompson DNA extraction buffer. Plant tissue was harvested (approx. 100 mg) into a 1.5 tube (Eppendorf, Hamburg, Germany) and mixed with 400 μl Thompson DNA extraction buffer. Next, tissue was ground with a pestle until the tissue was disrupted. Then, the samples were centrifuged at 20000 g for 3 min and 200 μl of the supernatant transferred to a new tube. The supernatant was mixed with equal volume of Isopropanol and incubated on ice for 10 min. The solutions were centrifuged at 20000 g for 15 min. The pellets were washed with 100 μL Ethanol (70%) and centrifuged for 1 min. The supernatant was removed and the pellet allowed to dry before being re-suspended in 30-50 μl ddH2O. Resulting DNA solutions was kept at -20 °C for long-term storage.

For genotyping of individual embryos, the protocol was modified as follows: Each embryo was disrupted and mixed with 100 μl of lysis buffer, Isopropanol was added to this mixture in a 1:1 ratio and the dried pellet was re-suspended into 30 μl of TE.

5.2.7.2   Agarose gel electrophoresis

DNA and RNA were separated on agarose gels according to standard protocols (Sambrook and Russell, 2001). Gels were prepared by dissolving agarose [0.8 – 3 % (w/v)] into 0.5 x TBE and adding ethidium bromide (0.25 μg/ml). Nucleicc acids were visualized on a GEL Stick "Touch" imager (INTAS Science Imaging Instruments, Goettingen, Germany). The size of the bands was estimated by comparison with molecular weight markers, GeneRuler 1 kb DNA Ladder and GeneRuler Low Range DNA Ladder (Thermo Fischer).

5.2.7.3   Polymerase chain reaction (PCR)

Standard PCR was prepared in a 20 μl reaction volume with 1 μl of Taq DNA polymerase, 1 x PCR reaction buffer, forward and reverse primers (0.5 μM) and dNTPs (125 μM). As DNA template, 1 μl of cDNA or genomic DNA were used. The standard PCR program was performed as follows: Initial denaturation for 3 min at 95 °C, 40 cycles of denaturation for 30 s at 95 °C, annealing for 30 s at 55 °C and elongation for1 min per kb at 72 °C and a final elongation step of 10 min at 72 °C. For colony PCR, a small portion of a bacterial colony was used as a template and boiled for 5 minutes before adding the enzyme. For generating DNA fragments for cloning the proofreading polymerases, Pfu DNA Polymerase or Q5 High-Fidelity DNA Polymerase were used according to the manufacturer instructions.

5.2.7.4   DNA sequencing

The DNA sequences were determined for confirmation of new constructs, molecular genotype, and determination of insertion sites. The sequencing was performed by GATC biotech (Konstanz, Germany). The sequences were analyzed with Lasergene software (DNASTAR, Madison, WI, USA).

5.2.7.5   Methods for molecular cloning and generation of constructs

Standard protocols were employed for conventional cloning (Sambrook and Russell, 2001) using enzymes indicated in Table 3. Restriction digestion was performed by incubation at designated temperatures overnight and enzymes were inactivated as instructed by the manufacturer. PCR products and digested DNA fragments used for cloning were purified from agarose gels using the High Pure PCR Product Purification. DNA fragment dephosphorylation was performed treating samples with alkaline phosphatase for 1 h at 37°C. DNA concentration was determined by Nanodrop or estimated by relative comparison of the signal in agarose gels. Ligation was

performed using T4 ligase and an insert to vector molar ratio of 3-5:1, at 16°C overnight. The T4 ligase enzyme was inactivated prior to the transformation of *E. coli* cells.

For Gateway cloning, BP and LR reactions were performed as described by the manufacturer's protocol. The final reaction volume was modified to 10 µl and the components were proportionally added.

After transformation of bacteria and selection on antibiotics, colonies were picked and analyzed by colony PCR. Colonies carrying the desired constructs were cultured into 5 mL of LB at 37°C with mild shaking for 16 – 18 h. Plasmid DNA was extracted and sequences were verified by restriction enzyme digestion. The bacteria carrying the correct plasmids was propagated and used for clean plasmid isolation with the Nucleospin plasmid purification kit.

5.2.7.6 Bacterial transformation

E. coli were transformed by heat shock of chemically competent as described below. Competent cells were prepared and aliquots of 50 – 100 µl frozen at -80°C for long-term storage. At the time of the transformation, aliquots of cells were thawed on ice and mixed with 50-100 ng plasmid. The mixture was shaken manually and incubated for 15 min on ice. The mixture was subjected to heat-shock at 42 °C for 90 s and subsequent cooling on ice for 5 min. Then, bacteria were regenerated in a 1 ml culture containing LB medium without antibiotics and incubated at 37 °C for 1 h. Finally, the cell suspension was centrifuged at 20000 g for 1 minute and the pelleted cells spread onto solid LB supplemented with antibiotics.

A. tumefasiens were transformed by electroporation of competent cells. To prepare competent cells: First, three to four single colonies were inoculated into 250 ml LB medium and cultured at 28°C until reaching an OD_{600} of 0.5. Next, the culture was centrifuged at 4000 g and 4°C for 10 min and the pellet resuspended into 300 ml of ice-cold water. The pellet was washed 3 times, each time with 300 ml ice-cold 10% (v/v) glycerol. A final was performed and the pellet was re-suspended in 1-2 ml 10% (v/v) glycerol. Aliquots of 40 µl were prepared, snap-frozen in liquid nitrogen and stored at -80°C for long-term.

At the time of the transformation, aliquots were placed on ice and mixed with 100-250 ng of plasmid DNA. The mixture was incubated on ice for 5-15 min and then electroporated using the MicropulserTM electroporator (Bio-Rad Laboratories, Munich, Germany) according to instructions of the manufacturer. Then, bacteria were regenerated in a 1 ml culture containing LB medium without antibiotics and incubated at 28 °C for 4 h. Finally, the cell suspension was centrifuged at 20000 g for 1 minute and the pelleted cells spread onto solid LB supplemented with antibiotics.

5.2.8 Cloning strategy for truncated SPA1 into pENTR 3C

For cloning of the truncated SPA1 ΔWD-repeats into the pENTR 3C vector, PCR amplification and traditional cloning were performed. pENTR SPA1 was used as a template for DNA amplification with specific primers (Section 5.1.7). The sequence of interest was flanked by SalI and XhoI restriction sites that were used to generate sticky ends and integrate the fragment into the vector backbone.

5.2.9   Cloning strategy for COLs into pENTR vectors

The coding sequences of *Arabidopsis thaliana* COLs from group III were cloned into pDONR vectors (Gateway®, Germany) to generate the corresponding pENTR vectors. Cloning was performed by BP recombination reactions, started from either pDest17 vectors or PCR amplicons generated using *A thaliana* cDNA and specific primers (Section 5.1.7). For *COL14,* traditional cloning was used to introduce the coding sequence into pDONR 3C, for this the CDS was flanked with EcoRI restriction sites.

The coding sequences that were cloned from pDest17 are: *COL9* (At3g07650), *COL10 (at5g48250), COL11 (at4g15250), COL12* (at3g21880) and *COL15* (at1g28050). The ones amplified from CDNA are *COL13* (at2g47890) and *COL14* (at2g33500).

5.2.10 Cloning strategy of deletion versions of COL12 into pENTR vectors

The COL12 deletion constructs were created using gene-specific primers (Table 9) and pENTR221_COL12 as a template. Domain regions were defined based on amino acid homology to *CO*. The cloned sequences span the nucleotide positions indicated in brackets: Lacking the N-terminal BBX1 domain (COL12 Δbbx1) (127 – 1073), without the bbx2 domain (COL12 Δbbx2) (1 – 126 + 277 -1073), without both BBX domains (COL12 Δbbx1 bbx2) missing the C-terminal CCT domain (COL12 Δcct) (1 - 920).

5.2.11 Cloning of Expression vectors

All the expression vectors were obtained by LR reactions (Gateway®, Germany).

5.2.12 Quantitative real-time PCR (qRT-PCR)

Samples of plant tissue (0.1 g) were harvested and snap-frozen in liquid nitrogen. Tissue was disrupted with mortar and pestle until obtaining a fine powder. Alternatively, frozen samples were ground by three cycles of shaking at 30 Hz for 1 min using a TissueLyser (Qiagen, Venlo, The Netherlands). Total RNA was extracted using the RNeasy Plant Mini Kit according to the manufacturers' protocol. The quality of the RNA was verified by visualization in agarose gels (0.8% w/v) and the RNA concentration quantified by spectrophotometry (NanoDrop, Thermoscientific).

DNase treatment and reverse transcription of mRNA were performed. For removal of genomic DNA, 1 µg of total RNA was treated with DNase I in a 20 µl reaction volume filled with RNAse-free water and incubated at 37 °C for 30 min. The DNase was inactivated by addition of 2 µl EDTA (50 µM) and incubation at 65°C for 20 min. To test if the RNA mixtures contained remaining DNA, 2 µl of the reaction mix were used as a template in a standard PCR with primers for UBQ10. DNase-treated RNA samples were either used immediately or stored at -80 °C.

Reverse transcription was performed in a reaction mix containing 1 µg of DNase-treated RNA, 0.5 µM oligo(dT)18 primers, 1mM dNTPs, 1 x reaction buffer and 1µl RevertAid H Minus Reverse transcriptase. First, the RNA was mixed with oligo-(dT) 18 primers and denatured at 65 °C for 5 min. After a short incubation on ice, the mixture was supplemented with dNTPs, reaction buffer and reverse transcriptase and the volume were filled to 40 µl with RNase-free water. The mixture was incubated at 42 °C for 3 h to allow cDNA synthesis. Subsequently, the reverse transcriptase was inactivated at 70 °C for 10 min. The cDNA samples were stored at -20 °C.

To perform the relative quantification of transcripts, a qRT-PCR reaction was prepared by mixing 1µ of diluted cDNA (1:10), 7.5 µl of SYBR FAST qPCR Mastermix and primers (0.15 µM) to a final volume of 15 µL. Samples were poured into 96-well plates, each sample was replicated twice. Each plate included the quantification of the reference gene (UBQ10) and the genes of interest. To compare samples among plates, a normalizing sample was tested on every plate. The real-time PCR was operated and quantified by the 7300 real-time PCR system (Applied Biosystems, Life Technologies, Karlsruhe, Germany). The PCR program consisted of an initial denaturation step at 95 °C for 2 min, followed by 40 cycles of a denaturation step at 95 °C for 2 s and a combined annealing and an elongation step at 60 °C for 30 s. For the melting curve analysis, a dissociation stage consisting of two cycles of 60 °C for 15 s and 95 °C for 15 s was performed at the end of each run. Relative transcript levels were calculated using the $2^{\Delta\Delta CT}$ method (Hellemans *et al.*, 2007, Schmittgen and Livak, 2008). For each experiment, two to four biological replicates were analyzed and statistically differences calculated with ANOVA using R software (R Development Core Team, 2005). Experiments were repeated two to three times.

The sequences of primers used in the quantification of genes of interest were obtained from the literature or designed by Primer3 software (Untergasser *et al.*, 2012) (Section 5.1.7). The primer efficiency was assessed performing the quantification of a dilution series and plotting the logarithm of the dilution factor against the corresponding C_T values. Then, efficiency was calculated using the formula: Efficiency=$10^{-1/slope}$.

5.2.13 Treatment with protease inhibitor

Seedlings were grown on solid MS, then were transferred to either water supplemented with MG132 (Calbiochem, EMD Millipore, Billerica, MA, USA) at a final concentration of 50 µM or water with the same volume of DMSO. Seedlings were incubated with the chemical for 4 hours under the same growing conditions. Subsequently, the seedlings were subjected to the different

light treatments. Protein was extracted as described in section 5.2.11. The experiments were repeated three times.

5.2.14 Protein isolation

Samples of plant tissue (100 mg) were harvested and snap-frozen in liquid nitrogen. Samples were ground using a TissueLyser (Qiagen, Venlo, The Netherlands) for 3-5 cycles of shaking at 30 Hz for 1 min. Alternatively, samples were ground with mortar and pestle and collected into 2 ml tubes. Nuclear enrichment protocol was performed as described in (Farrona *et al.*, 2011). The tissue powder was mixed throughout with 1.2 ml of nuclear enrichment buffer (Table 7) and centrifuged at 2790 *g* at 4°C, the supernatant was discarded and the pellet resuspended into 1 ml of the same buffer. The pellets were washed three more times, decreasing the rotation speed to 1780, 1000 and 690 g at 4°C. Next, the pellet was eluted into the same volume of 2 x Lämmli (50 – 100 µL), vortexed briefly and heated at 95°C for 10 minutes. Samples were centrifuged at 2790 g for 3 minutes and the supernatants collected into new tubes. Proteins were detected by western blotting and immunoblot as explained in section 5.2.12. Experiments were repeated at least three times.

5.2.15 Protein detection

Proteins were separated by SDS-polyacrylamide gel electrophoresis (SDS-PAGE) using the Mini-PROTEAN Tetra cell electrophoresis system (Bio-Rad Laboratories, Munich, Germany). Gel solutions were prepared and allowed to solidify (Section 5.1.6), stacking gels contained 5.0% acrylamide and resolving gels contained acrylamide in concentrations of 10, 12.5 or 15% (v/v). Solid gels were mixed with 1 x SDS running gel and loaded with samples together with the PageRuler Prestained Protein Ladder (Thermo Fisher Scientific, Schwerte, Germany) used to estimate the molecular weight of the proteins. A constant current of 15 mA was applied until the front line run out of the gel.

For Western blot, the separated protein samples were blotted onto PVDF membranes that had been activated in Methanol prior to assembly. Gels and PVDF were moisturized into 1 x carbonate blotting buffer and assembled together with filter paper. The assembly was immersed into 1 x carbonate buffer into a Mini-PROTEAN Tetra cell electrophoresis system. A constant voltage of 45 V was applied for 2 h.

After blotting, immunodetection was performed as follows. To avoid unspecific antibody binding, PVDF Membranes were blocked with a Rotiblock solution (Carl Roth GmbH, Karlsruhe, Germany) for 1 h at room temperature with mild rotation. Next, the primary antibody solutions were prepared into a solution containing skimmed milk 3% (w/v) in 1 x TBS. Membranes were placed into the antibody solutions into sealed plastic bags and incubated at 4 °C overnight with mild rotation. After incubation, membranes were washed with TBS-T three times for 10 mins. Then, membranes were incubated with a solution containing the horseradish peroxidase (HRP)-conjugated secondary antibody and skimmed milk 3% (w/v) in 1 x TBS, at room temperature for 1

h. Membranes were washed with TBS-T three times. Finally, the HRP activity was detected using the SuperSignal West Femto Maximum Sensitivity kit and visualized by a LAS-4000 Mini bioimager (GE Healthcare Life Sciences, Piscataway, USA). The signal intensities were quantified using FIJI software (Schindelin *et al.*, 2012).

5.2.16 Co-immunoprecipitation

The co-immunoprecipitation was performed as described in (Fernandez *et al.*, 2016). The epitope-tagged proteins of interest, HA-COL12, and CO-YFP, were expressed in *N. benthamiana* as described in section 5.2.4. The tobacco leaves were snap-frozen in liquid nitrogen, then ground with mortar and pestle and 300 mg were collected into 2 mL tubes. The powder was mixed with 1 mL of nuclear isolation buffer (Table 7), mixed thought and centrifuged at 2790 g (4000 rpm) at 4°C for 10 min, the supernatant was discarded and the pellet resuspended into 1 ml of the same buffer. The washes were repeated 3 times more. The pellet was re-suspended in 200 µl of sonication buffer. The samples were sonicated at high power for 10 minutes on intervals of 15 s sonication and 15 s pause, performed by a water bath sonicator (Bioruptor Plus, diagenode, Liege, Belgium) filled with cold water. The disrupted solutions were mixed with 2 volumes of sonication buffer and NaCl to a concentration of 0.1 M and incubated for 15 min at 4 °C. For clearing the lysate, the samples were centrifuged at maximum speed at maximum speed 4°C. Then the supernatant was collected and the input sample collected and mixed with equal volume of 2 x Lammli buffer. The rest of the cleared lysate was used for the Co-IP.

For the Co-IP, the lysate was mixed with 15 µl of anti-HA magnetic µMACS microbeads (Miltenyi Biotec, Germany) and incubated at 4°C for 30 min in a circular rotor. Next, the µ columns (Miltenyi Biotec, Germany) were placed in the magnetic field of the µMACSTM separator (Miltenyi, Germany) and the µ columns were moisturized by adding 200 µl of sonication buffer without protease inhibitors. Then, the mixture of lysate and microbeads was loaded into the µ columns and let it run through. The columns were rinsed with washing buffer (Table 7) 4 times. The immunoprecipitated fraction was eluted into 60 µl of elution buffer provided by the µMACS Epitope Tag Protein Isolation Kit.

The input and IP fractions were loaded on 12.5% acrylamide gels and detected with anti-HA-HRP and anti-GFP. The experiment was repeated three times.

5.2.17 Transformation of leek epidermal cells

The transient expression of chimeric fluorescent proteins in leek epidermal cells was achieved by particle bombardment. To this end, 5 µl of gold particles were mixed with 400 ng of each plasmid of interest, 10 µl of 2.5 M CaCl$_2$ and 4 µl of fresh spermidine 0.1 M. The mixture was incubated at RT for 15 min, then spinned down and the supernatant was discarded. The gold particles were washed with 100 µl 70% ethanol and 50% ethanol. Finally, the gold particles were resuspended in 12 µl 100% ethanol, distributed on a macrocarrier (Bio-Rad, Hercules, USA) and dried until the ethanol evaporated. Meanwhile, inner layers of leek were cut into small pieces (approximately 2

cm x 3 cm) and placed into Petri dishes. Particle bombardment was carried out with a helium Helios gun (Bio-Rad,Hercules, USA) according to manufacturer,s instructions and Rupture disks breaking at 900 psi were used in all experiments. After bombardment, the samples were incubated at RT for 15-24 h and then used for confocal microscope analysis.

5.2.18 Confocal microscopy and FRET-FLIM analysis

For the co-localization and FRET-FLIM analysis, living cells carrying YFP and mCherry fluorescent proteins were imaged using a confocal laser scanning microscope (SP8, Leica, Microsystems, Wetzlar, Germany). For the co-localization, the cells were imaged sequentially at both channels: YFP was excited with the pulsed picosecond laser emitting at 470 nm at a frequency of 40 MHz and detected in the 490 nm - 540 nm range, mCherry was excited with a laser emitting at 561 nm and detected in the range of 670 – 740 nm.

The occurrence of FRET was inferred by comparing of the florescence lifetime (FLIM) of the YFP donor alone or in presence of the acceptor. For the FLIM measurements, excitation of the donor was done with a pulsed picosecond laser emitting at 470 nm at a frequency of 40 MHz (Leica, Microsystems, Wetzlar, Germany). The fluorescence emission was acquired by the FLIM-PMT detector at a range of 490-540 nm. FLIM was determined by time-correlated single photon counting (TCSPC) using a time-correlated single photon counting unit (PicoHarp 300, PicoQuant, Germany). The nuclear speckles were delimited as regions of interest to generate the TCSPC histogram that were deconvoluted and fitted to monoexponential decay using the SymPhoTime software (PicoQuant, Germany). Thus, the lifetime and Chi square were obtained and only cells in which the Chi square was lower than one were considered for the analysis.

5.2.19 LUMIER assay

For the LUMIER assay, first chimeric proteins of interest were generated using the pTREX-dest30-Prot A and pcDNA-RLuc vectors. The proteins were expressed in HEK293TN cells that grew in an incubator at 37°C and 5% CO_2 (SANYO Electric, Japan). First, trypsinized cells were quantified and equal amounts seeded into the wells of a 24-well plate. The culture was completed with 1 ml/well of DMEM and incubated overnight. Then, the plasmid DNA (1 µg) was mixed with DMEM (100 µl) and 2 µl of peqFECT (PEQLAB, Erlangen, Germany) and incubated for 20 min at RT. Finally, the DNA-DMEM-peqFECT mixture was transferred to the wells containing the HEK293TN cells and incubated for 2 days.

For the ProtA Co-IP, the HEK293TN cell suspensions were harvested into 1.5 ml microtubes and centrifuged at 600 g for 15 min at 4°C. The pellets were collected and washed twice with 1 x PBS. The cell suspensions were resuspended in 80 µl of lysis buffer (Table 7), incubated on ice for 30 min and centrifuged at maximum speed (14000 rpm) for 10 min at 4°C. The supernatants were transferred to new microtubes and part of it separated for the input fraction. Then, 50 µl of the lysate were mixed with 5 µl of Dynabeads R Sheep-anti Mouse IgG (Life technologies, Carlsbad, CA, USA) and incubated at 4°C for 1 h in a circular rotator. The Dyna beads were collected using a

magnetic separator and washed for 5 times with 200 µl ice-cold PBS. After the washes, the beads were re-suspended in 50 µl PBS and transferred to a white microtiter plate. For the measurement of total luciferase protein, the input lysate was diluted 1:10 and 1:100 into 1 x PBS and transferred together with eluted beads into a microtiter plate. The concentration of luciferase activity was measured by monitoring the luminescence after addition of a buffer containing substrate using a TECAN luminometer (Infinite M200, TECAN). For each combination of RLuc and ProtA vectors, the luciferase measurements were performed triplicates.

5.2.20 Yeast-two-hybrid

Yeast-two-hybrid experiments were performed as described previously (Gietz *et al.*, 1995). The strain AH109 yeast strain was transformed with selected pAS, pACT and pGBKT7 plasmids to reconstitute the GAL4 transcription factor. Yeast cells were inoculated in 50 ml liquid YADP medium. The Erlenmeyer flask was incubated at 30°C on a rotary shaker until OD_{600} reached 0.6 – 1.0. Cells were harvested by centrifugation (3000 rpm, 5 min) in a 50 ml Falcon tube. The supernatant was discarded and the pellet washed with 20 ml sterile water. After another centrifugation step (3000 rpm, 5 min) the cells were re-suspended in 1.5 ml sterile 1x TE, 100 mM lithium acetate. For the transformation of yeast cells, 1 µg of bait and prey plasmids were mixed with 250 µg salmon sperm DNA (denatured by 2 min boiling) and 50 µl of yeast cell suspension. The samples were mixed with 300 µl of a solution containing PEG [40% (v/v)], lithium acetate 10 mM Tris. 1 mM EDTA, 100 mM lithium acetate (100 mM), 1x TE. Then, the mixtures were incubated and shaken for 30 min at 30°C. Afterward, 35 µl of DMSO were supplemented to the cell suspensions and incubated at 42°C for 15 min. After centrifugation for 1 min at 10000 rpm, the cells were resuspended in 100 µl of 1x TE. Transformed cells were plated onto synthetic "drop-out"media, -Trp -Leu as transformation control and -Trp-Leu-His as indicative of interaction. After plating, the samples were kept at 30 °C for 3 -5 days. In case auto-activation of the GAL4 was detected in the negative control sample, 3-amino-1,2,4-triazol (3-AT) solution was added to the media to enhance stringency. Experiments were repeated three times and for each set of experiments the positive and negative controls were grown on the same plate.

6 References

Abe, M., Kobayashi, Y., Yamamoto, S., Daimon, Y., Yamaguchi, A., Ikeda, Y., Ichinoki, H., Notaguchi, M., Goto, K. and Araki, T. (2005) FD, a bZIP protein mediating signals from the floral pathway integrator FT at the shoot apex. *Science*, **309**, 1052-1056.

Adrian, J. (2005) Interaction analysis between COP1 and SPA1 and CONSTANS-LIKE (COLs) in Arabidopsis. In *Botanical Institute*: University of Cologne.

Adrian, J., Farrona, S., Reimer, J.J., Albani, M.C., Coupland, G. and Turck, F. (2010) cis-Regulatory elements and chromatin state coordinately control temporal and spatial expression of FLOWERING LOCUS T in Arabidopsis. *Plant Cell*, **22**, 1425-1440.

Aguilar-Martínez, J.A., Poza-Carrión, C. and Cubas, P. (2007) Arabidopsis BRANCHED1 acts as an integrator of branching signals within axillary buds. *Plant Cell*, **19**, 458-472.

Albani, M.C. and Coupland, G. (2010) Comparative analysis of flowering in annual and perennial plants. *Curr Top Dev Biol*, **91**, 323-348.

Andres, F. and Coupland, G. (2012) The genetic basis of flowering responses to seasonal cues. *Nat Rev Genet*, **13**, 627-639.

Andres, F., Porri, A., Torti, S., Mateos, J., Romera-Branchat, M., Garcia-Martinez, J.L., Fornara, F., Gregis, V., Kater, M.M. and Coupland, G. (2014) SHORT VEGETATIVE PHASE reduces gibberellin biosynthesis at the Arabidopsis shoot apex to regulate the floral transition. *Proc Natl Acad Sci U S A*, **111**, 2760-2769.

Arsovski, A.A., Galstyan, A., Guseman, J.M. and Nemhauser, J.L. (2012) Photomorphogenesis. *Arabidopsis Book*, **10**, e0147.

Bajar, B.T., Wang, E.S., Zhang, S., Lin, M.Z. and Chu, J. (2016) A Guide to Fluorescent Protein FRET Pairs. *Sensors*, **16**, 1488.

Balcerowicz, M., Fittinghoff, K., Wirthmueller, L., Maier, A., Fackendahl, P., Fiene, G., Koncz, C. and Hoecker, U. (2011) Light exposure of Arabidopsis seedlings causes rapid de-stabilization as well as selective post-translational inactivation of the repressor of photomorphogenesis SPA2. *Plant J*, **65**, 712-723.

Barrios-Rodiles, M., Brown, K.R., Ozdamar, B., Bose, R., Liu, Z., Donovan, R.S., Shinjo, F., Liu, Y., Dembowy, J., Taylor, I.W., Luga, V., Przulj, N., Robinson, M., Suzuki, H., Hayashizaki, Y., Jurisica, I. and Wrana, J.L. (2005) High-throughput mapping of a dynamic signaling network in mammalian cells. *Science*, **307**, 1621-1625.

Ben-Naim, O., Eshed, R., Parnis, A., Teper-Bamnolker, P., Shalit, A., Coupland, G., Samach, A. and Lifschitz, E. (2006) The CCAAT binding factor can mediate interactions between CONSTANS-like proteins and DNA. *Plant J*, **46**, 462-476.

Böhlenius, H., Huang, T., Charbonnel-Campaa, L., Brunner, A.M., Jansson, S., Strauss, S.H. and Nilsson, O. (2006) Regulatory Module Controls Timing of Flowering and Seasonal Growth Cessation in Trees. *Science*, **312**, 1040-1043.

Boss, P.K., Bastow, R.M., Mylne, J.S. and Dean, C. (2004) Multiple pathways in the decision to flower: Enabling, promoting, and resetting. *Plant Cell*, **16**, S18-S31.

Buenning, E. (1936) Die endogene Tagesrhythmik als Grundlage der photoperiodischen Reaktion. *Bot. Ges*, **54**, 590-607.

Cao, S., Kumimoto, R.W., Gnesutta, N., Calogero, A.M., Mantovani, R. and Holt, B.F. (2014) A Distal CCAAT/NUCLEAR FACTOR Y Complex Promotes Chromatin Looping at the FLOWERING LOCUS T Promoter and Regulates the Timing of Flowering in Arabidopsis. *Plant Cell*, **26**, 1009-1017.

Casal, J.J. (2013) Photoreceptor Signaling Networks in Plant Responses to Shade. *Annu Rev Plant Biol*, **64**, 403-427.

Castillejo, C. and Pelaz, S. (2008) The balance between CONSTANS and TEMPRANILLO activities determines FT expression to trigger flowering. *Curr Biol*, **18**, 1338-1343.

Castle, L.A. and Meinke, D.W. (1994) A FUSCA gene of Arabidopsis encodes a novel protein essential for plant development. *Plant Cell*, **6**, 25-41.

Chang, C.S., Maloof, J.N. and Wu, S.H. (2011) COP1-mediated degradation of BBX22/LZF1 optimizes seedling development in Arabidopsis. *Plant Physiol*, **156**, 228-239.

Chen, F., Li, B.S., Li, G., Charron, J.B., Dai, M.Q., Shi, X.R. and Deng, X.W. (2014a) Arabidopsis Phytochrome A Directly Targets Numerous Promoters for Individualized Modulation of Genes in a Wide Range of Pathways. *Plant Cell*, **26**, 1949-1966.

Chen, H.D., Huang, X., Gusmaroli, G., Terzaghi, W., Lau, O.S., Yanagawa, Y., Zhang, Y., Li, J.G., Lee, J.H., Zhu, D.M. and Deng, X.W. (2010) Arabidopsis CULLIN4-Damaged DNA Binding Protein 1 Interacts with CONSTITUTIVELY PHOTOMORPHOGENIC1-SUPPRESSOR OF PHYA Complexes to Regulate Photomorphogenesis and Flowering Time. *Plant Cell*, **22**, 108-123.

Chen, M., MacGregor, D.R., Dave, A., Florance, H., Moore, K., Paszkiewicz, K., Smirnoff, N., Graham, I.A. and Penfield, S. (2014b) Maternal temperature history activates Flowering Locus T in fruits to control progeny dormancy according to time of year. *Proc Natl Acad Sci U S A*, **111**, 18787-18792.

Chen, S., Lory, N., Stauber, J. and Hoecker, U. (2015) Photoreceptor Specificity in the Light-Induced and COP1-Mediated Rapid Degradation of the Repressor of Photomorphogenesis SPA2 in Arabidopsis. *PLoS Genet*, **11**, e1005516.

Chen, S., Wirthmueller, L., Stauber, J., Lory, N., Holtkotte, X., Leson, L., Schenkel, C., Ahmad, M. and Hoecker, U. (2016) The functional divergence between SPA1 and SPA2 in Arabidopsis photomorphogenesis maps primarily to the respective N-terminal kinase-like domain. *BMC Plant Biol*, **16**, 165.

Cheng, X.F. and Wang, Z.Y. (2005) Overexpression of COL9, a CONSTANS-LIKE gene, delays flowering by reducing expression of CO and FT in Arabidopsis thaliana. *Plant J*, **43**, 758-768.

Clough, S.J. and Bent, A.F. (1998) Floral dip: a simplified method forAgrobacterium-mediated transformation ofArabidopsis thaliana. *Plant J*, **16**, 735-743.

Corbesier, L. and Coupland, G. (2006) The quest for florigen: a review of recent progress. *J Exp Bot*, **57**, 3395-3403.

Crocco, C.D., Locascio, A., Escudero, C.M., Alabadi, D., Blazquez, M.A. and Botto, J.F. (2015) The transcriptional regulator BBX24 impairs DELLA activity to promote shade avoidance in Arabidopsis thaliana. *Nat Commun*, **6**, 6202.

Datta, S., Hettiarachchi, G.H.C.M., Deng, X.W. and Holm, M. (2006) Arabidopsis CONSTANS-LIKE3 is a positive regulator of red light signaling and root growth. *Plant Cell*, **18**, 70-84.

Datta, S., Johansson, H., Hettiarachchi, C., Irigoyen, M.L., Desai, M., Rubio, V. and Holm, M. (2008) LZF1/SALT TOLERANCE HOMOLOG3, an Arabidopsis B-box protein involved in light-dependent development and gene expression, undergoes COP1-mediated ubiquitination. *Plant Cell*, **20**, 2324-2338.

Debeaujon, I. and Koornneef, M. (2000) Gibberellin requirement for Arabidopsis seed germination is determined both by testa characteristics and embryonic abscisic acid. *Plant Physiol*, **122**, 415-424.

Debeaujon, I., Leon-Kloosterziel, K.M. and Koornneef, M. (2000) Influence of the testa on seed dormancy, germination, and longevity in Arabidopsis. *Plant Physiol*, **122**, 403-414.

Deng, X.W., Matsui, M., Wei, N., Wagner, D., Chu, A.M., Feldmann, K.A. and Quail, P.H. (1992) Cop1, an Arabidopsis Regulatory Gene, Encodes a Protein with Both a Zinc-Binding Motif and a G-Beta Homologous Domain. *Cell*, **71**, 791-801.

Dickopf, S. (2015) The role of COP1 and SPA genes in the moss Physcomitrella patens. In *Botanical INstitute*. Cologne: University of Cologne.

Domagalska, M.A. and Leyser, O. (2011) Signal integration in the control of shoot branching. *Nat Rev Mol Cell Bio*, **12**, 211-221.

Dornan, D., Wertz, I., Shimizu, H., Arnott, D., Frantz, G.D., Dowd, P., O' Rourke, K., Koeppen, H. and Dixit, V.M. (2004) The ubiquitin ligase COP1 is a critical negative regulator of p53. *Nature*, **429**, 86-92.

Edwards, K., Johnstone, C. and Thompson, C. (1991) A simple and rapid method for the preparation of plant genomic DNA for PCR analysis. *Nucleic Acids Res*, **19**, 1349.

Endo, M., Tanigawa, Y., Murakami, T., Araki, T. and Nagatani, A. (2013) PHYTOCHROME-DEPENDENT LATE-FLOWERING accelerates flowering through physical interactions with phytochrome B and CONSTANS. *Proc Natl Acad Sci USA*, **110**, 18017-18022.

Fackendahl, P.C. (2012) Functional Analysis of Arabidopsis SPA Proteins in Plant Growth Control. In *Botanical institute*. Cologne: University of cologne.

Fan, X.Y., Sun, Y., Cao, D.M., Bai, M.Y., Luo, X.M., Yang, H.J., Wei, C.Q., Zhu, S.W., Sun, Y., Chong, K. and Wang, Z.Y. (2012) BZS1, a B-box Protein, Promotes Photomorphogenesis Downstream of Both Brassinosteroid and Light Signaling Pathways. *Mol Plant*, **5**, 591-600.

Farrona, S., Thorpe, F.L., Engelhorn, J., Adrian, J., Dong, X., Sarid-Krebs, L., Goodrich, J. and Turck, F. (2011) Tissue-specific expression of FLOWERING LOCUS T in Arabidopsis is maintained independently of polycomb group protein repression. *Plant Cell*, **23**, 3204-3214.

Feldmann, K.A. and Marks, M.D. (1987) Agrobacterium-mediated transformation of germinating seeds of Arabidopsis thaliana: a non-tissue culture approach. *Molecular and General Genetics MGG*, **208**, 1-9.

Fernandez, V., Takahashi, Y., Le Gourrierec, J. and Coupland, G. (2016) Photoperiodic and thermosensory pathways interact through CONSTANS to promote flowering at high temperature under short days. *Plant J*, **86**, 426-440.

Fittinghoff, K., Laubinger, S., Nixdorf, M., Fackendahl, P., Baumgardt, R.L., Batschauer, A. and Hoecker, U. (2006) Functional and expression analysis of Arabidopsis SPA genes during seedling photomorphogenesis and adult growth. *Plant J*, **47**, 577-590.

Fornara, F., de Montaigu, A. and Coupland, G. (2010) SnapShot: Control of flowering in Arabidopsis. *Cell*, **141**, 550, 550 e551-552.

Gangappa, S.N. and Botto, J.F. (2014) The BBX family of plant transcription factors. *Trends Plant Sci*, **19**, 460-470.

Gangappa, S.N., Crocco, C.D., Johansson, H., Datta, S., Hettiarachchi, C., Holm, M. and Botto, J.F. (2013) The Arabidopsis B-BOX Protein BBX25 Interacts with HY5, Negatively Regulating BBX22 Expression to Suppress Seedling Photomorphogenesis. *Plant Cell*, **25**, 1243-1257.

Gietz, R.D., Schiestl, R.H., Willems, A.R. and Woods, R.A. (1995) Studies on the transformation of intact yeast cells by the LiAc/ss-DNA/PEG procedure. *Yeast*, **11**, 355-360.

Gil, K.E., Park, M.J., Lee, H.J., Park, Y.J., Han, S.H., Kwon, Y.J., Seo, P.J., Jung, J.H. and Park, C.M. (2017) Alternative splicing provides a proactive mechanism for the diurnal CONSTANS dynamics in Arabidopsis photoperiodic flowering. *Plant J*, **89**, 128-140.

Goto, N., Kumagai, T. and Koornneef, M. (1991) Flowering Responses to Light-Breaks in Photomorphogenic Mutants of Arabidopsis-Thaliana, a Long-Day Plant. *Physiol Plantarum*, **83**, 209-215.

Graeff, M., Straub, D., Eguen, T., Dolde, U., Rodrigues, V., Brandt, R. and Wenkel, S. (2016) MicroProtein-Mediated Recruitment of CONSTANS into a TOPLESS Trimeric Complex Represses Flowering in Arabidopsis. *Plos Genetics*, **12**.

Griffiths, S., Dunford, R.P., Coupland, G. and Laurie, D.A. (2003) The evolution of CONSTANS-like gene families in barley, rice, and Arabidopsis. *Plant Physiol*, **131**, 1855-1867.

Guo, H.W., Yang, W.Y., Mockler, T.C. and Lin, C.T. (1998) Regulations of flowering time by Arabidopsis photoreceptors. *Science*, **279**, 1360-1363.

Hajdu, A., Adam, E., Sheerin, D.J., Dobos, O., Bernula, P., Hiltbrunner, A., Kozma-Bognar, L. and Nagy, F. (2015) High-level expression and phosphorylation of phytochrome B modulates flowering time in Arabidopsis. *Plant J*, **83**, 794-805.

Halliday, K.J., Salter, M.G., Thingnaes, E. and Whitelam, G.C. (2003) Phytochrome control of flowering is temperature sensitive and correlates with expression of the floral integrator FT. *Plant J*, **33**, 875-885.

Hartmann, U., Hohmann, S., Nettesheim, K., Wisman, E., Saedler, H. and Huijser, P. (2000) Molecular cloning of SVP: a negative regulator of the floral transition in Arabidopsis. *Plant J*, **21**, 351-360.

Hassidim, M., Harir, Y., Yakir, E., Kron, I. and Green, R.M. (2009) Over-expression of CONSTANS-LIKE 5 can induce flowering in short-day grown Arabidopsis. *Planta*, **230**, 481-491.

He, G., Elling, A.A. and Deng, X.W. (2011) The epigenome and plant development. *Annu Rev Plant Biol*, **62**, 411-435.

Heijde, M. and Ulm, R. (2012) UV-B photoreceptor-mediated signalling in plants. *Trends Plant Sci*, **17**, 230-237.

Hellemans, J., Mortier, G., De Paepe, A., Speleman, F. and Vandesompele, J. (2007) qBase relative quantification framework and software for management and automated analysis of real-time quantitative PCR data. *Genome Biol*, **8**, R19.

Hempel, F.D. and Feldman, L.J. (1994) Bi-directional inflorescence development inArabidopsis thaliana: Acropetal initiation of flowers and basipetal initiation of paraclades. *Planta*, **192**, 276-286.

Henschel, M. (2014) Analysis of protein-protein-interaction between COP1/SPA and CONSTANS-LIKE proteins in Arabidopsis thaliana: University of Cologne.

Hiraoka, K., Yamaguchi, A., Abe, M. and Araki, T. (2013) The Florigen Genes FT and TSF Modulate Lateral Shoot Outgrowth in Arabidopsis thaliana. *Plant Cell Physiol*, **54**, 352-368.

Hoecker, U. (2005) Regulated proteolysis in light signaling. *Curr Opin Plant Biol*, **8**, 469-476.

Hoecker, U. and Quail, P.H. (2001) The phytochrome A-specific signaling intermediate SPA1 interacts directly with COP1, a constitutive repressor of light signaling in Arabidopsis. *J Biol Chem*, **276**, 38173-38178.

Hoecker, U., Tepperman, J.M. and Quail, P.H. (1999) SPA1, a WD-repeat protein specific to phytochrome A signal transduction. *Science*, **284**, 496-499.

Holm, M., Hardtke, C.S., Gaudet, R. and Deng, X.W. (2001) Identification of a structural motif that confers specific interaction with the WD40 repeat domain of Arabidopsis COP1. *Embo J*, **20**, 118-127.

Holtkotte, X., Dieterle, S., Kokkelink, L., Artz, O., Leson, L., Fittinghoff, K., Hayama, R., Ahmad, M. and Hoecker, U. (2016) Mutations in the N-terminal kinase-like domain of the repressor of photomorphogenesis SPA1 severely impair SPA1 function but not light responsiveness in Arabidopsis. *Plant J*, **88**, 205-218.

Huang, X., Ding, J., Effgen, S., Turck, F. and Koornneef, M. (2013a) Multiple loci and genetic interactions involving flowering time genes regulate stem branching among natural variants of Arabidopsis. *New Phytol*, **199**, 843-857.

Huang, X., Ouyang, X.H. and Deng, X.W. (2014) Beyond repression of photomorphogenesis: role switching of COP/DET/FUS in light signaling. *Curr Opin Plant Biol*, **21**, 96-103.

Huang, X., Ouyang, X.H., Yang, P.Y., Lau, O.S., Chen, L.B., Wei, N. and Deng, X.W. (2013b) Conversion from CUL4-based COP1-SPA E3 apparatus to UVR8-COP1-SPA complexes underlies a distinct biochemical function of COP1 under UV-B. *Proc Natl Acad Sci U S A* **110**, 16669-16674.

Hyun, Y., Kim, J., Cho, S.W., Choi, Y., Kim, J.S. and Coupland, G. (2015) Site-directed mutagenesis in Arabidopsis thaliana using dividing tissue-targeted RGEN of the CRISPR/Cas system to generate heritable null alleles. *Planta*, **241**, 271-284.

Imaizumi, T., Tran, H.G., Swartz, T.E., Briggs, W.R. and Kay, S.A. (2003) FKF1 is essential for photoperiodic-specific light signalling in Arabidopsis. *Nature*, **426**, 302-306.

Jaeger, K.E. and Wigge, P.A. (2007) FT protein acts as a long-range signal in Arabidopsis. *Current Biology*, **17**, 1050-1054.

Jang, S., Marchal, V., Panigrahi, K.C., Wenkel, S., Soppe, W., Deng, X.W., Valverde, F. and Coupland, G. (2008) Arabidopsis COP1 shapes the temporal pattern of CO accumulation conferring a photoperiodic flowering response. *Embo J*, **27**, 1277-1288.

Jang, S., Torti, S. and Coupland, G. (2009) Genetic and spatial interactions between FT, TSF and SVP during the early stages of floral induction in Arabidopsis. *Plant J*, **60**, 614-625.

Jiao, Y.L., Ma, L.G., Strickland, E. and Deng, X.W. (2005) Conservation and divergence of light-regulated genome expression patterns during seedling development in rice and Arabidopsis. *Plant Cell*, **17**, 3239-3256.

Jung, J.-H., Domijan, M., Klose, C., Biswas, S., Ezer, D., Gao, M., Khattak, A.K., Box, M.S., Charoensawan, V., Cortijo, S., Kumar, M., Grant, A., Locke, J.C.W., Schäfer, E., Jaeger, K.E. and Wigge, P.A. (2016) Phytochromes function as thermosensors in Arabidopsis. *Science*, **354**, 886-889.

Kami, C., Lorrain, S., Hornitschek, P. and Fankhauser, C. (2010) Light-Regulated Plant Growth and Development. *Plant Development*, **91**, 29-66.

Kardailsky, I., Shukla, V.K., Ahn, J.H., Dagenais, N., Christensen, S.K., Nguyen, J.T., Chory, J., Harrison, M.J. and Weigel, D. (1999) Activation tagging of the floral inducer FT. *Science*, **286**, 1962-1965.

Kim, D.Y., Scalf, M., Smith, L.M. and Vierstra, R.D. (2013) Advanced proteomic analyses yield a deep catalog of ubiquitylation targets in Arabidopsis. *Plant Cell*, **25**, 1523-1540.

Kim, S.Y., Yu, X. and Michaels, S.D. (2008) Regulation of CONSTANS and FLOWERING LOCUS T expression in response to changing light quality. *Plant Physiol*, **148**, 269-279.

Kobayashi, Y., Kaya, H., Goto, K., Iwabuchi, M. and Araki, T. (1999) A pair of related genes with antagonistic roles in mediating flowering signals. *Science*, **286**, 1960-1962.

Koornneef, M., Hanhart, C.J. and Vanderveen, J.H. (1991) A Genetic and Physiological Analysis of Late Flowering Mutants in Arabidopsis-Thaliana. *Mol Gen Genet*, **229**, 57-66.

Krzymuski, M., Andres, F., Cagnola, J.I., Jang, S., Yanovsky, M.J., Coupland, G. and Casal, J.J. (2015) The dynamics of FLOWERING LOCUS T expression encodes long-day information. *Plant J*, **83**, 952-961.

Lau, O.S. and Deng, X.W. (2012) The photomorphogenic repressors COP1 and DET1: 20 years later. *Trends Plant Sci*, **17**, 584-593.

Laubinger, S., Fittinghoff, K. and Hoecker, U. (2004) The SPA quartet: A family of WD-repeat proteins with a central role in suppression of photomorphogenesis in arabidopsis. *Plant Cell*, **16**, 2293-2306.

Laubinger, S., Marchal, V., Le Gourrierec, J., Wenkel, S., Adrian, J., Jang, S., Kulajta, C., Braun, H., Coupland, G. and Hoecker, U. (2006) Arabidopsis SPA proteins regulate photoperiodic flowering and interact with the floral inducer CONSTANS to regulate its stability. *Development*, **133**, 3213-3222.

Lazaro, A., Mouriz, A., Pineiro, M. and Jarillo, J.A. (2015) Red Light-Mediated Degradation of CONSTANS by the E3 Ubiquitin Ligase HOS1 Regulates Photoperiodic Flowering in Arabidopsis. *Plant Cell*, **27**, 2437-2454.

Lazaro, A., Valverde, F., Pineiro, M. and Jarillo, J.A. (2012) The Arabidopsis E3 Ubiquitin Ligase HOS1 Negatively Regulates CONSTANS Abundance in the Photoperiodic Control of Flowering. *Plant Cell*, **24**, 982-999.

Leivar, P. and Quail, P.H. (2011) PIFs: pivotal components in a cellular signaling hub. *Trends Plant Sci*, **16**, 19-28.

Lian, H.L., He, S.B., Zhang, Y.C., Zhu, D.M., Zhang, J.Y., Jia, K.P., Sun, S.X., Li, L. and Yang, H.Q. (2011) Blue-light-dependent interaction of cryptochrome 1 with SPA1 defines a dynamic signaling mechanism. *Gene Dev*, **25**, 1023-1028.

Liu, B., Zuo, Z.C., Liu, H.T., Liu, X.M. and Lin, C.T. (2011) Arabidopsis cryptochrome 1 interacts with SPA1 to suppress COP1 activity in response to blue light. *Gene Dev*, **25**, 1029-1034.

Liu, L., Farrona, S., Klemme, S. and Turck, F.K. (2014) Post-fertilization expression of FLOWERING LOCUS T suppresses reproductive reversion. *Front Plant Sci*, **5**, 164.

Liu, L.J., Zhang, Y.C., Li, Q.H., Sang, Y., Mao, J., Lian, H.L., Wang, L. and Yang, H.Q. (2008) COP1-mediated ubiquitination of CONSTANS is implicated in cryptochrome regulation of flowering in Arabidopsis. *Plant Cell*, **20**, 292-306.

Losi, A. and Gartner, W. (2012) The Evolution of Flavin-Binding Photoreceptors: An Ancient Chromophore Serving Trendy Blue-Light Sensors. *Annu Rev Plant Biol*, **63**, 49-72.

Lu, X.D., Zhou, C.M., Xu, P.B., Luo, Q., Lian, H.L. and Yang, H.Q. (2015a) Red-light-dependent interaction of phyB with SPA1 promotes COP1-SPA1 dissociation and photomorphogenic development in Arabidopsis. *Mol Plant*, **8**, 467-478.

Lu, X.D., Zhou, C.M., Xu, P.B., Luo, Q., Lian, H.L. and Yang, H.Q. (2015b) Red-Light-Dependent Interaction of phyB with SPA1 Promotes COP1-SPA1 Dissociation and Photomorphogenic Development in Arabidopsis. *Mol Plant*, **8**, 467-478.

Ma, L.G., Gao, Y., Ou, L.J., Chen, Z.L., Li, J.M., Zhao, H.Y. and Deng, X.W. (2002) Genomic evidence for COP1 as a repressor of light-regulated gene expression and development in Arabidopsis. *Plant Cell*, **14**, 2383-2398.

Maier, A., Schrader, A., Kokkelink, L., Falke, C., Welter, B., Iniesto, E., Rubio, V., Uhrig, J.F., Hulskamp, M. and Hoecker, U. (2013) Light and the E3 ubiquitin ligase COP1/SPA control the protein stability of the MYB transcription factors PAP1 and PAP2 involved in anthocyanin accumulation in Arabidopsis. *Plant J*, **74**, 638-651.

Mateos, J.L., Madrigal, P., Tsuda, K., Rawat, V., Richter, R., Romera-Branchat, M., Fornara, F., Schneeberger, K., Krajewski, P. and Coupland, G. (2015) Combinatorial activities of SHORT VEGETATIVE PHASE and FLOWERING LOCUS C define distinct modes of flowering regulation in Arabidopsis. *Genome Biol*, **16**, 31.

McNellis, T.W., Vonarnim, A.G., Araki, T., Komeda, Y., Misera, S. and Deng, X.W. (1994) Genetic and Molecular Analysis of an Allelic Series of Cop1 Mutants Suggests Functional Roles for the Multiple Protein Domains. *Plant Cell*, **6**, 487-500.

Menje, M. (2016) Domain mapping analysis of Arabidopsis COL12 protein-protein interaction. Cologne: University of Cologne.

Menon, C., Sheerin, D.J. and Hiltbrunner, A. (2016) SPA proteins: SPAnning the gap between visible light and gene expression. *Planta*, **244**, 297-312.

Michaels, S.D. and Amasino, R.M. (1999) FLOWERING LOCUS C Encodes a Novel MADS Domain Protein That Acts as a Repressor of Flowering. *Plant Cell*, **11**, 949-956.

Mockler, T., Yang, H., Yu, X., Parikh, D., Cheng, Y.-c., Dolan, S. and Lin, C. (2003) Regulation of photoperiodic flowering by Arabidopsis photoreceptors. *Proc Natl Acad Sci U S A*, **100**, 2140-2145.

Niwa, M., Daimon, Y., Kurotani, K., Higo, A., Pruneda-Paz, J.L., Breton, G., Mitsuda, N., Kay, S.A., Ohme-Takagi, M., Endo, M. and Araki, T. (2013) BRANCHED1 Interacts with FLOWERING LOCUS T to Repress the Floral Transition of the Axillary Meristems in Arabidopsis. *Plant Cell*, **25**, 1228-1242.

Ordonez-Herrera, N., Fackendahl, P., Yu, X., Schaefer, S., Koncz, C. and Hoecker, U. (2015) A cop1 spa Mutant Deficient in COP1 and SPA Proteins Reveals Partial Co-Action of COP1 and SPA during Arabidopsis Post-Embryonic Development and Photomorphogenesis. *Mol Plant*, **8**, 479-481.

Pacin, M., Legris, M. and Casal, J.J. (2014) Rapid Decline in Nuclear COSTITUTIVE PHOTOMORPHOGENESIS1 Abundance Anticipates the Stabilization of Its Target ELONGATED HYPOCOTYL5 in the Light. *Plant Physiol*, **164**, 1134-1138.

Peng, H.Z., Begg, G.E., Schultz, D.C., Friedman, J.R., Jensen, D.E., Speicher, D.W. and Rauscher, F.J. (2000) Reconstitution of the KRAB-KAP-1 repressor complex: A model system for defining the molecular anatomy of RING-B box-coiled-coil domain-mediated protein-protein interactions. *J Mol Biol*, **295**, 1139-1162.

Putterill, J., Robson, F., Lee, K., Simon, R. and Coupland, G. (1995) The CONSTANS gene of Arabidopsis promotes flowering and encodes a protein showing similarities to zinc finger transcription factors. *Cell*, **80**, 847-857.

Reed, J.W., Nagpal, P., Poole, D.S., Furuya, M. and Chory, J. (1993) Mutations in the gene for the red/far-red light receptor phytochrome B alter cell elongation and physiological responses throughout Arabidopsis development. *Plant Cell*, **5**, 147-157.

Robson, F., Costa, M.M., Hepworth, S.R., Vizir, I., Pineiro, M., Reeves, P.H., Putterill, J. and Coupland, G. (2001) Functional importance of conserved domains in the flowering-time gene CONSTANS demonstrated by analysis of mutant alleles and transgenic plants. *Plant J*, **28**, 619-631.

Rodríguez-Falcón, M., Bou, J. and Prat, S. (2006) Seasonal control of tuberization in potato: conserved elements with the flowering response. *Annu Rev Plant Biol*, **57**, 151-180.

Romera-Branchat, M., Andres, F. and Coupland, G. (2014) Flowering responses to seasonal cues: what's new? *Curr Opin Plant Biol*, **21**, 120-127.

Romero-Campero, F.J., Lucas-Reina, E., Said, F.E., Romero, J.M. and Valverde, F. (2013) A contribution to the study of plant development evolution based on gene co-expression networks. *Front Plant Sci*, **4**.

Saijo, Y., Sullivan, J.A., Wang, H.Y., Yang, J.P., Shen, Y.P., Rubio, V., Ma, L.G., Hoecker, U. and Deng, X.W. (2003) The COP1-SPA1 interaction defines a critical step in phytochrome A-mediated regulation of HY5 activity. *Gene Dev*, **17**, 2642-2647.

Saijo, Y., Zhu, D., Li, J., Rubio, V., Zhou, Z., Shen, Y., Hoecker, U., Wang, H. and Deng, X.W. (2008a) Arabidopsis COP1/SPA1 complex and FHY1/FHY3 associate with distinct phosphorylated forms of phytochrome A in balancing light signaling. *Mol Cell*, **31**, 607-613.

Saijo, Y., Zhu, D.M., Li, J.G., Rubio, V., Zhou, Z.Z., Shen, Y.P., Hoecker, U., Wang, H.Y. and Deng, X.W. (2008b) Arabidopsis COP1/SPA1 complex and FHY1/FHY3 associate with distinct phosphorylated forms of phytochrome a in balancing light signaling. *Mol Cell*, **31**, 607-613.

Salazar, J.D., Saithong, T., Brown, P.E., Foreman, J., Locke, J.C.W., Halliday, K.J., Carre, I.A., Rand, D.A. and Millar, A.J. (2009) Prediction of Photoperiodic Regulators from Quantitative Gene Circuit Models. *Cell*, **139**, 1170-1179.

Samach, A. and Coupland, G. (2000) Time measurement and the control of flowering in plants. *Bioessays*, **22**, 38-47.

Samach, A., Onouchi, H., Gold, S.E., Ditta, G.S., Schwarz-Sommer, Z., Yanofsky, M.F. and Coupland, G. (2000) Distinct roles of CONSTANS target genes in reproductive development of Arabidopsis. *Science*, **288**, 1613-1616.

Sambrook, J. and Russell, D. (2001) *Molecular cloning: a laboratory manual. Cold Spring 798 Harbor Laboratory Press*: Cold Spring Harbor, NY.

Sarid-Krebs, L., Panigrahi, K.C., Fornara, F., Takahashi, Y., Hayama, R., Jang, S., Tilmes, V., Valverde, F. and Coupland, G. (2015) Phosphorylation of CONSTANS and its COP1-dependent degradation during photoperiodic flowering of Arabidopsis. *Plant J*, **84**, 451-463.

Schindelin, J., Arganda-Carreras, I., Frise, E., Kaynig, V., Longair, M., Pietzsch, T., Preibisch, S., Rueden, C., Saalfeld, S., Schmid, B., Tinevez, J.Y., White, D.J., Hartenstein, V., Eliceiri, K., Tomancak, P. and Cardona, A. (2012) Fiji: an open-source platform for biological-image analysis. *Nat Methods*, **9**, 676-682.

Schmid, M., Davison, T.S., Henz, S.R., Pape, U.J., Demar, M., Vingron, M., Scholkopf, B., Weigel, D. and Lohmann, J.U. (2005) A gene expression map of Arabidopsis thaliana development. *Nat Genet*, **37**, 501-506.

Schmittgen, T.D. and Livak, K.J. (2008) Analyzing real-time PCR data by the comparative CT method. *Nature protocols*, **3**, 1101-1108.

Searle, I. and Coupland, G. (2004) Induction of flowering by seasonal changes in photoperiod. *Embo J*, **23**, 1217-1222.

Seo, H.S., Yang, J.Y., Ishikawa, M., Bolle, C., Ballesteros, M.L. and Chua, N.H. (2003) LAF1 ubiquitination by COP1 controls photomorphogenesis and is stimulated by SPA1. *Nature*, **423**, 995-999.

Serrano, G., Herrera-Palau, R., Romero, J.M., Serrano, A., Coupland, G. and Valverde, F. (2009) Chlamydomonas CONSTANS and the evolution of plant photoperiodic signaling. *Curr Biol*, **19**, 359-368.

Shalit, A., Rozman, A., Goldshmidt, A., Alvarez, J.P., Bowman, J.L., Eshed, Y. and Lifschitz, E. (2009) The flowering hormone florigen functions as a general systemic regulator of growth and termination. *Proc Natl Acad Sci U S A* **106**, 8392-8397.

Sheerin, D.J., Menon, C., Oven-Krockhaus, S.Z., Enderle, B., Zhu, L., Johnen, P., Schleifenbaum, F., Stierhof, Y.D., Huq, E. and Hiltbrunner, A. (2015) Light-Activated Phytochrome A and B Interact with Members of the SPA Family to Promote Photomorphogenesis in Arabidopsis by Reorganizing the COP1/SPA Complex. *Plant Cell*, **27**, 189-201.

Sheldon, C.C., Burn, J.E., Perez, P.P., Metzger, J., Edwards, J.A., Peacock, W.J. and Dennis, E.S. (1999) The FLF MADS Box Gene: A Repressor of Flowering in Arabidopsis Regulated by Vernalization and Methylation. *Plant Cell*, **11**, 445-458.

Simon, R., Igeno, M.I. and Coupland, G. (1996) Activation of floral meristem identity genes in Arabidopsis. *Nature*, **384**, 59-62.

Simon, S., Ruhl, M., de Montaigu, A., Wotzel, S. and Coupland, G. (2015) Evolution of CONSTANS Regulation and Function after Gene Duplication Produced a Photoperiodic Flowering Switch in the Brassicaceae. *Mol Biol Evol*, **32**, 2284-2301.

Song, Y.H., Estrada, D.A., Johnson, R.S., Kim, S.K., Lee, S.Y., MacCoss, M.J. and Imaizumi, T. (2014) Distinct roles of FKF1, GIGANTEA, and ZEITLUPE proteins in the regulation of CONSTANS stability in Arabidopsis photoperiodic flowering. *Proc Natl Acad Sci U S A*, **111**, 17672-17677.

Song, Y.H., Smith, R.W., To, B.J., Millar, A.J. and Imaizumi, T. (2012) FKF1 Conveys Timing Information for CONSTANS Stabilization in Photoperiodic Flowering. *Science*, **336**, 1045-1049.

Suarez-Lopez, P. and Coupland, G. (1998) Plants see the blue light. *Science*, **279**, 1323-1324.

Telfer, A., Bollman, K.M. and Poethig, R.S. (1997) Phase change and the regulation of trichome distribution in Arabidopsis thaliana. *Development*, **124**, 645-654.

Teper-Bamnolker, P. and Samach, A. (2005) The flowering integrator FT regulates SEPALLATA3 and FRUITFULL accumulation in Arabidopsis leaves. *Plant Cell*, **17**, 2661-2675.

Tiwari, S.B., Shen, Y., Chang, H.C., Hou, Y.L., Harris, A., Ma, S.F., McPartland, M., Hymus, G.J., Adam, L., Marion, C., Belachew, A., Repetti, P.P., Reuber, T.L. and Ratcliffe, O.J. (2010) The flowering time regulator CONSTANS is recruited to the FLOWERING LOCUS T promoter via a unique cis-element. *New Phytologist*, **187**, 57-66.

Trimborn, L. (2015) Molecular characterization of CONSTANS LIKE 12 in Arabidopsis thaliana: University of Cologne.

Turck, F. and Coupland, G. (2014) Natural variation in epigenetic gene regulation and its effects on plant developmental traits. *Evolution*, **68**, 620-631.

Turck, F., Fornara, F. and Coupland, G. (2008) Regulation and identity of florigen: FLOWERING LOCUS T moves center stage. *Annu Rev Plant Biol*, **59**, 573-594.

Uljon, S., Xu, X., Durzynska, I., Stein, S., Adelmant, G., Marto, J.A., Pear, W.S. and Blacklow, S.C. (2016) Structural Basis for Substrate Selectivity of the E3 Ligase COP1. *Structure*, **24**, 687-696.

Untergasser, A., Cutcutache, I., Koressaar, T., Ye, J., Faircloth, B.C., Remm, M. and Rozen, S.G. (2012) Primer3--new capabilities and interfaces. *Nucleic Acids Res*, **40**, e115.

Valverde, F., Mouradov, A., Soppe, W., Ravenscroft, D., Samach, A. and Coupland, G. (2004) Photoreceptor regulation of CONSTANS protein in photoperiodic flowering. *Science*, **303**, 1003-1006.

Velten, J. and Schell, J. (1985) Selection-expression plasmid vectors for use in genetic transformation of higher plants. *Nucleic Acids Research*, **13**, 6981-6998.

Vonarnim, A.G. and Deng, X.W. (1994) Light Inactivation of Arabidopsis Photomorphogenic Repressor Cop1 Involves a Cell-Specific Regulation of Its Nucleocytoplasmic Partitioning. *Cell*, **79**, 1035-1045.

Wang, C.Q., Guthrie, C., Sarmast, M.K. and Dehesh, K. (2014) BBX19 Interacts with CONSTANS to Repress FLOWERING LOCUS T Transcription, Defining a Flowering Time Checkpoint in Arabidopsis. *Plant Cell*, **26**, 3589-3602.

Wang, C.Q., Sarmast, M.K., Jiang, J. and Dehesh, K. (2015) The Transcriptional Regulator BBX19 Promotes Hypocotyl Growth by Facilitating COP1-Mediated EARLY FLOWERING3 Degradation in Arabidopsis. *Plant Cell*, **27**, 1128-1139.

Wang, H.G., Zhang, Z.L., Li, H.Y., Zhao, X.Y., Liu, X.M., Ortiz, M., Lin, C.T. and Liu, B. (2013) CONSTANS-LIKE 7 regulates branching and shade avoidance response in Arabidopsis. *J Exp Bot*, **64**, 1017-1024.

Wang, J.W., Czech, B. and Weigel, D. (2009) miR156-Regulated SPL Transcription Factors Define an Endogenous Flowering Pathway in Arabidopsis thaliana. *Cell*, **138**, 738-749.

Wenkel, S., Turck, F., Singer, K., Gissot, L., Le Gourrierec, J., Samach, A. and Coupland, G. (2006) CONSTANS and the CCAAT box binding complex share a functionally important domain and interact to regulate flowering of Arabidopsis. *Plant Cell*, **18**, 2971-2984.

Wigge, P.A., Kim, M.C., Jaeger, K.E., Busch, W., Schmid, M., Lohmann, J.U. and Weigel, D. (2005) Integration of spatial and temporal information during floral induction in Arabidopsis. *Science*, **309**, 1056-1059.

Wollenberg, A.C., Strasser, B., Cerdán, P.D. and Amasino, R.M. (2008) Acceleration of flowering during shade avoidance in Arabidopsis alters the balance between FLOWERING LOCUS C-mediated repression and photoperiodic induction of flowering. *Plant Physiol*, **148**, 1681-1694.

Xu, D.Q., Jiang, Y., Li, J.G., Lin, F., Holm, M. and Deng, X.W. (2016a) BBX21, an Arabidopsis B-box protein, directly activates HY5 and is targeted by COP1 for 26S proteasome-mediated degradation. *Proc Natl Acad Sci U S A*, **113**, 7655-7660.

Xu, F., Li, T., Xu, P.B., Li, L., Du, S.S., Lian, H.L. and Yang, H.Q. (2016b) DELLA proteins physically interact with CONSTANS to regulate flowering under long days in Arabidopsis. *FEBS Lett*, **590**, 541-549.

Yamaguchi, A., Kobayashi, Y., Goto, K., Abe, M. and Araki, T. (2005) TWIN SISTER OF FT (TSF) acts as a floral pathway integrator redundantly with FT. *Plant Cell Physiol*, **46**, 1175-1189.

Yang, J., Lin, R., Hoecker, U., Liu, B., Xu, L. and Wang, H. (2005a) Repression of light signaling by Arabidopsis SPA1 involves post-translational regulation of HFR1 protein accumulation. *Plant J*, **43**, 131-141.

Yang, J., Lin, R., Sullivan, J., Hoecker, U., Liu, B., Xu, L., Deng, X.W. and Wang, H. (2005b) Light regulates COP1-mediated degradation of HFR1, a transcription factor essential for light signaling in Arabidopsis. *Plant Cell*, **17**, 804-821.

Yang, J.P. and Wang, H.Y. (2006) The central coiled-coil domain and carboxyl-terminal WD-repeat domain of Arabidopsis SPA1 are responsible for mediating repression of light signaling. *Plant J*, **47**, 564-576.

Yanovsky, M.J. and Kay, S.A. (2002) Molecular basis of seasonal time measurement in Arabidopsis. *Nature*, **419**, 308-312.

Yi, C.L. and Deng, X.W. (2005) COP1 - from plant photomorphogenesis to mammalian tumorigenesis. *Trends Cell Biol*, **15**, 618-625.

Yoo, S.K., Chung, K.S., Kim, J., Lee, J.H., Hong, S.M., Yoo, S.J., Yoo, S.Y., Lee, J.S. and Ahn, J.H. (2005) CONSTANS activates SUPPRESSOR OFOVEREXPRESSION OFCONSTANS 1 through FLOWERING LOCUS T to promote flowering in Arabidopsis. *Plant Physiol*, **139**, 770-778.

Yoshida, S., Mandel, T. and Kuhlemeier, C. (2011) Stem cell activation by light guides plant organogenesis. *Gene Dev*, **25**, 1439-1450.

Zhang, B.L., Wang, L., Zeng, L.P., Zhang, C. and Ma, H. (2015) Arabidopsis TOE proteins convey a photoperiodic signal to antagonize CONSTANS and regulate flowering time. *Gene Dev*, **29**, 975-987.

Zhang, Z.L., Ji, R.H., Li, H.Y., Zhao, T., Liu, J., Lin, C.T. and Liu, B. (2014) CONSTANS-LIKE 7 (COL7) Is Involved in Phytochrome B (phyB)-Mediated Light-Quality Regulation of Auxin Homeostasis. *Mol Plant*, **7**, 1429-1440.

Zheng, X., Wu, S.W., Zhai, H.Q., Zhou, P., Song, M.F., Su, L., Xi, Y.L., Li, Z.Y., Cai, Y.F., Meng, F.H., Yang, L., Wang, H.Y. and Yang, J.P. (2013) Arabidopsis Phytochrome B Promotes SPA1 Nuclear Accumulation to Repress Photomorphogenesis under Far-Red Light. *Plant Cell*, **25**, 115-133.

Zhu, D.M., Maier, A., Lee, J.H., Laubinger, S., Saijo, Y., Wang, H., Qu, L.J., Hoecker, U. and Deng, X.W. (2008) Biochemical Characterization of Arabidopsis Complexes Containing CONSTITUTIVELY PHOTOMORPHOGENIC1 and SUPPRESSOR OF PHYA Proteins in Light Control of Plant Development. *Plant Cell*, **20**, 2307-2323.

Zobell, O., Coupland, G. and Reiss, B. (2005) The family of CONSTANS-like genes in Physcomitrella patens. *Plant Biol (Stuttg)*, **7**, 266-275.

Zuo, Z.C., Liu, H.T., Liu, B., Liu, X.M. and Lin, C.T. (2011) Blue Light-Dependent Interaction of CRY2 with SPA1 Regulates COP1 activity and Floral Initiation in Arabidopsis. *Curr Biol*, **21**, 841-847.

7 Supplementary figures
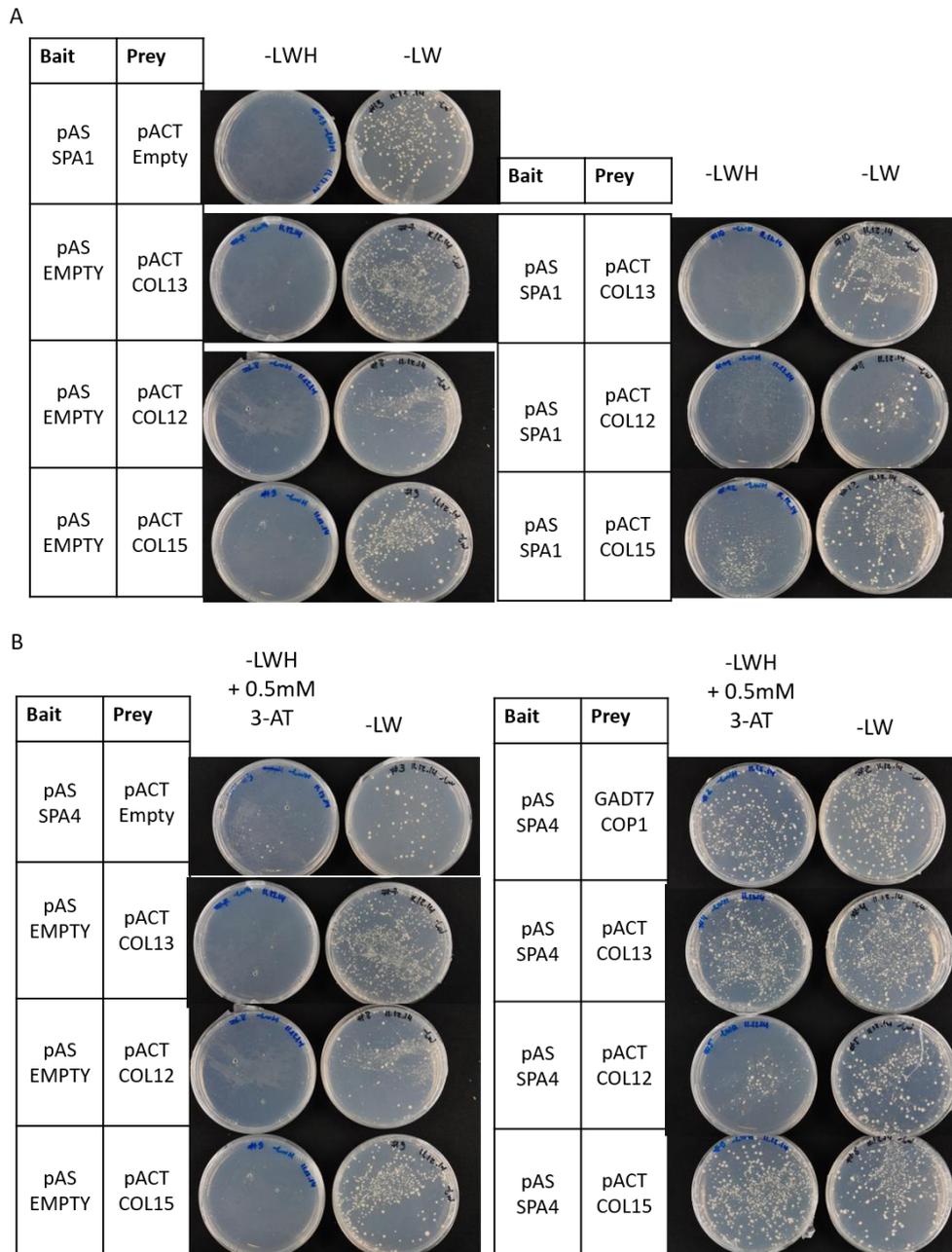
Supplementary Figure 1. COL12 and COL13 do not interact with SPA1 in the Yeast-two hybrid system

Y2H experiment testing interactions of SPA1 and SPA4 used as baits fused to pAS and COL proteins as prey fused to pACT. Yeast was co-transformed with prey and bait constructs and plated in non-selective (-LW) medium and selective (-LWH) supplied with 3-AT as indicated as indicated. The experiment was repeated three times.
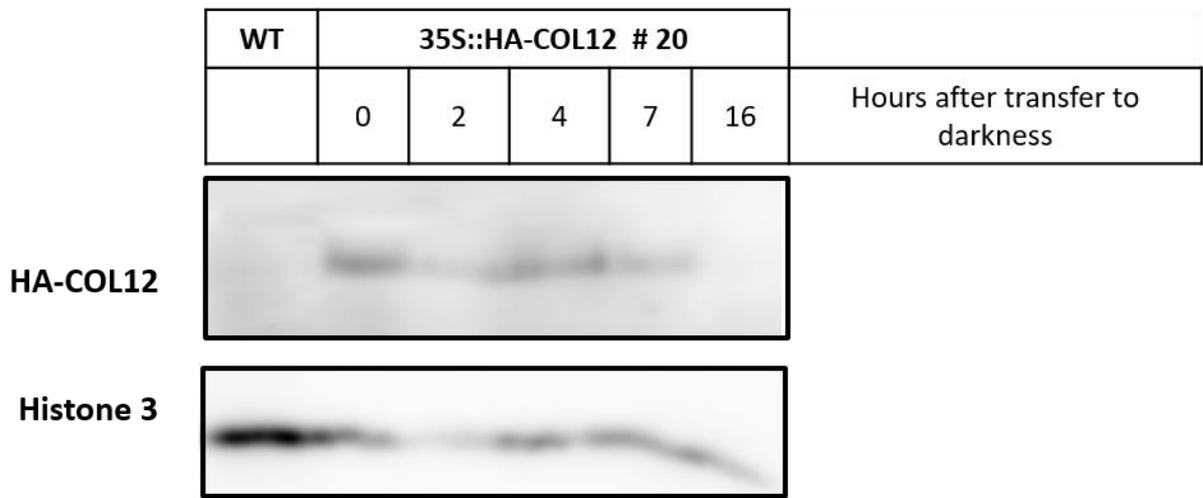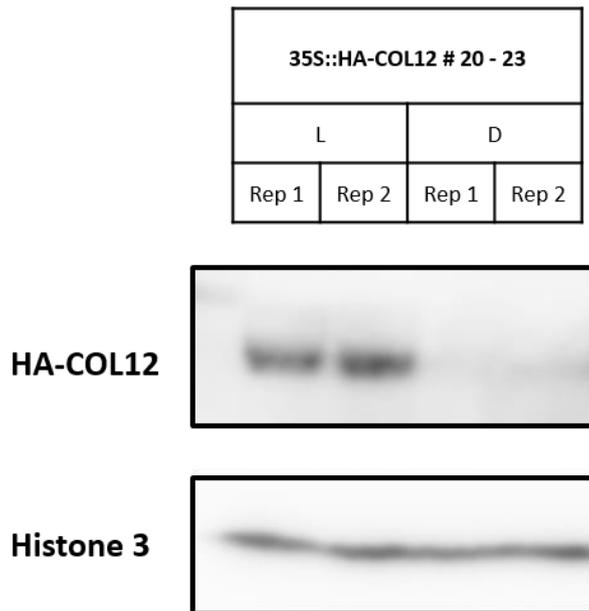
(A) SPA1 interact weakly with COL15 and does not interact with COL12.

(B) SPA4 interacts with COL13 and COL15 and might interact with COL12. For COL12 experimental replicates show contradicting results, here one replicate is shown.
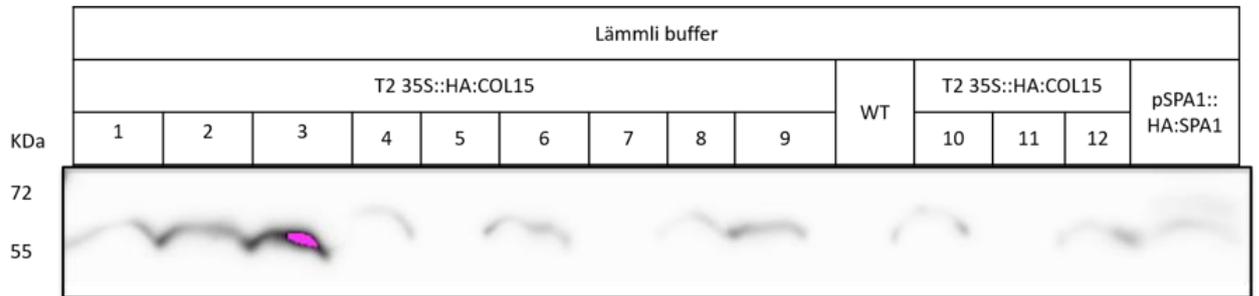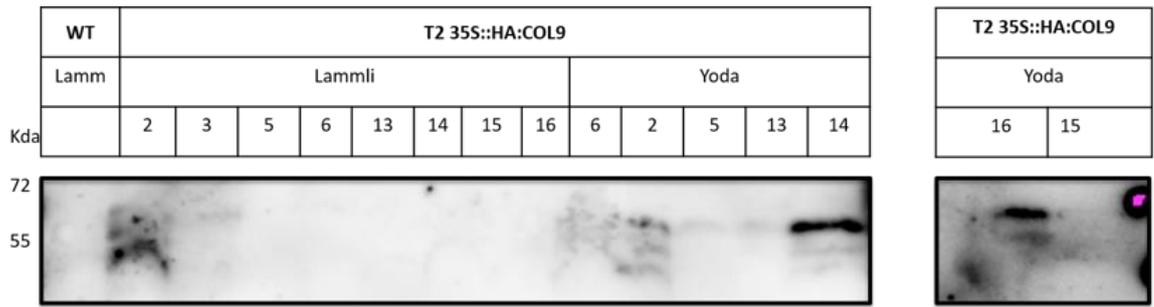
Supplementary Figure 2. Detection of HA:COL9 and HA:COL15 proteins from T2 independent transgenic lines.

Independent T2 generation seedlings grown for 10 days under continuous Wc. Tissue was harvested and immediately mixed with equal volume if 2x Lämmli buffer or Yoda buffer as indicated. Inmunoblot was performed using anti-HA antibody. HA:COL15 has a predicted size of 47 kDa and HA:COL9 of 40 kDa.

35S::HA-COL12 # 20 - 23			
L		D	
Rep 1	Rep 2	Rep 1	Rep 2

HA-COL12

Histone 3

WT	35S::HA-COL12 # 20					
	0	2	4	7	16	Hours after transfer to darkness

HA-COL12

Histone 3

Supplementary Figure 3.

Everything as in Figure 7, using a second independent transgenic line.
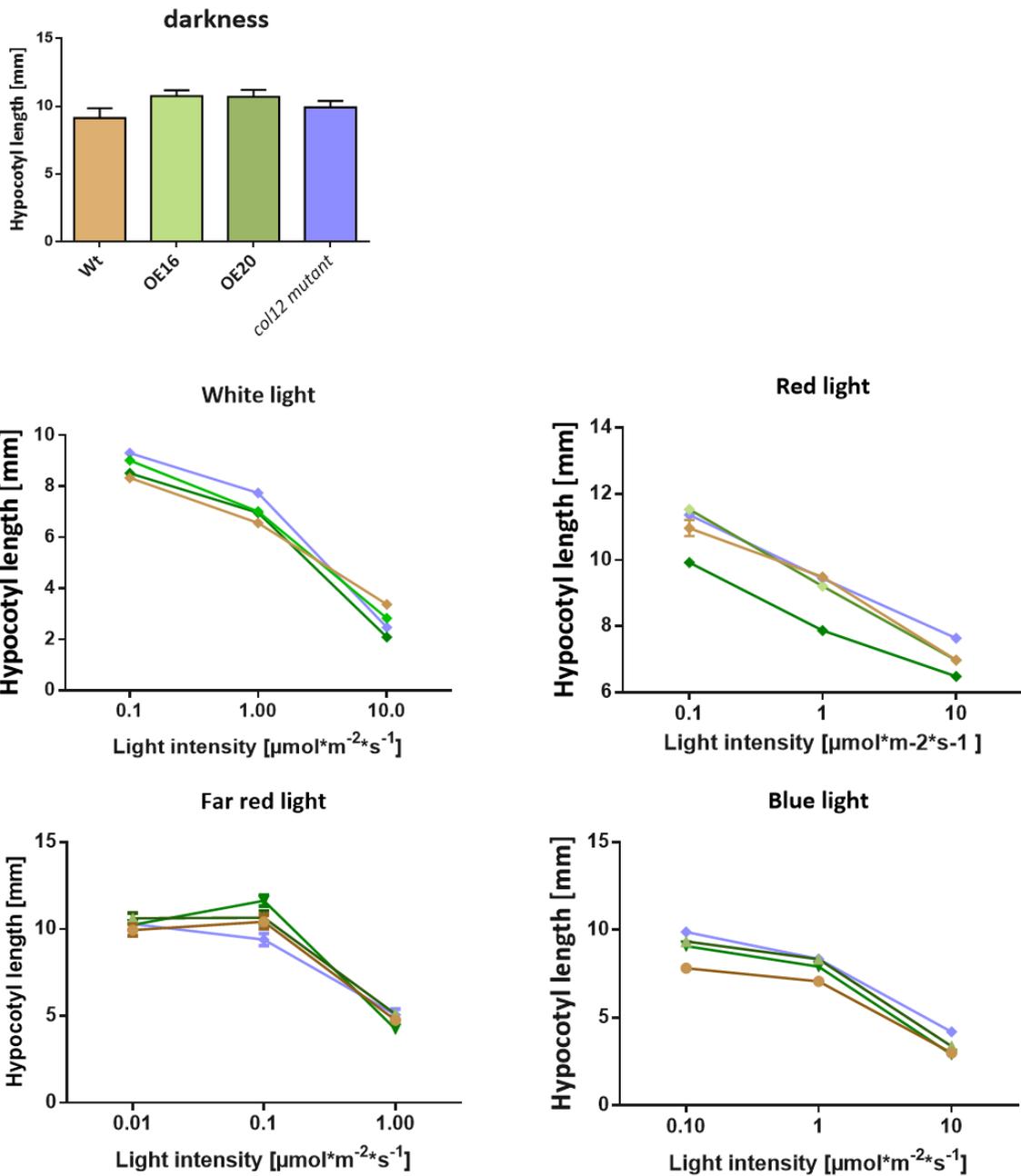
Supplementary Figure 4. COL12 does not play a role in seedling photomorphogenesis

Fluence dose response test the response of the hypocotyl length of light treatments with D, Wc or monochromatic R, B and Fr. Experiment compares the following genotypes: WT, *col12*, COL12 ox 16 and COL12 ox 20. Seedlings were allowed to grow for 4 days before being photographed and measured with the IMAJEJ software. Data shows the average of 15 -20 seedlings ± SEM. The experiment was replicated three times (Trimborn, L 2015. Bachelor Thesis).

WT	F3 *ft* x COL12 ox 16				COL12 OX 16	F3 *ft* x COL12 ox 20	
	4	5	11	16		1	4

70 kDa
55 kDa
40 kDa

◄ HA:COL12
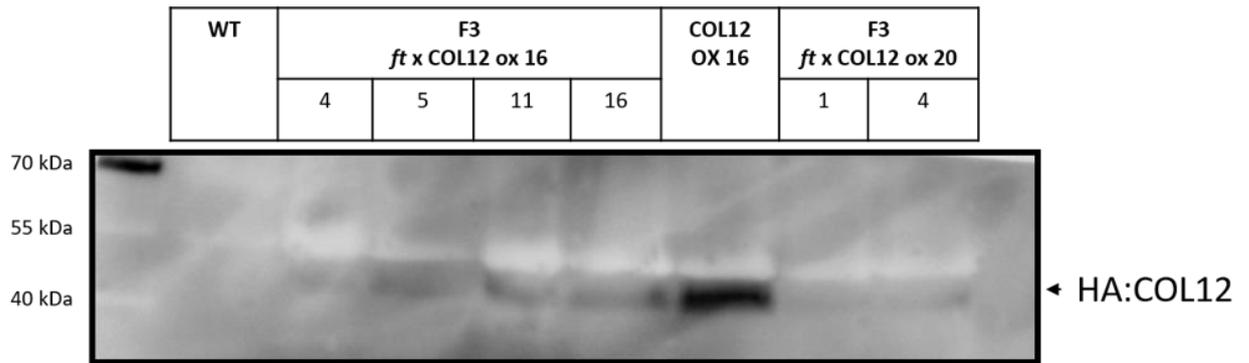
Supplementary Figure 5. COL12 protein levels in double ft col12 ox lines and single COL12 ox

Immunoblot shows COL12 protein levels in COL12 ox line 16 or double mutants *ft* x COL12 ox 16 and ox 20.

MS + GA (10uM)
Germination rate
95 %   18%

WT   *cop1-5 (-/-)*
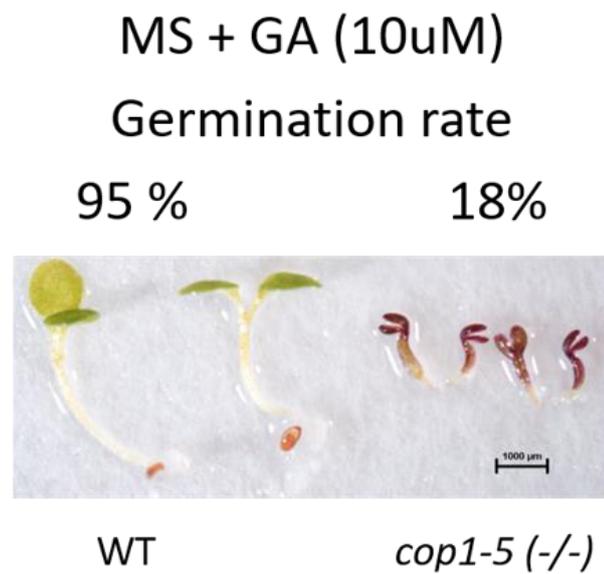
Supplementary Figure 6. *cop1-5* seeds germinate in medium supplied with GA

Phenotype of 8-days old seedlings growing in MS supplied with GA at a concentration of 10uM and calculation of germination rate from 50 seeds. Experiment was replicated once.
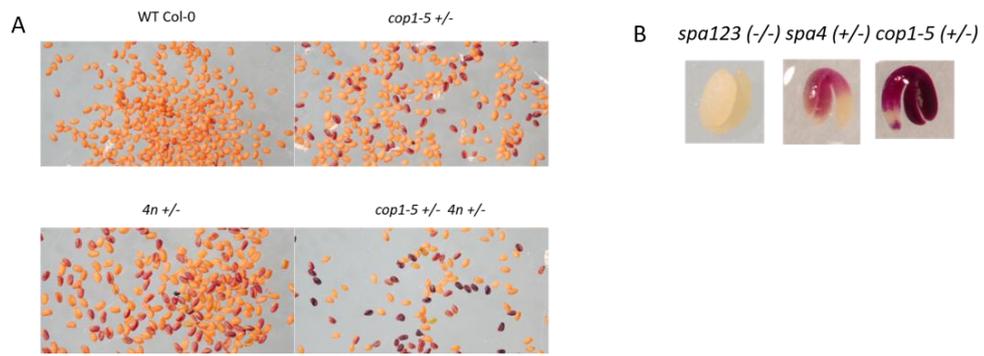
Supplementary Figure 7.

(A) Seed color phenotype shows the offspring seed from indicated segregating parents.

(B) Mature embryos exhibiting different degrees of purple color are the offspring of segregating *cop1-5 +/-4n +/-.*

8 Supplementary Table

Supplementary Table1. List of mutant lines with T-DNA insertion within the COL genes and primers

Mutant line ID	Accession	Gene	Salk code	Location of insertion ATG = 0	RP primer WT/Mut sequence	LP primer WT allele sequence	LP Mut allele
N629040	at1g28050	COL15	SALK_129040 (BZ)	154 bp first exon	CCTCAACATCTCTTGACCAT	GGAGAGAGTACCGTGCGATT	Lb1.3
N640552	at2g33500	COL14	SALK_140552	-894 bp promoter?	TTAGGCACATTAATTGGCTGCCCTC	TTCTTGTGTGTGGGGTCT	Lb1.3
N674509	at2g47890	COL13	SALK_037623C	1500 bp 3' UTR	CAATTCGTGCAGAGAGTCTCC	GAAGATTAGGCCCCAACAAAC	Lb1.3
N862394	at3g21880	COL12	SAIL_318_F05	1089 bp exon C-terminus	AGACAAGGCTCTAGAGGTCTC	ATTGGTTCTAAACCAGTGGGG	LB sail
N685620	at4g15250	COL11	SALK_034952C	exon terminus C-terminus	TGAAATGGAAGGTGGAGAGTG	AATGGTTCATCAACTTCCGTG	Lb1.3
N662685	at5g48250	COL10	SALK_0619961C	1886 bp exon C-terminus	TCACAGTCAAGTCATGATGCC	AGCAGCCAGCATTAAGCAAT	Lb1.3
N637167	At3g07650	COL9	SALK_137167 (BY)	First exon	CCGAGAGCTGTATGGAAGATG	GAGCCAAGGAAGATGGGTTAC	Lb1.3

9 Acknowledgements

Declaration

I hereby declare that except where specific reference is made to the work of others, the contents of this dissertation are original and have not been submitted in whole or in part for consideration for any other degree or qualification in this, or any other University. This dissertation is the result of my own work and includes the contribution of students, from the University of Cologne, who performed the following experiments:

Name	Contribution	Related Documents
Melanie Menje	- Molecular cloning of truncated *COL12* into pDONR and pAMARENA vectors - Co-localization and FRET Analysis of COP1/SPA vrs COL12	Bachelor Thesis
Laura Trimborn	- Transcriptional analysis of COL12 effects. - Assessment of *COL12* circadian and developmental regulation. - Molecular characterization of *col12* allele. - Light response curves.	Bachelor Thesis
Monique Henschel	- Molecular cloning of *COLs* (*9,10,11,12,15*) into pDONR, pENSG_CFP and pEarlyGate 201 vectors. - Co-localization analysis of COP1/SPA vrs COLs	Bachelor Thesis
Lennart Robers	- Analysis of COL12 protein stability under different light qualities. - Effects of COL12 on CO protein stability	Masters Module

Natalia Maria Ordoñez Herrera

Erklärung

Ich versichere, dass ich die von mir vorgelegte Dissertation selbständig angefertigt, die benutzten Quellen und Hilfsmittel vollständig angegeben und die Stellen der Arbeit einschließlich Tabellen, Karten und Abbildungen, die anderen Werken im Wortlaut oder dem Sinn nach entnommen sind, in jedem Einzelfall als Entlehnung kenntlich gemacht habe; dass diese Dissertation noch keiner anderen Fakultät oder Universität zur Prüfung vorgelegen hat; dass sie _ abgesehen von unten angegebenen Teilpublikationen noch nicht veröffentlicht worden ist sowie dass ich eine solche Veröffentlichung vor Abschluss des Promotionsverfahrens nicht vornehmen werde.

Die von mir vorgelegte Dissertation ist von Prof. Dr. Ute Höcker betreut worden.

Natalia Maria Ordoñez Herrera

Teilpublikationen:

Ordonez-Herrera, N., Fackendahl, P., Yu, X., Schaefer, S., Koncz, C., and Hoecker, U. (2015). A cop1 spa Mutant Deficient in COP1 and SPA Proteins Reveals Partial Co-Action of COP1 and SPA during Arabidopsis Post-Embryonic Development and Photomorphogenesis. Mol Plant *8*, 479-481.

Lebenslauf

Natalia Maria Ordoñez Herrera

Rungiustrasse 40, 12347 Berlin

Tel. (mobil): +49 (01) 766)4759042

E-mail: nataliaordonez@gmail.com

Geburtsdatum: 18/01/1987

Geburtsort: Bogota- Kolumbien

Hochschulausbildung

seit 10/2012	**Promotion am Botanischen Institut der Universität zu Köln - Deutschland** unter Betreuung von Prof. Dr. Ute Höcker Titel: " Analysis of COP1/SPA signalling events in plant developmental responses "
09/2010-08/2012	**Masterstudium Biologie - Biologisches Institut, King Abdullah University of Science and Technology (KAUST) - Saudi Arabien.** unter Betreuung von Prof. Dr. Christoph Gehring Titel: " Physiological and molecular effects of the cyclic nucleotides cAMP and cGMP on Arabidopsis thaliana"
01/2004 – 09/2009	**Studium der Biologie an der Universität zu Kolumbien - Kolumbien** unter Betreuung von Prof. Dr. Adriana Umana Titel: "Effects of sinvastatins in the apoptosis and activation of the JAK-STAT signalling pathway in a human trophoblast cell line line"

Publikationen

- Ordonez-Herrera, N., P. Fackendahl, X. Yu, S. Schaefer, C. Koncz, and U. Hoecker. 2015. A *cop1 spa* Mutant Deficient in COP1 and SPA Proteins Reveals Partial Co-Action of COP1 and SPA during Arabidopsis Post-Embryonic Development and Photomorphogenesis. *Molecular Plant*. 8:479-481.

- Ordonez, N.M., C. Marondedze, L. Thomas, S. Pasqualini, L. Shabala, S. Shabala, and C. Gehring. 2014. Cyclic mononucleotides modulate potassium and calcium flux responses to H2O2 in Arabidopsis roots. *Febs Letters*. 588:1008-1015.

- Ordoñez, N.M., Shabala L., Gehring C., Shabala, S. 2013. Noninvasive Microelectrode Ion Flux Estimation Technique (MIFE) for the Study of the Regulation of Root Membrane

Transport by Cyclic Nucleotides. *In* Cyclic nucleotide signaling in plants. C. Gehrig, editor. Humana Press, New York. 95-106.

Teilnahme an wissenschaftlichen Konferenzen

09/2015	Signalling in plant development, Brünn, Tschechien
06/2014	Plant Biology Europe FESPB/EPSO, Dublin, Ireland
06/2013	International Symposium on Plant Photobiology, Edinburgh, Schottland

Stipendien und Auszeichnungen

2012-2017	Promotionsstipendium von der International Max Planck Research School
09/2010-08/2012	Promotionsstipendium von der King Abdullah University of Science and Technology (KAUST)

Akademische und Forschungserfahrung

seit 10/2012	**Wissenschaftlicher Mitarbeiter** am Botanischen Institut der Universität zu Köln
05/2012 -6/2012	**Wissenschaftlicher Mitarbeiter,** University of Tasmania, Australia unter Betreeuung von Prof Sergey Shabala Projekt: Non-invasive measurement of ionic fluxes in response to cyclic monophosphates.
05/2011- 07/2011	**Studentische Hilfskraft** am Institut für Genombiologie, University of Illinois, USA unter Betreeuung von Dr. Andrew Leakey Projekt : Soybean responses to Drought and Elevated CO_2
08/2007- 06/2008	**Akademischer Austausch**, Biologisches Institut, University of Sao Paulo, Brazil

Wichtige Wissenschaftliche Methoden

Biochemie	Proteinisolation, Western-Blot, Immunpräzipitation
Molekularbiologie	Molekulare Klonierung, RNA- und DNA-Extraktion, qRT-PCR
Pflanzenbiologie	Photomorphogenese, Blütezeit, Embryo-Dissektion, Ionenfluss-Messungen, Dürre-Stress, Photosynthese, Stomatal-Leitfähigkeit,
Zellen-Biologie	Konfokale-Mikroskopie, FRET-FLIM

Weiterbildungen

Scientific Writing Kurs, BioScript, Graduate School for Biological Sciences, Universität zu Köln
FIJI Bioimaging, Graduate School for Biological Sciences, Universität zu Köln

Lehre und Mentoring

2013 – 2015	Aufsicht auf 4 Bachelorstudenten für 4 Monaten jede.

Sprachen

Spanisch, Muttersprache
Englisch und Portugiesisch, fließend in Wort und Schrift
Deutsche, fortgeschritten

Datum   Unterschrift